

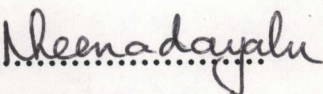
**THE DETERMINATION OF ACTIVITY COEFFICIENTS AT INFINITE
DILUTION USING GAS-LIQUID CHROMATOGRAPHY**

**Submitted in partial fulfilment of the requirements for the degree of
Master of Science in the Department of Chemistry,
University of Natal
1996**

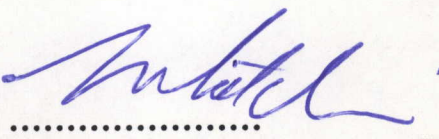
by

**Nirmala Deenadayalu
University of Natal
Durban**

I hereby certify that this research is the result of my own investigations, which has not already been accepted in substance for any degree, and is not being concurrently submitted for any other degree.

signed : 
N. Deenadayalu

I hereby certify that the above statement is correct.

signed : 
Prof. T.M. Letcher

ACKNOWLEDGEMENTS

Prof. T.M. Letcher for his helpful criticism, guidance and constant encouragement;

My colleagues Warren, Penny, Paul and Megan for their helpfulness.

The technical staff : Jody and Dave for helping me with my equipment, Kishore for solving my computer "problems", Gregory, Raj and Jay for obtaining my chemicals and other necessities that enabled me to conduct my research.

My husband, Vijay, for his patience and encouragement.

ABSTRACT

Gas chromatography is an accepted technique for the determination of activity coefficients at infinite dilution, γ_{13}^{∞} . The method produces rapid and reliable results for systems in which the solutes are non-polar and volatile and in which the solvents are involatile. At the same time the glc technique is also limited to solutes that are not adsorbed onto the support packing.

In this work the scope of the glc technique was extended to include polar solutes which are adsorbed onto the support packing and a solvent which is moderately volatile.

The systems chosen to investigate extending the technique to include polar solutes were C1, C2, and C3 alkanols in the solvent n-hexadecane. These polar solutes are adsorbed onto the celite which is the support packing used in this work. Their retention volumes were found to be dependent on sample size, flowrate and column loading. It was therefore necessary to correct retention volumes for these effects. The systems were studied at two temperatures namely 293.15 K and 303.15 K.

The systems chosen to investigate extending the glc technique to include a volatile solvent were solutes pentane, hexane, cyclopentane, cyclohexane and benzene in the moderately volatile solvent, decane. This technique has been tested and reported by my colleagues for weakly volatile solvents such as cis- and trans - decalin. In this work a more volatile solvent namely decane was used to further test the technique. This work was conducted at two temperatures namely 278.15 K and 293.15 K and the excess enthalpies at infinite dilution, $H_1^{E\infty}$, calculated.

The infinite dilution activity coefficients and infinite dilution excess enthalpies for related systems are compared with data found in the literature.

Glossary

Symbol	Definition
n_3	Moles of solvent on the column
t_r	Infinite dilute retention times of the solute
t_r^*	retention times of the solute at finite concentration
t_g	retention time of an unretained gas
P_w	Pressure of water-vapour in the atmosphere
P_o	Outlet pressure (atmospheric)
J_3^2	correction factor for the compressibility of the mobile phase
U_o	Flowrate corrected for temperature and water-vapour pressure
V_N	Net retention volume corrected for compressibility of the mobile phase an at infinite dilution
W_s	Mass of celite per mole of solvent
T	temperature of the waterbath
V_N^*	net retention volume corrected to zero mean column flowrate
V_N^o	net retention volume corrected to zero sample size and to zero flowrate per mole of solvent
$V_N/$	net retention volume corrected to zero sample size, zero mean flowrate per mole of solvent
t	time of injection of the solute
P_3'	partial pressure of the solvent in the carrier gas
a	intercept of the graph of $U_o t/n_3$
b	slope of the graph of $U_o t/n_3$
γ_{13}^∞	activity coefficient at infinite dilution
$H_1^{E\infty}$	excess enthalpy at infinite dilution
$\gamma(x)$	activity coefficient at finite concentration
V_1^*	molar volume of solute
P_1^*	saturated vapour pressure of solute

TABLE OF CONTENTS

	page
1. INTRODUCTION	1
2. THE ACTIVITY COEFFICIENT	4
2.1. Definition of the activity coefficient at Infinite Dilution	
2.2. Importance of the activity Coefficient Data at Infinite Dilution	5
2.2.1. The Flory Huggins Theory	5
2.2.2. Environmental and Chemical Engineering	6
2.3. Experimental Methods Available for the Determination of γ_{13}^{∞}	
2.3.1. Dynamic Chromatography	7
2.3.2. Differential Ebulliometry	7
2.3.3. Dew Point	8
2.3.4. Headspace Analysis	8
2.3.5. Differential Static Cell	9
2.3.6. Gas Stripping	9
2.3.7. Liquid-Liquid Solubility	9
2.4. Advantages and Limitations of the GLC Technique	10
3. THEORY OF GAS-LIQUID CHROMATOGRAPHY	
3.1. The Gas Chromatographic Method	11
3.2 Summary of glc Theory	11
3.2.1. Relationship of the Net Retention Volume and Activity Coefficient at Infinite Dilution to the Partition Coefficient	15
3.2.2. Theoretical Plate Concept and the Activity Coefficient at Infinite Dilution	24
3.2.3. Fugacity Effects	30
3.2.4. Mixed Virial Coefficients	32
3.3. Determination of $H_1^{E\infty}$	
3.3.1. $H_1^{E\infty}$ from γ_{13}^{∞} values	37
3.3.2. Roosenboom's Method	38

	page
3.4. Treatment of a Polar Solute	41
3.5. Treatment of a Volatile Solvent	42
4. APPARATUS AND EXPERIMENTAL PROCEDURE	
4.1. Introduction	44
4.1.1 Column Thermostat	46
4.1.2. Pressure Control and Measurement	46
4.1.3. Soap Bubble Flowmeters	46
4.1.4. Injectors	47
4.1.5. Detectors	51
4.2.1. Experimental Procedure for a Simple System	55
4.2.2. Experimental and Measurement Procedure for polar solutes	
4.2.2.1. Experimental Procedure	55
4.2.2.2. Measurement Procedure	56
4.2.2.2.1. Retention Times at Infinite Dilution	57
4.2.2.2.2. Net Retention Volume at Zero Flowrate	57
4.2.2.2.3. Net Retention Volume at Infinite Coverage	57
4.2.3. Experimental Procedure for a Volatile Solvent	59
5. POLAR SOLUTES IN HEXADECANE	
5.1. Introduction	61
5.2. Results	62
5.3. Error Analysis	101
5.4. Discussion	103
5.4.1. Experimental Error in γ_{13}^{∞} for a Polar Solute in a Non-polar Solvent	107
5.4.2. Solute size	108
5.4.3. Flowrate	109
5.4.4. Percentage Loading	109
5.5. Conclusion	113

6. NON-POLAR SOLUTES IN DECANE	
6.1. Introduction	114
6.2. Results	135
6.3. Error Analysis	138
6.4. Sample Calculations	138
6.5. Discussion	141
6.6. Conclusion	146
APPENDIX i	147
APPENDIX ii	152
APPENDIX iii	157
REFERENCES	189

1. INTRODUCTION

The glc technique for the determination of activity coefficients at infinite dilution, γ_{13}^∞ , was first described by Martin and Synge⁽¹⁾ and later refined by Everett⁽²⁾ and Cruickshank⁽³⁾. Their equation relates γ_{13}^∞ to simple properties of chromatography such as n_3 the number of moles of solvent on the column packing, V_N the net retention volume, P_o the column outlet pressure and P_1^* the vapour pressure of the solute by

$$\ln \gamma_{13}^\infty = \ln \frac{n_3 RT}{V_N P_1^*} - \left[\frac{(B_{11} - V_1^*)}{RT} \right] P_1^* + \left[\frac{(2B_{12} - V_1^\infty)}{RT} \right] P_o J_3^2 \quad (1.1.)$$

where V_1^* is the molar volume of the solute, V_1^∞ is the partial molar volume of solute at infinite dilution in the stationary phase, J_3^2 is the gas compressibility factor of the mobile phase, B_{11} the second virial coefficient of pure solute and B_{12} the mixed second virial coefficient of the solute and the carrier gas. The subscripts 1, 2, and 3 will be used to represent the solute, carrier gas and the solvent respectively.

This technique developed by Everett⁽²⁾ and Cruickshank⁽³⁾ works very well for volatile, nonpolar solutes such as pentane, hexane and heptane in involatile solvents such as hexadecane, octadecane and dotricontane. However for systems in which solute adsorption on the diatomaceous earth occurs, the simple technique has to be altered. In this work the method was extended to include alkanols that adsorb on the surface of the solid support (see chapter 4).

For the alkanol-hexadecane systems equation 1.1. was extended to include the dependence of solute retention time on sample size and the dependence of net retention volume on mean column flowrate, $U_o J_3^2$, and solvent coverage, W_s (see chapter 3).

For the alkanol-hexadecane system equation 1.2., developed in chapter 3, was used

$$\ln V'_N = \ln \left[\frac{RT}{\gamma_{13}^\infty P_1^*} \right] - \left[\frac{(B_{11} - V_1^*)}{RT} \right] P_1^* + \left[\frac{(2B_{12})P_o}{RT} \right] \quad (1.2.)$$

The approach used here was first tested by Cruickshank *et al*⁽³⁾ for the benzene-glycerol system in which the solute benzene is weakly polar and adsorbed onto the glycerol and the solid support. Equation 1.2. was used in the extrapolation of the net retention volume to zero flowrate and to infinite solvent coverage on the column packing, and hence to calculate the activity coefficients at infinite dilution.

The theory developed by Everett⁽²⁾ and Cruickshank⁽³⁾ also does not take into account the possibility of determining γ_{13}^∞ for a moderately volatile solvent.

Letcher *et al*⁽⁴⁾ have extended the Everett⁽²⁾ and Cruickshank⁽³⁾ theory to include a moderately volatile solvent by relating the solvent evaporation from the column to its partial pressure (P_3')

$$\frac{V_N}{n_3 e^C} = \frac{RT}{\gamma_{13}^\infty P_1^*} - \frac{U_o t}{n_3} \left[\frac{P_3'}{\gamma_{13}^\infty P_1^*} \right] \quad (1.3.)$$

where

$$C = - \left[\frac{B_{11} - V_1^*}{RT} \right] P_1^* + \left[\frac{2B_{12} - V_1^\infty}{RT} \right] P_o J_2^3 \quad (1.4.)$$

U_o is the volumetric flowrate corrected to column temperature and for the presence of water vapour and t is the time at injection of the solute onto the column.

In order to extend and test the technique previously developed for moderately volatile solvents (decalin and dodecane), an even more volatile solvent, decane, was chosen.

The definition and importance of the activity coefficient is given in chapter 2.

Chapter 3 contains a detailed theory of gas liquid chromatography. The apparatus used and the experimental procedure are outlined in chapter 4. The results together with literature values are given in chapters 5 and 6.

2. THE ACTIVITY COEFFICIENT

2.1. Definition

The activity coefficient at infinite dilution, γ_{13}^{∞} , for a solute 1 in a solvent 3 for an ideally dilute solution is related to the activity of the solute a by

$$a_1 = \gamma_{13}^{\infty} x_1 \quad (2.1)$$

where a_1 is the activity of solute 1 and x_1 is the mole fraction of solute 1.

In this work an ideally dilute solution will be defined as follows : if $a_1 \rightarrow x_1$ and $x_1 \rightarrow 0$ then $\gamma_{13}^{\infty} \rightarrow 1$. In this work, systems for which γ_{13}^{∞} is very much larger than 1 (alkanol and hexadecane) and systems for which γ_{13}^{∞} is *close* to 1 (hydrocarbons and decane) are studied.

2.2. Importance of Activity Coefficient Data at Infinite Dilution

Activity coefficients obtained at infinite dilution are of importance to chemical engineers, theoreticians and solution chemists. γ_{13}^{∞} is important for separation processes and distillation of azeotropic mixtures. Solution chemists interpret activity coefficient data in order to understand interactions in solutions. Theoreticians apply these data for the testing of various solution theories. Biological and environmental chemists⁽⁵⁾ have found new uses for the activity coefficient measured at infinite dilution.

2.2.1. Use of Infinite Dilution Activity Coefficients to Calculate Activity Coefficients at Finite Concentrations

Although the glc method produces only one γ_{13}^{∞} value, the result can be used in predicting the activity coefficient at finite concentration, $\gamma(x)$, from models of liquid-liquid mixtures. One such model is the **Guggenheim-Miller-Flory - Huggins**^{(6),(7),(8),(9)} equation. solvent, ie. γ_{13}^{∞} . The GMFH equation relates the activity coefficient of a component of a binary mixture of molecules of different sizes to the composition according to:

$$\ln \gamma_1 = \ln(1 - \phi_2) \left(\frac{1}{x_1} \right) + \left(1 - \frac{1}{r} \right) \phi_2 + \chi \phi_2^2 \quad (2.2.)$$

where:

ϕ_2 = the volume fraction of component 2

χ = the Flory - Huggins interaction parameter

x_1 = the mole fraction of component 1

γ_1 = the activity coefficient at a finite concentration

The value of r can be chosen to be the ratio of the size of molecules $(V_2/V_1)^{(10)}$.

At infinite dilution equation (2.2.) becomes:

$$\ln \gamma_1^{\infty} = \ln \left(\frac{1}{r} \right) + \left(1 - \frac{1}{r} \right) + \chi \quad (2.3.)$$

The interaction parameter, χ can be calculated from equation 2.3. and substituted into equation 2.2. Equation 2.2. is then used to calculate the activity coefficient at a finite concentration. This model and equation 2.2. and 2.3. can be applied to the activity coefficient at infinite dilution related to the hydrocarbon-decane systems as determined in this work.

2.2.2. Environmental and Chemical Engineering

Infinite dilution activity coefficients are useful for the determination of excess Gibbs free energy model parameters and in design separation for very dilute systems, such as in the production of high purity reagents for chromatography and pharmaceuticals and for the separation of pollutants from the environment. In environmental engineering the chemical species of interest is often very dilute so that only the infinite dilution activity coefficient of the component is important. Thermodynamic modelling⁽¹¹⁾ can be used to predict the fate of a long-lived chemical. The partitioning between the aqueous and the organic phase of many long-lived pollutants is indicated by the hydrophobicity of the compound which is determined by the value of the infinite dilution activity coefficient of the pollutant in water. For example the distribution of benzo[a]pyrene in water, air, soil, sediment and fish was calculated from the infinite dilution activity coefficients and favourably compared with those values obtained by other conventional methods⁽¹¹⁾.

Many of the theoretical models of liquid mixtures contain two parameters, and can in principle be solved if the infinite dilution activity coefficients of each species in the other are found i.e. γ_{13}^{∞} and γ_{31}^{∞} . These model parameters can then be fixed and predictions of vapour-liquid, liquid-liquid and vapour-liquid-liquid equilibria over the whole composition range⁽¹¹⁾ can be made. Models have also been developed to extend the scope of γ_{13}^{∞} data. Together with equations of state γ_{13}^{∞} can be used to extrapolate over a large range of temperatures and pressures. γ_{13}^{∞} can also be used to estimate UNIFAC group interaction parameters⁽¹²⁾.

2.3. Experimental Methods Available for Determination of γ_{13}^{∞}

A number of different methods⁽¹¹⁾ are now available for the direct measurement of γ_{13}^{∞} . These methods are complementary and cover a range of relative volatilities of the two components.

2.3.1. Dynamic Chromatography

The work done in this project uses this glc technique. In this method the solvent is packed onto a chromatographic column and a small amount of solute is injected. The time taken for a solute to elute is a measure of the gas-liquid partition coefficient, and can be used to calculate γ_{13}^{∞} (see pp 34).

2.3.2. Differential Ebulliometry

This method involves accurately measuring the effect of solute concentration on the difference in boiling point temperature between a solution and a reference solvent at constant pressure. Eckert *et al*⁽¹³⁾ pioneered this technique when they solved the problem of pressure fluctuations and loss of volatile components. The equipment consists of ebulliometers connected through condensers to a common manifold which keeps the pressure in each ebulliometer the same and thereby minimises any pressure fluctuations. The ebulliometers are connected to a quartz thermometer and to a printer. The theory relates γ_{13}^{∞} to the limiting composition derivative of the difference in boiling point temperature at constant pressure⁽¹³⁾.

2.3.3. Dew Point

The method developed by Trampe and Eckert⁽¹⁴⁾ is a complementary method to the ebulliometric method. This method is best suited for systems in which the relative velocities are very low. In this method the change in temperature of the dew point temperature with respect to a reference solvent when very small amounts of solute are added is measured. The dew point temperature change is obtained from the difference between the average dew point temperature for a run and the pure solvent dew point temperature. The theory relates γ_{13}^{∞} to the relative volatilities, α , of a solute which is infinitely dilute in a solvent. The derivative of the dew point temperature change and different solvent composition is related linearly to α and γ_{13}^{∞} . The apparatus consists of a peristaltic pump, a preheater, the dew point sensor in a constant temperature air bath and a trap or condenser.

2.3.4. Headspace Analysis

Hussam and Carr⁽¹⁵⁾ pioneered this method which relates γ_{13}^{∞} to the peak area or peak height of a gas standard of known composition and to the peak area or peak height of a sample. The apparatus consists of sample cells placed in a waterbath, sampling valves, a capillary gas chromatograph, a barometer, a manometer and a computer. A known amount of dilute solute is dissolved in a thermostatted solvent and allowed to equilibrate. For a set of measurements the gas lines are evacuated and then reopened to allow the sample vapour to fill the sample loop from where the sample vapour is injected into the capillary gas column. The method is good when solute-solute interactions are negligible. The drawbacks of the technique are that solute can be lost by adsorption on the container surface and thermodynamic correction factors must be obtained from other experimental measurements or by empirical calculations.

2.3.5. Differential Static Cell

The differential static cell method was developed by Alessi *et al*⁽¹⁶⁾. γ_{13}^{∞} is related to the saturated vapour pressure of solute, the saturated vapour pressure of solvent and to the limiting slope of total pressure versus mole fraction of solute. The apparatus consists of two glass cells, placed in a constant waterbath, and connected to a differential transducer. The apparatus is designed to measure the total equilibrium pressure difference of a gravimetrically prepared binary mixture at constant temperature.

2.3.6. Gas Stripping

Gas stripping has been used by Carr *et al*⁽¹⁷⁾ for measuring γ_{13}^{∞} at very high values of relative volatilities. Leroi *et al*⁽¹⁸⁾ pioneered this technique. In this method a binary solute-solvent is kept in an equilibrium still which is placed in a constant temperature bath. An inert carrier gas at constant flow is introduced into the still and strips the solute from the solution into the vapour phase. The outlet gas flow is periodically injected into a chromatograph by means of a gas sampling valve maintained at a higher temperature to prevent any condensation of the vapour phase. The total pressure at equilibrium, the carrier gas flow rate and the total amount of solvent in the still are measured. The activity coefficient at infinite dilution is obtained from an exponential relationship between the solute peak area and time.

2.3.7. Liquid-Liquid Solubility

In this method the infinite dilution activity coefficient of the solute in one of the phases must be known together with the partition coefficient to enable the calculation of the infinitely dilute activity coefficient in the other phase. The two phases chosen must be mutually insoluble in each other.

2.4. Comparison of GC and Static Methods: Advantages and Limitations

Advantages

The glc used is easy to build, operate and maintain. Once the system is working it can be used for months with only frequent checks being made for pressure leakages. Solutes are required in very small amounts ($\pm 0.1 \text{ mm}^3$). This technique is therefore particularly useful for solutes that are only available in small quantities. The chromatographic column separates impurities from the solute therefore solutes of high purity are not essential. When several solutes are to be studied they can be injected as a premixed sample provided that their retention times differ significantly. This technique gives rapid results for most systems.

Limitations

The solutes chosen must be volatile and of a relatively high vapour pressure at the temperature of measurement in order to have a retention time not exceeding 10 minutes. When retention times are large (>10 minutes), peaks tend to become very broad. For systems in which adsorption occurs these effects must be correctly accounted for by extrapolation to infinite coverage. Corrections must also be made for imperfect gas phase behaviour. The carrier gas must be insoluble or nearly insoluble in the stationary phase. It should not interact with the solute vapour nor should it be adsorbed in or on the stationary liquid phase or on the solid support. The solute should be non-polar or the effect of the solute polarity must be taken into account and the solvent should be involatile.

3. THEORY OF GAS-LIQUID CHROMATOGRAPHY

3.1. The Gas Chromatographic Method

In all chromatographic processes two immiscible phases are brought together at a common interface.

The one phase (**mobile phase**) is made to flow over the other phase (**stationary phase**). When a third component is injected into the system, it is partitioned between the two phases and it is also carried (**eluted**) through the system by the mobile phase.

In glc a small quantity of solute is injected into a column packed with support coated with solvent. In the column, equilibrium is attained between the liquid phase and the carrier gas phase so that a proportion of solute always remains in the gas phase. Assuming equilibrium takes place the properties of glc can be related to the thermodynamic properties of the solute and the solvent.

3.2. Summary of GLC Theory

In 1941 **Martin and Synge**⁽¹⁾ related the **equilibrium partition coefficient, K** , to retardation properties using a plate theory. Their general equation relates the **retention volume of the solute, V_R** , to the **gas hold-up volume, V_G** , and the **solvent volume V_3** according to the equation:

$$V_R = V_G + KV_3 \quad (3.1.)$$

The solute being component 1, the carrier gas component 2 and the solvent component 3.

Martin and James⁽¹⁹⁾ presented the first theory that took into account the compressibility of the mobile phase. They applied a correction factor, J_n^m , to the gas volumes of equation 3.1. In terms of **Everett's**⁽²⁾ notation this correction term can be generalised as :

$$J_n^m = \frac{n}{m} \frac{\left(\frac{P_i}{P_o}\right)^m - 1}{\left(\frac{P_i}{P_o}\right)^n - 1} \quad (3.2.)$$

where P_i and P_o refer to the inlet and outlet pressures respectively.

In 1956 **Porter et al**⁽²⁰⁾ related the **net retention volume**, V_N , to the activity coefficient of the solute at infinite dilution according to the equation :

$$V_N = \frac{n_3 RT}{\gamma_{13}^\infty P_i^*} \quad (3.3.)$$

The retention volume V_N is determined from the column outlet flowrate U_o by:

$$V_N = J_3^2 U_o (T_r - T_g) = J_3^2 U_o T_r - V_D \quad (3.4.)$$

where t_r and t_g are the **retention times** for the solute and an **unretained gas** respectively, and V_D is the **dead space volume** or **gas hold-up volume** at mean column pressure, $P_o J_3^2$.

Desty⁽²¹⁾ used an extrapolation procedure based on the equation:

$$\ln V_N = \ln V_N^o + \beta P_o J_2^3 \quad (3.5.)$$

V_N^o is the extrapolated retention volume at zero mean column pressure where

$$\ln V_N^o = \frac{n_3 RT}{\gamma_{13}^\infty P_1^*} - \left[\frac{B_{11} - V_1^*}{RT} \right] P_1^* \quad (3.6.)$$

and

$$\beta = \frac{2B_{12} - V_1^\infty}{RT} \quad (3.7.)$$

V_1^* is the molar volume of the solute, B_{11} the second virial coefficient of pure solute and V_1^∞ is the partial molar volume of solute at infinite dilution in the stationary phase.

Neither of these workers took into account the solubility of the carrier gas in the stationary phase.

The **Bristol group**⁽³⁾ suggested a third extrapolation procedure

$$\ln V_N = \ln V_N^o + \beta P_o J_3^4 \quad (3.8.)$$

This extrapolation is suitable for carrier gases such as hydrogen, helium, nitrogen, oxygen and argon.

For non-ideal carrier gases they proposed :

$$\ln V'_N = \ln \left[\frac{V_N(1+bP_o J_2^3)}{(1+bP_o)} \right] = \ln V_N^o + \beta P_o J_3^4 \quad (3.9.)$$

where $b = B_{22}/RT$ and B_{22} is the second virial coefficient of the carrier gas.

This is identical to equation 1.1. for pressures P_o and P_i less than 1 atm since under these conditions $J_3^4 \approx J_3^2$.

A further refinement done by the Bristol group⁽³⁾ involved the solubility of the carrier gas in the stationary liquid.

$$\ln V'_N = \ln V_N^o + \beta' P_o J_3^4 \quad (3.10.)$$

where

$$\beta' = \beta + \lambda \left[1 - \frac{\partial \ln \gamma_{13}^\infty}{\partial x_2} \right] \quad (3.11.)$$

and λ is defined by the expansion of x_2 (mole fraction of carrier gas in the solvent as a series in the local carrier gas pressure) :

$$x_2 = \lambda p_2 + \phi p_2^2 + \dots$$

where ϕ is the coefficient of the second order pressure term.

For polar solutes none of the above equations can be used since the net retention volume has to be corrected to zero sample size, zero mean column flowrate, and to infinite solvent coverage.

In this work the following equation was used for the alkanol-hexadecane work (see chapter 4)

$$\ln V'_N = \ln \left[\frac{RT}{\gamma_{13}^\infty P_1^*} \right] - \left[\frac{(B_{11} - V_1^*)}{RT} \right] P_1^* + \left[\frac{(2B_{12})P_o}{RT} \right] \quad (1.2.)$$

Since the previous equations are valid only for nonvolatile solvents, equation 1.3. was used for the hydrocarbon-decane work (see chapter 4)

$$\frac{V_N}{n_3 e^C} = \frac{RT}{\gamma_{13}^\infty P_1^*} - \frac{U_o t}{n_3} \left[\frac{P_3'}{\gamma_{13}^\infty P_1^*} \right] \quad (1.3.)$$

3.2.1. Relationship of the Net Retention Volume and Activity Coefficient at Infinite Dilution to the Partition Coefficient

The distribution of a solute between stationary (L) and mobile (G) phases at constant temperature and pressure corresponds to equilibrium when the solute free energy is a minimum⁽²²⁾.

Under these conditions its chemical potential in one phase is equal to its chemical potential in the other phase.

$$u_L = u_G \quad (3.12.)$$

where

$$u_i = u_i^0 + RT \ln a_i \quad (3.13.)$$

a_i is the solute activity coefficient in the i th phase and μ_i^0 is the solute chemical potential at unit activity.

Replacing activities by concentrations and using equations (3.12.) and (3.13.)

$$\mu_L^0 = RT \ln C_L = \mu_G^0 + RT \ln C_G \quad (3.14.)$$

Rearranging equation (3.14.)

$$\frac{C_L}{C_G} = e^{\left(\frac{\Delta u^0}{RT}\right)} = K_R \quad (3.15.)$$

where

$$\Delta u^{\circ} = u_G^{\circ} - u_L^{\circ} \quad (3.16.)$$

Both $\Delta\mu^{\circ}$ and K_r are constants.

For elution at infinite dilution the linear rate of travel is equal to the average carrier velocity, \bar{u} multiplied by the fraction of time the solute spends in the mobile phase.

$$\text{rate of travel} = \bar{u} \left(\frac{C_G V_G}{C_G V_G + C_L V_L} \right) \quad (3.17.)$$

V_G is the mobile phase volume

V_L is the stationary phase volume

Rearranging equation (3.17.) gives :

$$\text{rate of travel} = \bar{u} \left(1 + \frac{C_L V_L}{C_G V_G} \right)^{-1} \quad (3.18.)$$

Equation (3.18.) can be rewritten as :

$$\text{rate of travel} = \bar{u} \left(1 + K_R \frac{V_L}{V_G} \right)^{-1} \quad (3.19.)$$

The solute rate of travel is also given by the expression :

$$\text{rate of travel} = \frac{\text{column length (L)}}{t_r} \quad (3.20.)$$

t_r is defined as the time required for the centre of gravity of the solute band to pass completely through the column (the column retention time).

Equating equations (3.19.) and (3.20.) and on rearranging yields

$$t_r = \frac{L}{u} \left(1 + K_R \frac{V_L}{V_G} \right) \quad (3.21.)$$

The quantity L/u is the dead time t_D , the time a nonsorbed solute requires to pass through the column.

$$\Rightarrow t_r = t_D \left(1 + K_R \frac{V_L}{V_G} \right) \quad (3.22.)$$

Equation (3.22.) was first deduced by Martin and Synge⁽¹⁾.

To convert retention times to gas volumes the mobile phase flow rate usually measured at the column outlet must be known.

The measured flow rate (U_o) must be corrected to conditions prevailing in the column (U_c)

$$U_c = U_o \left(\frac{T_c}{T_{fm}} \right) \left(\frac{P_{fm} - P_w}{P_{fm}} \right)$$

T_c and T_{fm} are the column and flowmeter temperatures.

P_{fm} and P_w are the flowmeter and water vapour pressures at T_{fm} .

The dead volume (V'_D) and retention volumes (V'_R) are given by

$$V'_D = t_D U_o \quad (3.24.)$$

$$V'_R = t_r U_o \quad (3.25.)$$

By substituting equations (3.24.) and (3.25.) into equation (3.22.) the true retention volume (V_R) is defined as

$$V_R = V'_R - V'_D \quad (3.26.)$$

$$V_r = U_o(t_r - t_D) \quad (3.27.)$$

In 1952 Martin and James⁽¹⁹⁾ introduced a gas compressibility correction factor. Consider a carrier gas flowing through a packed column of uniform cross section, A , at a pressure, P , and velocity, u . The volume within the column must be constant so that by Boyles law:

$$Pu = p_o u_o = \overline{Pu} \quad (3.28.)$$

where \overline{P} is the average pressure, P_o the outlet pressure, \overline{u} the average velocity, u_o the outlet velocity.

The velocity at any given point is given by

$$u = P_o \frac{u_o}{P} \quad (3.29.)$$

The velocity can be related to the pressure gradient dp within a length dx along the column, the column specific permeability coefficient K , porosity e and gas viscosity η through Darcy's law

$$u = -K \frac{dP}{e\eta dx} \quad (3.30.)$$

Also,

$$\Rightarrow P_o = \frac{uP}{u_o} \quad (3.31.)$$

$$P_o = -\frac{KPdP}{e\eta u_o dx} \quad (3.32.)$$

$$\Rightarrow dx = \frac{-KPdP}{e\eta u_o P_o} \quad (3.33.)$$

Multiplying equation (3.34.) by P

$$Pdx = -\frac{K}{e\eta u_o P_o} P^2 dP \quad (3.34.)$$

The average value of a continuous function $\bar{F}(x)$ is

$$\bar{F}(x) = \frac{\int F(x) dx}{\int dx} \quad (3.35.)$$

The average pressure \bar{P} over the column is represented by

$$\bar{P} = \frac{\int -\frac{K}{e\eta u_o P_o} P^2 dP}{\int -\frac{K}{e\eta u_o P_o} P dP} \quad (3.36.)$$

Integrating over the column gradient, which is bound by the inlet and outlet

pressures (P_i and P_o) respectively

$$\Rightarrow \bar{P} = \frac{2}{3} \left\{ \frac{(P_i^3 - P_o^3)}{(P_i^2 - P_o^2)} \right\} \quad (3.37.)$$

$$\Rightarrow \frac{\bar{P}}{P_o} = \frac{2}{3} \left\{ \frac{\left(\frac{P_i}{P_o}\right)^3 - 1}{\left(\frac{P_i}{P_o}\right)^2 - 1} \right\} \quad (3.38.)$$

Everett⁽¹⁾ suggested that the gas compressibility be represented as:

$$J_n^m = \frac{n}{m} \left\{ \frac{\left[\left(\frac{P_i}{P_o}\right)^m - 1\right]}{\left[\left(\frac{P_i}{P_o}\right)^n - 1\right]} \right\} \quad (3.39.)$$

The retention volume which is corrected for gas compressibility is the product of V_R'/J_n^m and is represented by V_R^o and is known as the corrected retention volume.

Similarly, the fully corrected dead volume is represented by V_D and is the product of V_D'/J_n^m .

Equation (3.22.) can be rewritten as:

$$V_R^o = V_D \left(1 + K_R \frac{V_L}{V_G} \right) \quad (3.40.)$$

after taking into account the gas compressibility correction. Also

$$V_D = V_G \quad (3.41.)$$

Therefore equation (3.40.) can be rewritten as :

$$V_R^o = V_D + K_R V_L \quad (3.42.)$$

The product $K_R V_L$ is the net retention volume V_N , which is defined as the total volume less the mobile phase volume.

$$V_N = V_R^o - V_D \quad (3.43.)$$

$$V_N = J_n^m \dot{V}_R - J_n^m \dot{V}_D \quad (3.44.)$$

$$= K_R V_L \quad (3.45.)$$

From equation (3.24.) and (3.25.)

$$V_N = U_o J_n^m (t_r - t_D) \quad (3.46.)$$

The solute partial pressure over its infinitely dilute solution in the liquid phase ie. the region for which Henry's law is valid is

$$P_1 = \gamma_{13}^{\infty} x_1^L P_1^* \quad (3.47.)$$

γ_{13}^{∞} is the solute activity coefficient at infinite dilution, P_1 is the solute partial pressure, P_1^* is the saturated vapour pressure of the solute, x_1^L is the solute mole fraction in the liquid phase, also, $x_1^L \approx n_1^L / n_L$ where n_1^L is the number of moles of solute in the liquid phase and n_L is the total number of moles of the liquid phase.

Dividing both sides of equation (3.47.) by V_L and rearranging

$$\frac{n_1^L}{V_L} = \frac{P_1 n_L}{\gamma_{13}^{\infty} P_1^{\circ} V_L} \quad (3.48.)$$

For an ideal gas

$$\frac{n_1^G}{V_G} = \frac{P_1}{RT} \quad (3.49.)$$

n_1^G is the number of moles of gas

V_G is the volume occupied by the gas

P_1 is the pressure exerted by the gas

$$K_R = \frac{n_1^L V_G}{n_1^G V_L} \quad (3.50.)$$

$$K_R = \frac{P_1 n_3 V_G}{n_1^G \gamma_{13}^\infty P_1^* V_L} \quad (3.51.)$$

Using equation (3.49.)

$$K_R = \frac{P_1 n_3 RT}{P_1 \gamma_{13}^\infty P_1^* V_L} \quad (3.52.)$$

$$= \frac{n_3 RT}{\gamma_{13}^\infty \bar{V}_L P_1^*} \quad (3.53.)$$

Since,

$$\bar{V}_L = \frac{V_L}{n_3} \quad (3.54.)$$

\bar{V}_L is the molar volume of the liquid phase.

Also from equation (3.53.)

$$n_3 = \frac{\text{mass of stationary phase } W_L}{\text{molar mass of stationary phase } M_L} \quad (3.55.)$$

Multiplying equation (3.53.) by V_L

$$K_R V_L = \frac{RT n_3}{\gamma_{13}^\infty P_1^*} \quad (3.56.)$$

But from equation (3.45.)

$$K_R V_L = V_N \quad (3.57.)$$

Therefore

$$V_N = \frac{RTn_3}{\gamma_{13}^\infty P_1^*} \quad (3.58.)$$

Equation (3.58.) represents the net retention volume without taking into account gas imperfections, solvent volatility and non-equilibrium processes or solute adsorption.

3.2.2. Theoretical Plate Concept and the Activity Coefficient at Infinite Dilution

In glc an injected solute (1) is allowed to partition between a carrier gas (2) and a liquid solvent (3). The solvent is supported on an inert material.

Let y and z be the fractions of solute in the liquid and gas phases respectively.

Consider a single plate. Let the volumes of liquid and gas phases be $V_{(l)}$ and $V_{(g)}$ respectively. This is any part of the glc column. At the very first plate of the column, the moment the solute is injected it immediately vaporizes. All the solute is in the gas phase of the plate. A moment later, the solute partitions itself between the gas and liquid phases.

At equilibrium⁽²³⁾, for each plate the partitioning of the solute between the gas and liquid phases satisfies the relation

$$k = \frac{y}{z} \quad (3.59.)$$

In general if r volumes of carrier gas have passed through the column and the number of any plate is designated N , the quantity of solute in the $(N+1)^{\text{th}}$ plate can be shown to be:

$$Q_{N+1} = \frac{r!y^{(r-N)}z^N}{N!(r-N)!} \quad (3.60.)$$

where Q is the quantity of material at equilibrium.

Assuming that the $(N+1)^{\text{th}}$ plate is the detector point then the amount of solute at equilibrium, Q_{N+1} , is greater than the amount of solute when $(r-1)$ volumes or $(r+1)$ volumes of carrier has entered the column.

ie.

$$\frac{r!y^{(r-N)}z^N}{N!(r-N)!} > \frac{(r+1)!y^{(r-N+1)}z^N}{N!(r-N+1)!} \quad (3.61.)$$

$$1 > \frac{r+1}{r-N+1}y \quad (3.62.)$$

$$r-N+1 > (r+1)(1-z) \quad (3.63.)$$

$$N < rz+z \quad (3.64.)$$

Also

$$\frac{r!}{N!(r-N)!}y^{r-N}z^N > \frac{(r-1)!y^{r-N-1}z^N}{N!(r-N-1)!} \quad (3.65.)$$

$$\frac{ry}{(r-N)} > 1 \quad (3.66.)$$

$$r(1-z) > r-N \quad (3.67.)$$

$$N > rz \quad (3.69.)$$

From equations (3.64.) and (3.68.) and for a large number of N and r

$$N = rz \quad (3.69.)$$

The fraction of solute in the gas phase in any plate is given by where V_G and V_L have been previously defined and ΔV_G and ΔV_L represent a change in V_G and V_L .

$$z = \frac{C_G \Delta V_G}{C_G \Delta V_G + C_L \Delta V_L} \quad (3.70.)$$

where C_G is the solute concentration in the gas and C_L is the solute concentration in the liquid.

The solute partition coefficient K' is given by the expression

$$K' = \frac{C_L}{C_G} \quad (3.71.)$$

$$\Rightarrow z = \frac{\Delta V_G}{\Delta V_G + K' \Delta V_L} \quad (3.72)$$

Also,

$$K' = \frac{\text{moles of solute per unit volume in liquid}}{\text{moles of solute per unit volume in gas}} \quad (3.73)$$

The maximum of the elution curve is found at the $(N + 1)^{\text{th}}$ plate, where $N = rz$.
Therefore the total number of plates in the column is N .

And

$$\frac{N}{r} = \frac{\Delta V_G}{\Delta V_G + \Delta V_L K'} \quad (3.74)$$

Also

$$N \Delta V_G + N \Delta V_L K' = r \Delta V_G \quad (3.75)$$

where

$$N \Delta V_G = V_{\text{deadspace}} \quad (3.76.)$$

$$K' \Delta V_L = V_{\text{liquid}} \quad (3.77.)$$

$$r\Delta V_G = V_{retention} \quad (3.78.)$$

$$V_{retention} = V_{deadspace} + K'V_{liquid} \quad (3.79.)$$

Using the corrected Raoult's Law (which can be considered as Henry's Law at infinite dilution)

$$\gamma_{13}^{\infty} x_{13} = \frac{P_1}{P_1^*} \quad (3.80.)$$

where

x_{13} is the mole fraction of solute in the liquid phase.

P_1^* is pure solute vapour pressure at some temperature T

P_1 is the solute partial pressure at the same temperature T

Also,

$$x_{13} = \frac{\text{moles of solute / volume of solvent}}{\text{moles of solvent / volume of solvent}} \quad (3.81.)$$

But moles of solute is \ll moles of solvent.

$$\therefore x_{13} = \frac{C_{13}}{(m_3/M_3)/V_3} \quad (3.82.)$$

Now from Raoult's corrected law

$$\frac{\gamma_{13}^{\infty} C_{13} M_3 V_3}{m_3} = \frac{P_1}{P_1^*} \quad (3.83.)$$

And

$$C_{13} = \frac{P_1 m_3}{P_1^* M_3 \gamma_{13}^\infty V_3} \quad (3.84.)$$

Also,

$$C_{12} = \frac{n_{12}}{V_1} = \frac{P_1}{RT} \quad (3.85.)$$

Now ,

$$K' = \frac{C_{13}}{C_{12}} = \frac{RTm_3}{P_1^* M_3 \gamma_{13}^\infty V_3} \quad (3.86.)$$

And substituting equation (3.86.) into equation (3.79.) results in equation (3.87.)

$$V_{retention} - V_{deadspace} = \frac{RTn_3}{P_1^* \gamma_{13}^\infty} \quad (3.87.)$$

This is the basic equation and is used when there are no gas phase corrections or when non-ideality effects are absent and is identical to equation 3.58.

3.2.3. Fugacity Effects

At constant temperature the fugacity f_i and absolute activity a_i of the components of a binary gaseous mixture⁽²⁴⁾ is represented by

$$\frac{f_i}{a_i} = \text{constant} \quad (3.88.)$$

$$\frac{f_i}{x_i P_i} \rightarrow 1 \text{ as } P_i \rightarrow 0 \quad (3.89.)$$

In terms of solute 1 and carrier 2

$$f_i = x_1 P_{12} \exp[(B_{11} + 2x_2^2 \delta_{12})] \frac{P_{12}}{RT} \quad (3.90.)$$

$$\delta_{12} = B_{12} - \frac{1}{2}(B_{11} + B_{22}) \quad (3.91.)$$

P_{12} is the partial pressure of solute in the carrier gas, B_{11} and B_{22} are the solute - solute and carrier - carrier fugacity coefficients and B_{12} is the solute - carrier mixed second - interaction virial coefficient.

As $x_2 \rightarrow 0$, equation (3.90.) can be rewritten as:

$$f_i^o = P_1^* e^{\left(\frac{B_{11} P_1^*}{RT}\right)} \quad (3.92.)$$

f_1^o is the solute saturation fugacity. The activity coefficient at infinite dilution is given by

$$\gamma_{13}^\infty = \frac{RTn_3}{V_N P_1^*} \quad (3.93.)$$

In terms of fugacity

$$\gamma_1^\infty = \frac{RTn_3}{V_N f_1^o} \quad (3.94.)$$

Equations (3.93.) and (3.94.) are related through equation (3.92.) by

$$\ln \gamma_1^\infty = \ln \gamma_{13}^\infty - B_{11} \frac{P_1^*}{RT} \quad (3.95.)$$

Guggenheim⁽²⁵⁾ showed that the solute chemical potential on being diluted by the carrier gas be included in equation (3.95.) to give

$$\ln \gamma_1^\infty = \ln_{13}^\infty - \frac{P_1^*(B_{11} - V_1^*)}{RT} \quad (3.96.)$$

V_1^* is the solute bulk molar volume. This equation includes correction for solute-solute gas phase interactions.

3.2.4. Mixed Virial Coefficients

Different carrier gases alter elution times and in some cases can produce reversals in relative retention behaviour⁽²⁶⁾. Gas-phase solute-carrier (mixed) second virial interactions^(27,28) should be taken into account because **gas solubility in the stationary is significant at low column pressures**^(29,30).

The rate of travel dl/dt of solute molecules through an infinitely thin cross section of a column is represented by

$$\frac{dl}{dt} = uv_m \left(\frac{1}{v_m + K_R V_L} \right) \quad (3.97.)$$

where V_M and V_L are the mobile and stationary phase volumes respectively within the column segment and u is the linear carrier velocity.

Since,

$$uv_m = f \quad (3.98.)$$

Where f is the cross sectional volume flowrate

$$f dt = (V_M + K_R V_L) dl \quad (3.99.)$$

The mobile phase flowrate varies along the column as the inverse of the pressure and is denoted by

$$f = \frac{RT + B_{22}p}{p} \quad (3.100.)$$

Also, at the column outlet

$$f_o = \frac{RT + B_{22}P_o}{P_o} \quad (3.101.)$$

Combining equations (3.100.) and (3.101.) and substituting the result into equation (3.99.)

$$f_o dt = \frac{P(K_R V_L + V_M)(1 + bP_o)}{P_o(1 + bP)} dl \quad (3.102.)$$

where $b = B_{22}/RT$

The term

$$V_M \left[\frac{p(1 + bp_o)}{p_o(1 + bp)} \right] dl \quad (3.103.)$$

is the dead volume in the segment corrected to conditions at the outlet so that equation (3.102.) can be rewritten as :

$$f_o dt - V_M \left[\frac{p(1 + bp_o)}{p_o(1 + bp)} \right] dl = dV_N = K_R V_L \left[\frac{p(1 + bp_o)}{p_o(1 + bp)} \right] dl \quad (3.104.)$$

From Darcy's Law

$$\frac{\partial P}{\partial l} = -\frac{\epsilon \mu \eta}{K} \quad (3.105.)$$

For $P < 50$ atmospheres at $P_i - P_o < 5$ atmospheres

and

$$\eta = \eta^o (1 + ap) \quad (3.106.)$$

where

$$a = 0,175 B_{22} / RT \quad (3.107.)$$

Substituting into equation (3.105.)

$$dl = - \left[\frac{K/\varepsilon}{n^o(1+ap)} \right] \left[\frac{1+bp_o}{p_o u_o} \right] \left[\frac{p}{1+bp} \right] dp \quad (3.108.)$$

Dividing dl by the column length L yields:

$$\frac{dl}{L} = \frac{\int_{P_o}^{P_i} \frac{p dp}{(1+ap)(1+bp)}}{\int_{P_o}^{P_i} \frac{p dp}{(1+ap)(1+bp)}} \quad (3.109.)$$

Cruickshank and co-workers⁽²⁸⁾ combined Everett's earlier treatment⁽²⁷⁾ with Buckingham⁽³¹⁾ to relate the solute partition coefficient to that at zero pressure drop:

$$\ln K_R = \ln K_R^o + \beta \bar{p} + \zeta \bar{p}^2 + \dots \quad (3.110.)$$

K_R^o is given by :

$$\ln K_R^o = \ln \frac{RT}{\bar{V}_L P_1^* \gamma_{13}^\infty} - \frac{P_1^*(B_{11} - V_1^o)}{RT} - \left(\frac{P_1^*}{RT} \right)^2 (B_{11}^2 - C_{111}) + \dots \quad (3.111.)$$

Where,

$$\beta' = \frac{2B_{12} - V_1^\infty}{RT} + \lambda \left[1 - \left(\frac{\partial \ln \gamma_{13}^\infty}{\partial x_2} \right)_o \right] \quad (3.112.)$$

$$\zeta' = \frac{3C_{122} - 4B_{12}B_{22}}{2(RT)^2} + \phi \left[1 - \left(\frac{\partial \ln \gamma_{13}^\infty}{\partial x_2} \right)_o \right] + \frac{\lambda^2}{2} \left[1 - \left(\frac{\partial^2 \ln \gamma_{13}^\infty}{\partial x_2^2} \right)_o \right] + \frac{K'V_1^\infty}{RT} \quad (3.113.)$$

C_{111} and C_{122} are the third virial coefficients that take into account trimolecular interactions, λ and ϕ are the carrier molal solubility in the stationary phase and the last term takes into account the effect of the pressure and composition on V_1^∞ .

Combining equations (3.102.) and (3.103.) with equation (3.111.) yields

$$V_N = \frac{K_R^o V_L \frac{[1 + bP_o + cP_o + \dots]}{P_o} \int_{P_o}^{P_i} \frac{(P^2 \exp(b' + \delta'P^2 + \dots))}{(1 + aP)(1 + bP + cP^2 + \dots)} dp}{\int_{P_o}^{P_i} \frac{P}{(1 + aP)(1 + bP + cP^2 + \dots)} dP} \quad (3.114.)$$

This equation expresses the dependence of V_N (and K_R) on pressure as a function of K_R^o , b , β' and ζ' .

In this work the basic equation used to test the glc technique and also used as a starting point for further refinements was equation 1.1.

$$\ln \gamma_{13}^\infty = \ln \frac{n_3 RT}{V_N P_1^*} - \left[\frac{(B_{11} - V_1^*)}{RT} \right] P_1^* + \left[\frac{(2B_{12} - V_1^\infty)}{RT} \right] P_o J_3^2 \quad (1.1.)$$

The following equation was used for the alkanol-hexadecane work

$$\ln V'_N = \ln \left[\frac{RT}{\gamma_{13}^\infty P_1^*} \right] - \left[\frac{(B_{11} - V_1^*)}{RT} \right] P_1^* + \left[\frac{(2B_{12})P_o}{RT} \right] \quad (1.2.)$$

Equations such as 3.58. could not be used since for polar solutes adsorption occurs on the the solid packing. The net retention volume has to be corrected to zero sample size, zero mean column flowrate, and to infinite solvent coverage.

Since equation 3.58. is valid for only nonvolatile solvents, equation 1.3. was used for the hydrocarbon-decane work

$$\frac{V_N}{n_3 e^C} = \frac{RT}{\gamma_{13}^\infty P_1^*} - \frac{U_o t}{n_3} \left[\frac{P_3'}{\gamma_{13}^\infty P_1^*} \right] \quad (1.3.)$$

3.3. Determination of the Partial Molar Excess Enthalpy at Infinite Dilution, $H_1^{E\infty}$

3.3.1. $H_1^{E\infty}$ from γ_{13}^∞ Values

The activity coefficient at infinite dilution, γ_{13}^∞ , based on the pure component standard state is related to the partial molar excess free energy by

$$\ln \gamma_{13}^\infty = \frac{G_1^{E\infty}}{RT} \quad (3.115.)$$

Applying the Gibbs-Helmholtz equation directly to equation 3.115.

$$\left(\frac{\partial \ln \gamma_{13}^\infty}{\partial T} \right)_P = \left[\frac{\partial G_1^{E\infty}}{\partial T} \right]_P = -\frac{H_1^{E\infty}}{RT^2} \quad (3.116.)$$

Integrating from some reference temperature, T_1

$$\ln \gamma_{13(T_1)}^\infty - \ln \gamma_{13(T_2)}^\infty = \int_{T_2}^{T_1} \frac{H_1^{E\infty}}{R} d\left(\frac{1}{T}\right) \quad (3.117.)$$

Hence,

$$\ln \gamma_{13(T_1)}^\infty - \ln \gamma_{13(T_2)}^\infty = \frac{H_1^{E\infty}}{R} \left(\frac{1}{T_1} - \frac{1}{T_2} \right) \quad (3.118.)$$

Equation 3.118. was used to calculate the partial molar excess enthalpy at infinite dilution for the hydrocarbon-decane system.

3.3.2. The Tangent to Intercept Method (Roosenboom's method)⁽³²⁾ for the Determination of Partial Molar Quantities

The molar excess enthalpy of a solution is given by

$$H_m^E = \frac{H^E}{n_1 + n_2} \quad (3.119.)$$

Then the excess partial molar enthalpy of a solute 1 in a solvent 2 is given by

$$H_1^E = \left(\frac{\partial H^E}{\partial n_1} \right)_{n_2} = H_m^E + (n_1 + n_2) \left(\frac{\partial H_m^E}{\partial n_1} \right)_{n_2} \quad (3.120.)$$

where

$$n = n_1 + n_2 \quad (3.121.)$$

Now the derivative with respect to mole number of 1, n_1 , is transformed into a derivative with respect to mole fraction 2, x_2 ,

where

$$x_2 = \frac{n_2}{(n_1 + n_2)} \quad (3.122.)$$

$$\left(\frac{\partial H_m^E}{\partial n_1} \right)_{n_2} = \frac{\partial H_m^E}{\partial x_2} \left(\frac{\partial x_2}{\partial n_1} \right)_{n_2} \quad (3.123.)$$

and

$$\left(\frac{\partial x_2}{\partial n_1} \right)_{n_2} = - \frac{n_2}{(n_1 + n_2)^2} \quad (3.124.)$$

Now

$$\frac{\partial x_2}{\partial n_1} = \frac{\frac{\partial(n_2)}{(n_1+n_2)}}{\frac{\partial(n_1+n_2)}{\partial n_1}} \quad (3.125.)$$

$$\frac{\partial x_2}{\partial n_1} = -\left(\frac{n_2}{n^2}\right) \quad (3.126.)$$

Thus equation 3.120. becomes

$$H_1^E = H_m^E - \frac{n_2}{n_1+n_2} \frac{\partial H_m^E}{\partial x_2} \quad (3.127.)$$

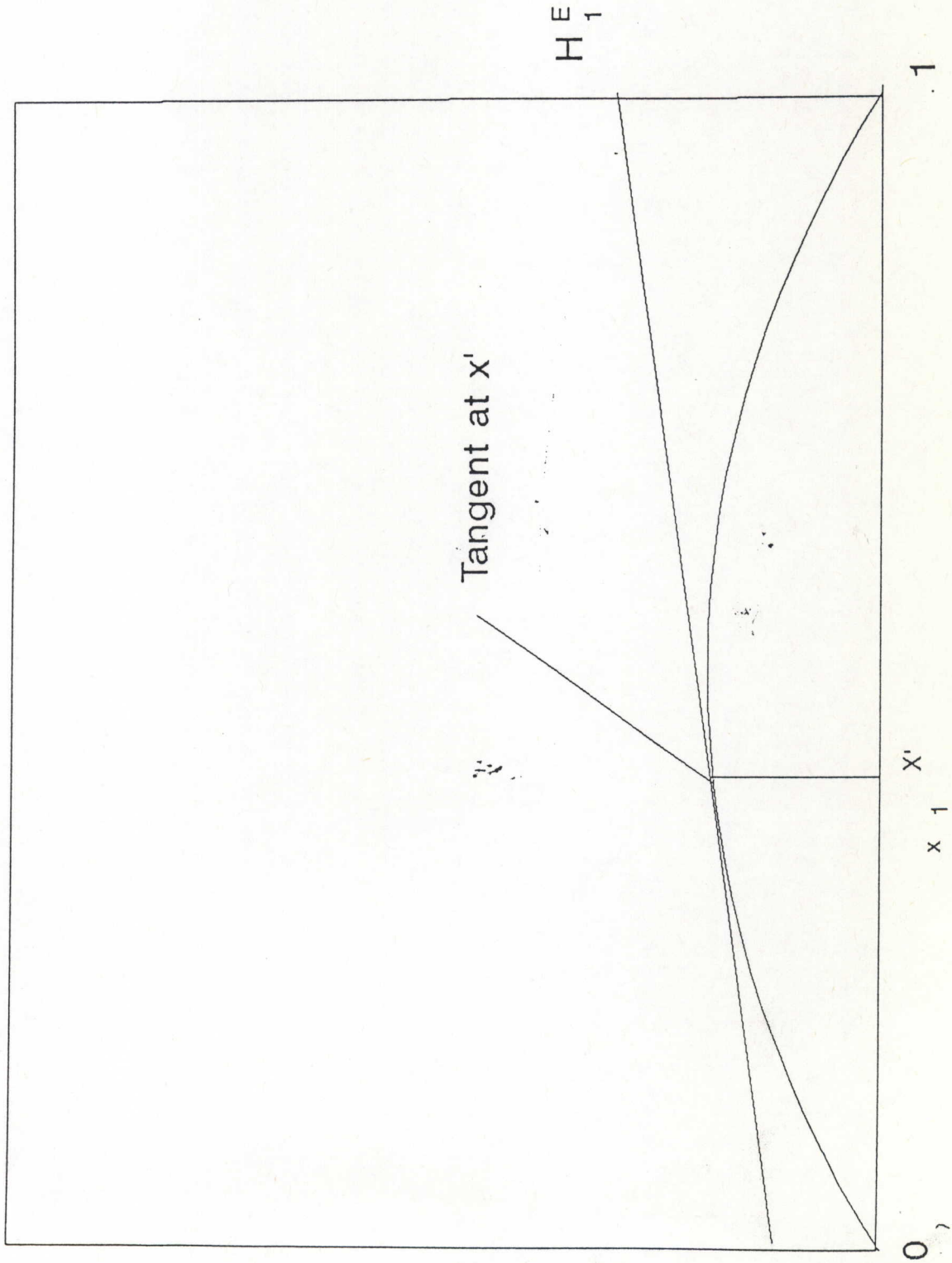
$$H_1^E = H_m^E - x_2 \frac{\partial H_m^E}{\partial x_2} \quad (3.128.)$$

The application of this equation is illustrated in figure 3.1. where H^E is plotted against mole fraction. By drawing a tangent to the curve, the intercepts at $x_2 = 0$ and $x_2 = 1$ gives the value for the partial molar enthalpies of both components at the specified mixture composition.

To determine the partial molar enthalpies at infinite dilution a tangent has to be drawn at $x_1 = 0$ and extrapolated to $x_1 = 1$ axis. The intercept at $x_1 = 1$ is $H_1^{E\infty}$. For best results values as close to $x_1 = 0$ should be taken, otherwise the tangent method would produce large errors in $H_1^{E\infty}$.

This equation was used to calculate the partial molar excess enthalpies at infinite dilution for the hydrocarbon-decane systems (pp. 137) together with data obtained from the literature.

FIG. 3.1.
Determination of Partial Molar enthalpies from the Tangent to Intercept
Method



3.4. Treatment of a Polar Solute

The equation developed by Everett⁽²⁾ and Cruickshank⁽³⁾

$$\ln \gamma_{13}^{\infty} = \ln \frac{n_3 RT}{V_N P_1^*} - \left[\frac{(B_{11} - V_1^*)}{RT} \right] P_1^* + \left[\frac{(2B_{12} - V_1^{\infty})}{RT} \right] P_o J_3^2 \quad (1.1.)$$

can only be used when adsorption effects are absent and for solvents that are involatile.

Polar solutes have retention times that are dependent on sample size, and net retention volumes that are dependent on mean column flowrate and percentage column loading. Solute retention times, t_r^* , must be extrapolated to zero solute size, t_r , and the net retention volume, V_N , extrapolated to zero mean column pressure, $U_o J_3^2 (= \bar{u})$ and to infinite solvent coverage, W_s .

The equation relating V_N to t_r , the retention time at infinitely dilute sample size, is

$$V_N = (t_r - t_g) U_o J_3^2 \quad (3.129.)$$

It is assumed that t_g is constant for the range of solute size and any variation of t_g is within the experimental error on V_N .

For polar solutes equation 1.1. is extended to include the dependence of net retention volume on mean column flowrate, $U_o J_3^2 (= \bar{u})$ and infinite solvent coverage.

$$\ln V_N' = \ln \left[\frac{RT}{\gamma_{13}^{\infty} P_1^*} \right] - \left[\frac{(B_{11} - V_1^*)}{RT} \right] P_1^* + \left[\frac{(2B_{12}) P_o}{RT} \right] \quad (3.130.)$$

where

$$V'_N = V_N^o + \phi U_o J_3^2 \quad (3.131.)$$

V_N^o is the net retention volume corrected to zero mean flowrate per mole of solvent i.e. the molal net retention volume, V'_N is the molal retention volume extrapolated to infinite solvent coverage and ϕ is a function of net retention volume at infinite dilution V_N and mean column flowrate $U_o J_3^2$. Since V_N^o is small in magnitude and J_3^2 approaches one at the limit of zero flowrate (Le Hospital's rule) these variables were excluded from equation 3.130.

Cruickshank *et al*⁽³⁾ found that V_N remained a linear function of $U_o J_3^2$ therefore by plotting $U_o J_3^2$ against V_N , V_N^* is obtained from the intercept. $V_N^o (=V_N^*/n_3)$ is then plotted against W_s to obtain V'_N . The value of γ_{13}^∞ is then obtained from this relationship.

3.5. Treatment of a Volatile Solvent

The equation devised by Everett⁽²⁾ and Cruickshank⁽³⁾

$$\ln \gamma_{13}^\infty = \ln \frac{n_3 RT}{V_N P_1^*} - \left[\frac{(B_{11} - V_1^*)}{RT} \right] P_1^* + \left[\frac{(2B_{12} - V_1^\infty)}{RT} \right] P_o J_3^2 \quad (1.1.)$$

relates the net retention volume to the total number of moles of solvent on the column. The equation developed by Letcher⁽⁴⁾ relates the net retention volume to the loss of solvent due to evaporation from the column. During its passage through the column the carrier gas becomes charged with solvent vapour. The total amount of solvent lost from the column, n'_3 , may be expressed in terms of the total volume of gas which has passed through the column, the partial pressure, P'_3 , of the solvent in the gas at the column outlet and the time, t , elapsed from the start of the carrier gas passing through the column. The observed retention times are assumed to be negligible compared to

the total flow time through the column. The gas flowrate, U_o , measured at the outlet is maintained constant throughout the whole experiment. The expression for n_3' is given by

$$n_3' = \frac{U_o t P_3'}{RT} \quad (3.132.)$$

In this work the partial pressure of the solvent in the carrier was less than 1 percent of the total. It is probably reduced further in the flowmeter. Therefore no correction was

applied to the flowrate for the presence of the solvent.

Equation 1.1. becomes

$$\frac{V_N}{n_3 e^C} = \frac{RT}{\gamma_{13}^\infty P_1^*} - \frac{U_o t}{n_3} \left[\frac{P_3'}{\gamma_{13}^\infty P_1^*} \right] \quad (3.133.)$$

where

$$C = - \left[\frac{B_{11} - V_1^*}{RT} \right] P_1^* + \left[\frac{2B_{12} - V_1^\infty}{RT} \right] P_o J_2^3 \quad (3.134.)$$

hence

$$\frac{V_N}{n_3 e^C} = \frac{RT}{\gamma_{13}^\infty P_1^*} - \frac{U_o t}{n_3} \left[\frac{P_3'}{\gamma_{13}^\infty P_1^*} \right] = a - b \left[\frac{U_o t}{n_3} \right] \quad (3.135.)$$

By plotting $V_N/n_3 e^C$ against $U_o t/n_3$ a straight line is obtained, giving an intercept of $RT/\gamma_{13}^\infty P_1^*$ ($= a$) and a slope P_3'/RT ($= b$).

The values of γ_{13}^∞ and P_3' are obtained from this linear relationship.

4. APPARATUS AND EXPERIMENTAL PROCEDURE

4.1. INTRODUCTION

The following equations were used to calculate the net retention volumes.

(a) For the work related to the alkanol - hexadecane systems :

$$\ln V'_N = \ln \left[\frac{RT}{\gamma_{13}^\infty P_1^*} \right] - \left[\frac{(B_{11} - V_1^*)}{RT} \right] P_1^* + \left[\frac{(2B_{12})P_o}{RT} \right] \quad (4.1.)$$

where

$$V'_N = V_N^o + \phi U_o J_3^2 \quad (4.2.)$$

(b) For the work related to the hydrocarbon - decane systems :

$$\frac{V_N}{n_3 e^c} = \frac{RT}{\gamma_{13}^\infty P_1^*} - \frac{U_o t}{n_3} \left[\frac{P_3'}{\gamma_{13}^\infty P_1^*} \right] = a - b \left[\frac{U_o t}{n_3} \right] \quad (4.3.)$$

where

$$V_N = (t_r - t_g) U_o J_3^2 \quad (4.4.)$$

and

$$U_c = U_o \left(\frac{T^c}{T_{fm}} \right) \left(\frac{P_{fm} - P_w}{P_{fm}} \right) \quad (4.5.)$$

The retention time, t_r , gas hold-up time, t_g , column flowmeter temperature, T_{fm} , temperature of the waterbath, T^c , measured flowrate, U_o , corrected flowrate, U_c , flowmeter pressure, P_{fm} , and water vapour pressure, P_w had to be accurately measured. The details of the experimental procedures have been reported in the literature⁽³³⁾. In this work the procedure used by Cruickshank⁽²⁾ and Moollan⁽³⁴⁾ have been followed.

The peaks obtained for the alkanol - hexadecane systems were not symmetrical with greater amount of tailing at a lower percentage loading. The reason being that at a lower liquid loading the solute molecules are adsorbed to a greater extent on the diatomaceous earth due to incomplete coverage of the solid support thus enhancing the non-ideality effect⁽²²⁾. Also, for a higher flowrate but at a lower loading peaks were more sharper. For the alkanols the retention time was obtained by recording the time taken from injection of the solute to the emergence of the peak maximum for peaks that were less than ideal and for peaks that were symmetrical the tangent method⁽²²⁾ was adopted. In this method the retention time is calculated from the distance measured on the chart from the point of injection to the point at which the tangent to the peak intersect. These are then converted to retention times using the chart speed which is accurately measured using a stopwatch (the tangent to peak method). For a moderately volatile solvent the retention time of the solute was obtained from the tangent method. The gas holdup time i.e. the time taken for an unretained sample of air to elute, was the time from injection of a gas sample to the emergence of the air peak. The flowrate was obtained by measuring the time taken for a soap film to travel through a 100 ml calibrated burette. Prior to measuring the flowrate a stream of bubbles were sent through the flowmeter to allow the interior of the walls of the burette to be thoroughly wetted by the soapy solution to avoid errors arising from uneven movement of the bubble film due to surface tension effects and the possibility that the burette was not fully saturated with water vapour.

The glc apparatus (figure 4.1) used consists of a temperature monitor for the accurate control of the waterbath, a packed column in a water bath, two soap bubble flowmeters to set the column outlet flowrate to the column inlet flowrate, a manometer

to measure the atmospheric pressure, a detector and a recorder for recording the signals.

4.1.1. Column Thermostat

(figure 4.2.)

Temperature control (± 0.01 K) was achieved by a Tronac temperature controller together with a light bulb heater. A calibrated Hewlett-Packard quartz thermometer was used to measure the water bath temperature. The waterbath size was approximately 300mm x 350mm x 700 mm. To prevent any temperature gradients the water bath was well stirred. The carrier gas was passed through a pre-heater / pre-cooler before entering the column to ensure that the gas entering the column was of the same temperature as the column. The temperatures used ranged from 278.15 K to 303.15 K. To obtain the temperature of 278.15 K it was necessary to cool the waterbath using a refrigerated coil.

4.1.2. Pressure Control and Measurement

The outlet pressure, P_o , was atmospheric pressure and it was measured on a Fortin barometer (± 0.01 mmHg) which was at the same level as the glc apparatus. The column inlet pressure, P_i , was measured by the use of a mercury manometer using a kathetometer. The column inlet pressure was controlled (± 0.1 mmHg) by three pressure regulators, one attached to the cylinder head, a Negretti and Zambra precision pressure regulating valve and a needle valve attached before the column inlet to the gas line. The precision of the inlet pressure was estimated to be ± 2 Pa.

4.1.3. Soap Bubble Flowmeters

(figure 4.3.)

The flow rate was controlled (± 0.1 s) by measuring the time taken for a soap bubble to travel up a 100 ml calibrated flowmeter of uniform diameter. The flowrates used for each set of measurements ranged over at least fivefold. The flowrates used over all experiments ranged between $2 \times 10^{-7} \text{ m}^3\text{s}^{-1}$ and $1 \times 10^{-5} \text{ m}^3\text{s}^{-1}$ for the alkanol-hexadecane systems. The precision was estimated to be $1 \times 10^{-8} \text{ m}^3\text{s}^{-1}$.

4.1.4. Injectors

(figure 4.4.)

Samples were injected with a Hamilton microsyringe through a silicon septum. Sample sizes varied from 0.1 mm^3 to 1.0 mm^3 . The septum was frequently replaced to prevent pressure leaks.

FIG.4.1. GAS CHROMATOGRAPH FOR PHYSICOCHEMICAL MEASUREMENT

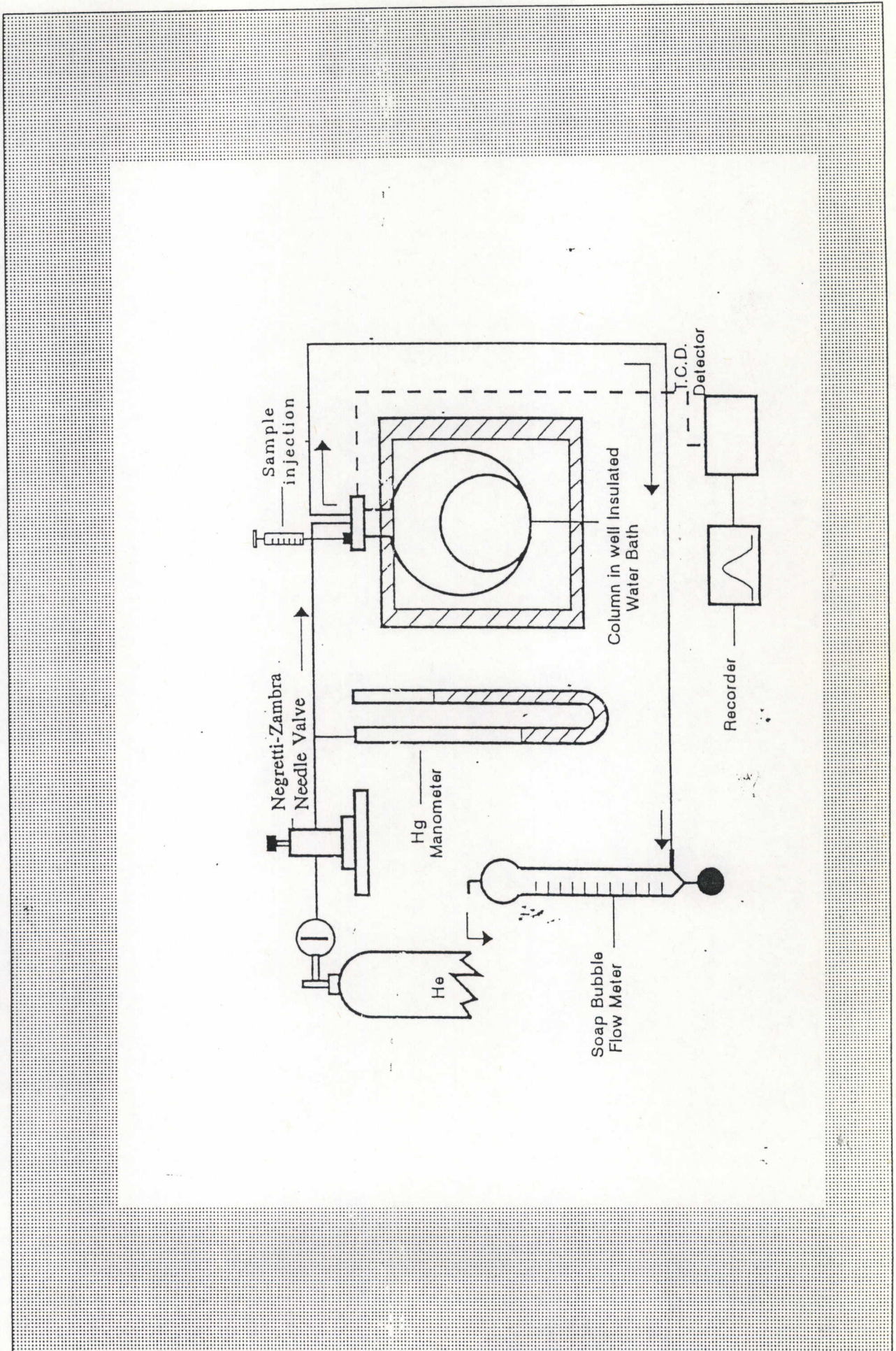


FIG.4.2. COOLING APPARATUS USED TO OBTAIN TEMPERATURE OF 278.15 K

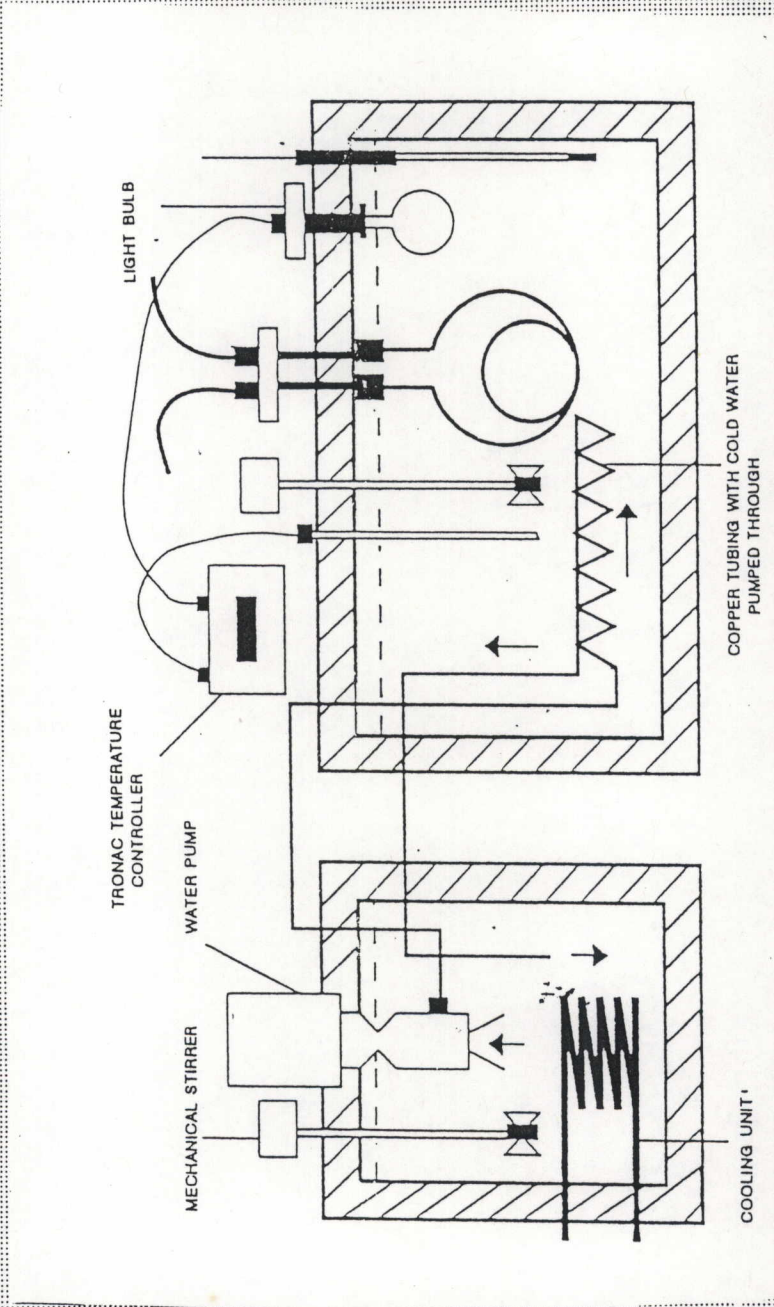


FIG.4.3 SOAP BUBBLE FLOWMETER

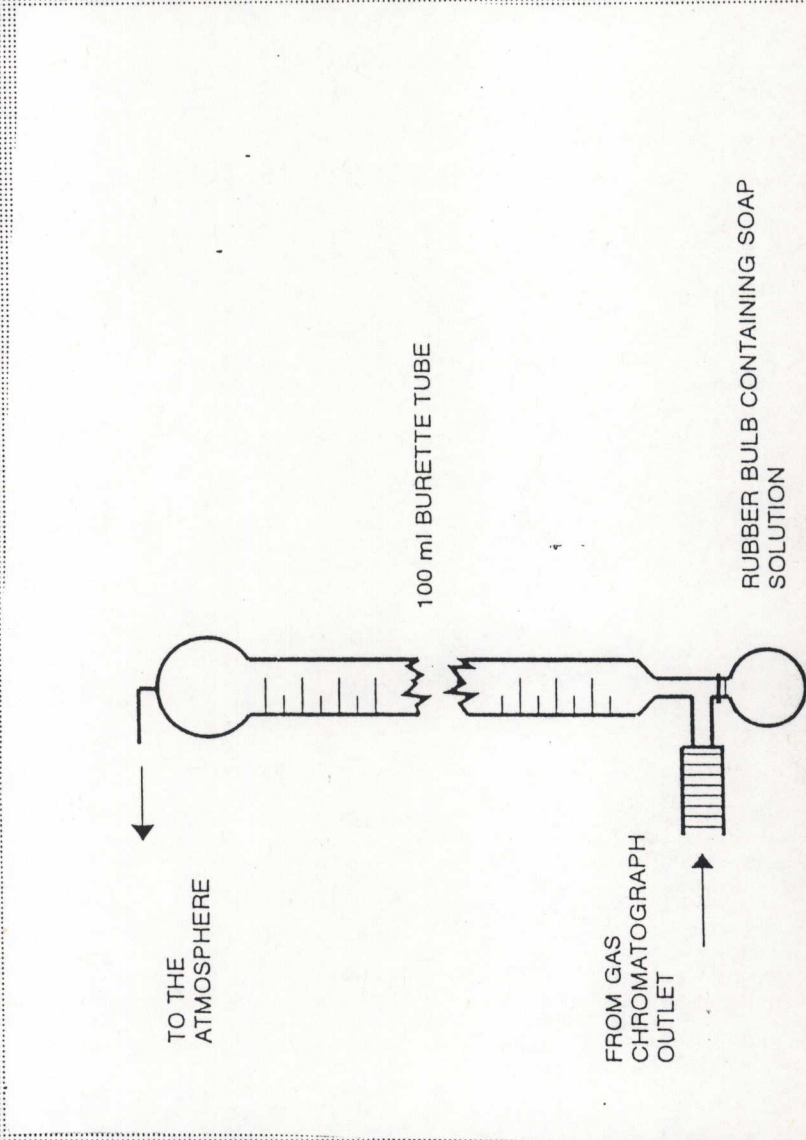
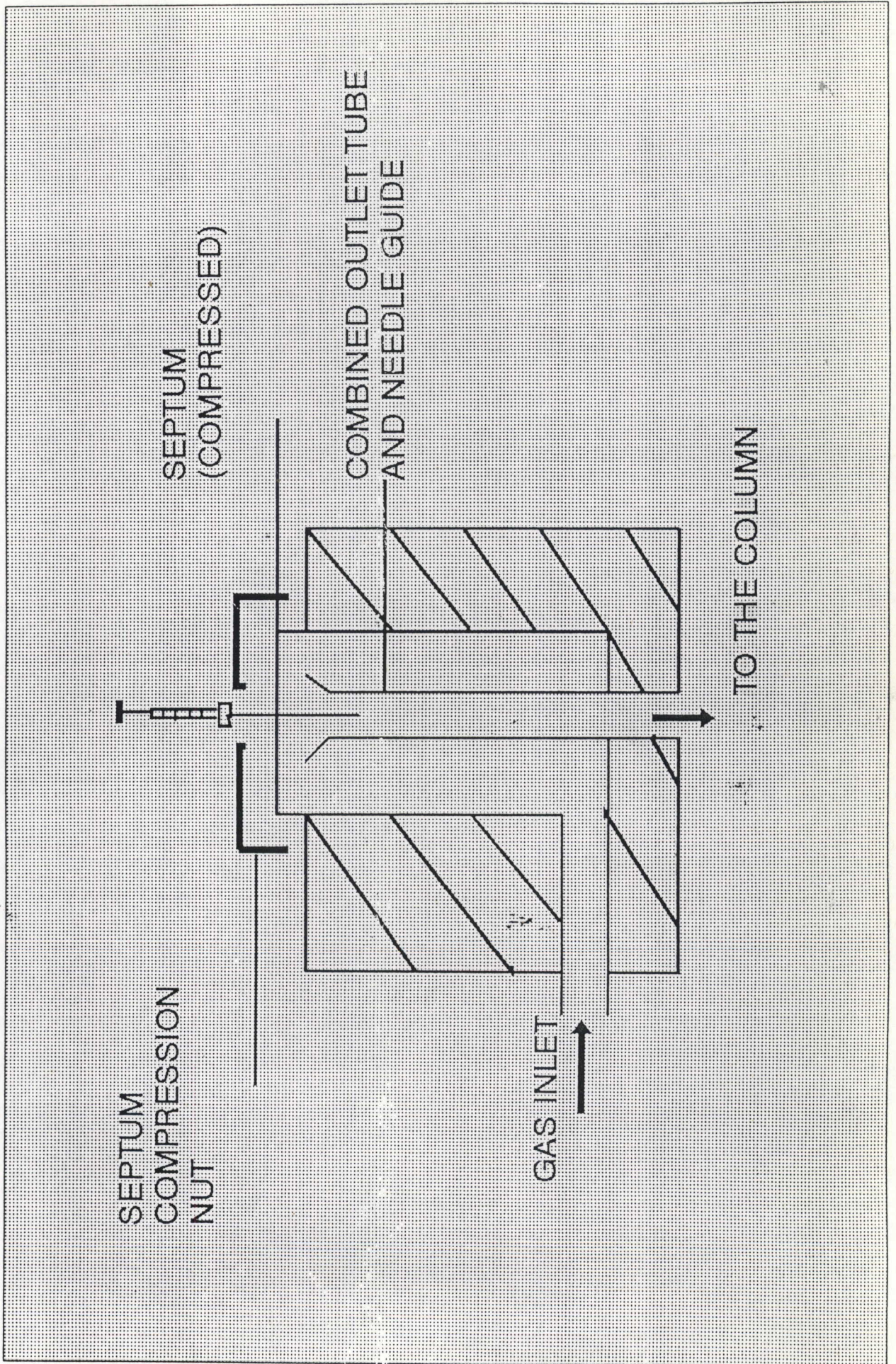


FIG. 4.4. THE INJECTION SYSTEM



4.1.5. Detectors

(figures 4.5. and 4.6.)

Two types of thermal conductivity detectors were used, a Gow-Mac gas chromatograph and a Shandon U.K.3 gas chromatograph.

The Gow-Mac detector used consists of four filaments. The geometrical configuration of each pair of filaments are identical. The filaments formed two arms of an electrical Wheatstone bridge circuit. A stream of pure gas is split equally into the two arms of the bridge. One half of the gas enters the column and the other half of the gas enters the reference filaments. The gas emerging from the column flows over the measuring filaments. The thermocouple detector are placed in a metallic block containing a cavity through which the gas flows. A heated element is positioned in the cavity and loses heat to the block depending upon the thermal conductivity of the gas. The heated elements are connected electrically to a Wheatstone bridge. With the same gas flowing through both cavities the network is balanced by the balancing potentiometers so that the electrical output is zero. When the thermal conductivity of the gas in one of the cavities changes (the sample cavity) the temperature and resistance of the detector element of that cavity changes and the imbalance between the reference and sample cavities is the recorded signal. The filaments are made of gold-plated Kovar with a rhenium tungsten filament.

The Shandon U.K.3 Detector consists of two matched, electrically heated, helically coiled, tungsten filaments. These are mounted in the brass detector body by means of mechanical seal tube-nuts. In this way the two filaments are inserted directly into the gas stream, one (reference) in the pure carrier gas before it enters the column, and the other (measuring) in the column outlet. The geometric configuration of each filament is identical. The filaments form two arms of a Wheatstone bridge. The bridge is balanced when the gas flowing through both the reference and measuring arms are the same. When a solute is injected the gas flowing through the reference and measuring arms are different and the bridge is unbalance giving rise to an electrical output.

The signals were recorded by a GC strip chart recorder.

FIG.4.5. CIRCUIT DIAGRAM OF SHANDON U.K.T.C.DETECTOR

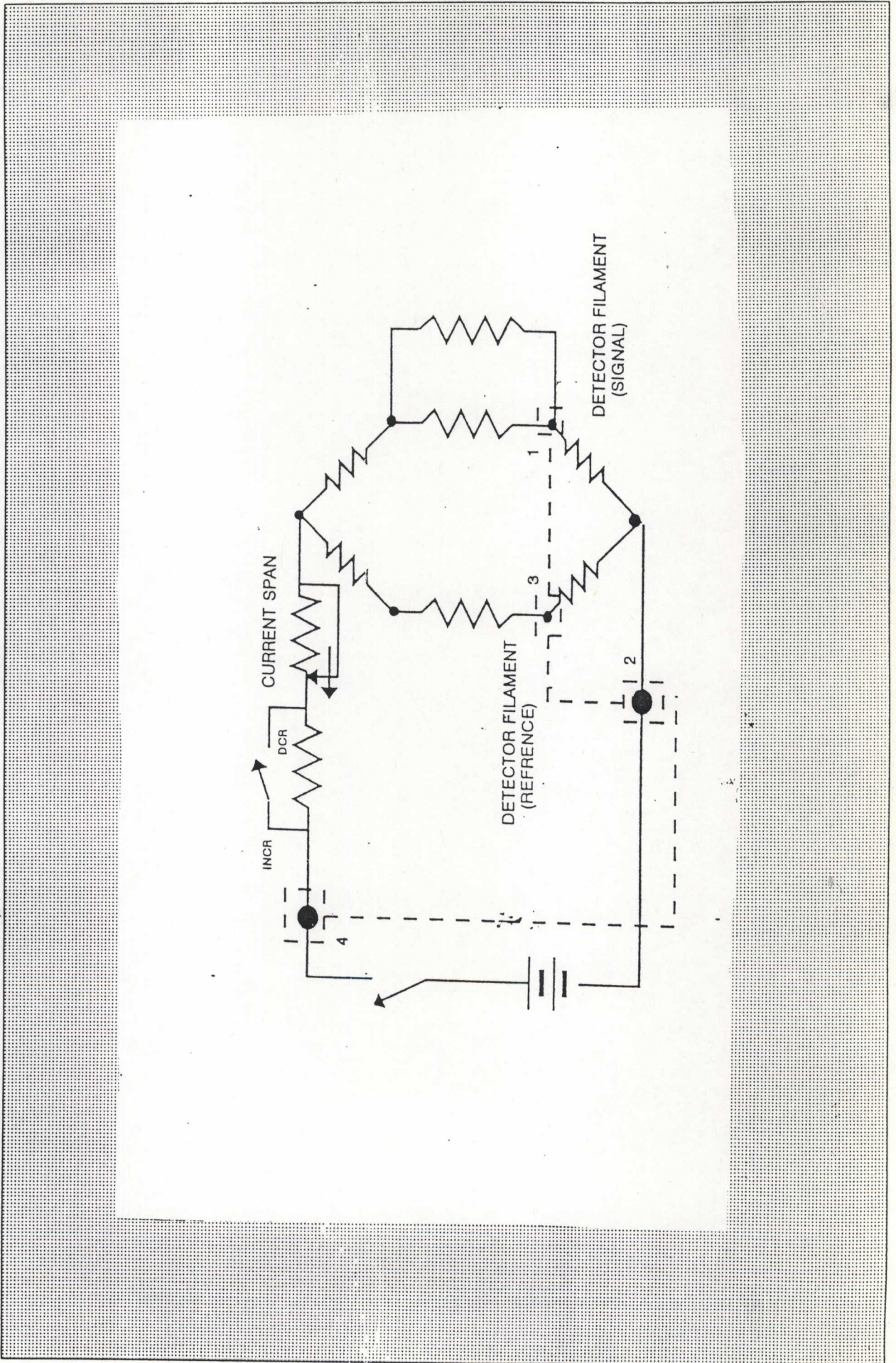
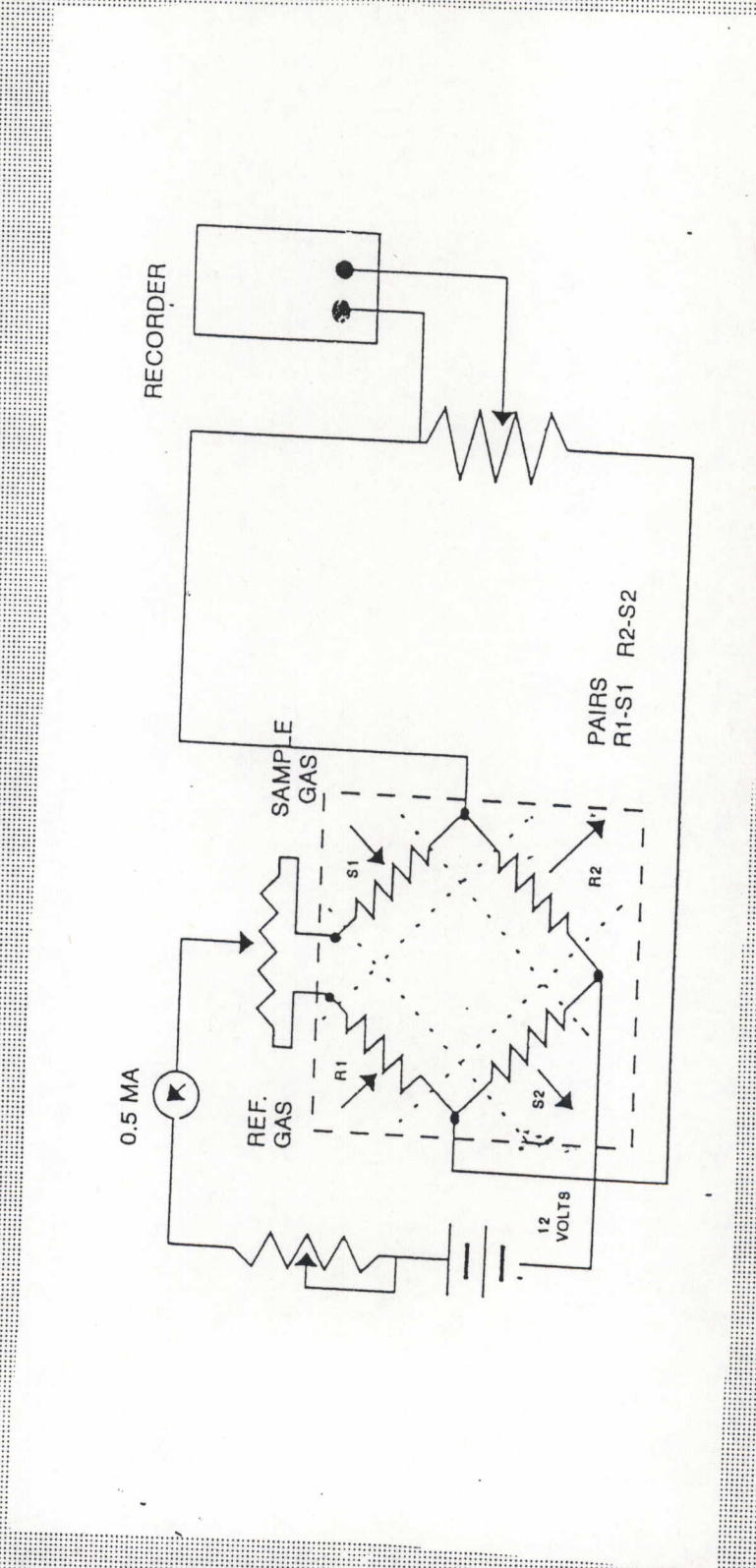


FIG. 4.6. CIRCUIT DIAGRAM OF GOW-MAC T.C.D. DETECTOR



4.2.1. Experimental Procedure for a Simple System used as a Test System for the GLC Technique

The equation used to calculate the activity coefficient at infinite dilution for a simple system such as hexane in hexadecane is given by equation 1.1.

$$\ln \gamma_{13}^{\infty} = \ln \frac{n_3 RT}{V_N P_1^*} - \left[\frac{(B_{11} - V_1^*)}{RT} \right] P_1^* + \left[\frac{(2B_{12} - V_1^{\infty})}{RT} \right] P_0 J_3^2 \quad (1.1.)$$

For a such a system the column is loaded with the solvent. The exact moles of solvent is recorded. The flowrate is set to obtain retention times of a few minutes. The solute is injected and gas hold-up time, flowrate, and atmospheric pressure are measured. The retention time is calculated from the distance measured on the chart from the point of injection to the point at which the tangents to the peak intersect. These are then converted to retention times using the chart speed which is accurately measured using a stopwatch (the tangent to peak method). These measured parameters together with the constants obtained from literature are used to calculate γ_{13}^{∞} .

4.2.2. Experimental and Measurement Procedure for Polar Solutes

4.2.2.1. Experimental Procedure

Stainless steel and copper columns of 6.35 mm in diameter and length between 1 - 1.5 m were used. Each column was thoroughly washed with hot soapy water, rinsed with acetone and air dried. The support used was Chromosorb W/HP 80 - 100 mesh. The celite and solvent were mixed with anhydrous diethyl ether. The diethyl ether was dried over a molecular sieve. The ether was slowly removed by the application of a vacuum using a Buchi rotary evaporator. Traces of ether were removed by placing the flask in a fume cupboard. The coated celite was weighed and reweighed on completion to check that all

the ether had been removed and that no stationary phase had been lost. The column was packed as described by Cruickshank *et al*⁽³⁾. One end of the column was sealed with glasswool and the packing introduced in small amounts into the column through a preweighed funnel. A rubber stopper was attached to the sealed end and the column was gently tapped on the floor and from top to bottom after each addition to ensure even packing. On completion the funnel was also weighed and the amount of stationary phase added was determined by difference. The column was then coiled and secured by means of nuts and bolts to the glc. Each column was allowed to equilibrate for about 10 -15 minutes to water bath temperature before taking any readings. Leaks at joints were checked for by pressurising the system with carrier gas and squirting a soapy solution on the outside of the joints.

4.2.2.2. Measurement Procedure

Cruickshank *et al*⁽³⁾ showed that in the limit of low coverage the solvent-gas interface is co-extensive with the total solid surface⁽³⁾, decreasing rapidly with increasing coverage ratio. It is in this region of low coverage that chromatographic non-ideality is high and surface effects predominate over solubility⁽³⁾. The adsorbing surface contributes independently to the total retention. Therefore to obtain meaningful retention volumes corrections have to be made for the adsorbing surface at low percentage loadings.

The equation used in the calculation of γ_{13}^{∞} is

$$\ln V'_N = \ln \left[\frac{RT}{\gamma_{13}^{\infty} P_1^*} \right] - \left[\frac{(B_{11} - V_1^*)}{RT} \right] P_1^* + \left[\frac{(2B_{12}) P_o}{RT} \right] \quad (4.1.)$$

where

$$V_N = V_N^* + \phi U_o J_3^2 \quad (4.2)$$

4.2.2.2.1. Retention Times at Infinite Dilution

Sample sizes ranging from 0.1mm^3 - 1.0mm^3 were injected at each flowrate. To obtain retention times at infinite dilution, t_r , graphs of retention time, t_r^* (s), versus solute size (mm^3) were plotted.

Retention times were obtained from the time of injection of the solute to the emergence of a solute peak. The retention volume, V_N , is related to the retention time at infinite dilution of the solute by

$$V_N = (t_r - t_g)U_o J_3^2 \quad (4.4.)$$

4.2.2.2.2. Net Retention Volume at Zero Flowrate

The measured flowrate, U_o , was adjusted to conditions prevailing in the column according to (see page 17)

$$U_c = U_o \left(\frac{T^c}{T_{fm}} \right) \left(\frac{P_{fm} - P_w}{P_{fm}} \right) \quad (4.5.)$$

V_N is expected to be a linear function of flowrate⁽³⁾. Hence V_N was plotted against $U_o J_3^2$ ($= u$, the mean flowrate) to obtain the net retention volume at zero sample size and zero mean column flowrate, V_N^* . The infinite dilution retention volume was extrapolated to zero flowrate for two reasons: to decrease the effects of longitudinal diffusion and to ensure data referred to an equilibrium process and thus overcome resistance to mass transfer⁽³⁾.

4.2.2.2.3. Net Retention Volume at Infinite Coverage

The variation of net retention volume (V_N) with coverage ratio as indicated by Cruickshank *et al*⁽³⁾ and Pecsok *et al*⁽³⁵⁾ led to a third extrapolation. Molal retention volume V_N^o (corresponding to zero injection volume and zero flowrate) was plotted against the mass of support per mole of solvent, W_s . The value of $\log V_N'$ (net retention volume at zero sample size, zero mean column flowrate and at infinite solvent coverage) was finally used to calculate γ_{13}^∞ according to the equation

$$\ln \gamma_{13}^\infty = \ln \left[\frac{RT}{V_N' P_1^*} \right] - \left[\frac{(B_{11} - V_1^*)}{RT} \right] P_1^* + \left[\frac{(2B_{12})}{RT} \right] P_o \quad (4.1.)$$

B_{11} and B_{12} values were calculated from extrapolation of data found in the literature⁽³⁶⁾. Vapour pressure data was calculated from the Antoine constants⁽³⁷⁾ and the molar volumes were calculated from the density values found in the literature⁽³⁷⁾.

4.2.3. Measurement Procedure for a Volatile Solvent

The procedure was similar to 4.2.1. above except for the preparation of the packing and the measurement of the net retention volume. The flask containing the packing was well sealed and placed onto a shaker to ensure mixing. This procedure was preferred to the use of the rotary evaporator since it minimised any loss of solvent. Measurement of flowrate (which was kept constant), retention times of solute and unretained gas, and temperature were made for each column. The flowrate was set depending on the length of column and the amount of solvent on the column, so that the column would have a lifespan of about 1- 1.5 hours.

Retention times were calculated from the tangent to peak method⁽²²⁾. The carrier gas flowrate was measured regularly throughout each run using an accurate stopwatch. Equation (4.3.) was used to calculate γ_{13}^{∞} .

$$\frac{V_N}{n_3 e^c} = \frac{RT}{\gamma_{13}^{\infty} P_1^*} - \frac{U_o t}{n_3} \left[\frac{P_3'}{\gamma_{13}^{\infty} P_1^*} \right] \quad (4.3.)$$

$$\frac{V_N}{e^c n_3} = a + b \left[\frac{U_o t}{n_3} \right] \quad (4.6)$$

The parameters have been defined on pages 2 and 43. The values of $V_N/n_3 e^c$ and $U_o t/n_3$ were fitted to the best straight line using a regression analysis. From the intercept the value of the quantity $RT/\gamma_{13}^{\infty} P_1^*$ was obtained and γ_{13}^{∞} was calculated. The partial pressure P_3' of the solvent in the gas was obtained from the slope of the straight line graph of $U_o t/n_3$ versus $V_N/n_3 e^c$. The time from the instant the gas flows into the column to the time at injection of a solute, t , is significant. Once the gas starts to flow over the support it slowly removes the solvent, since the solvent itself is moderately volatile. Measurements have to be taken every ten minutes over a short

period of time, between 1-1.5 hours before all the solvent has evaporated. t together with the flowrate, U_0 are related to the total volume of solvent, hence the number of moles of solvent that has evaporated off the column. B_{11} and B_{12} were calculated from McGlashan and Potter's equation⁽³⁸⁾ and Hudson and McCoubrey's combining rule⁽³⁹⁾ following Letcher *et al*⁽⁴⁰⁾.

Two **TURBO PASCAL** programs one for the calculation of V_N and $U_0 J_3^2$ and the other for $V_N/n_3 e^C$ and $U_0 t/n_3$ (See Appendices i and ii) were used.

5. POLAR SOLUTES IN HEXADECANE

5.1. INTRODUCTION

The purpose of this experiment was to obtain unambiguous values of γ_{13}^{∞} for the polar solutes methanol, ethanol, propan-1-ol and propan-2-ol in the solvent hexadecane. Polar solutes are surface adsorbed onto the column packing. Retention volumes for these systems are dependent on sample size, average mean column flowrate and column loading. The retention volumes have to be corrected for these parameters in order to obtain unambiguous values for γ_{13}^{∞} . The literature values for these systems were obtained from retention volumes that do not take into account all of these dependences and are therefore not truly reflective of the system interactions only.

Following the method of Cruickshank *et al*⁽³⁾, the following equation was used to determine γ_{13}^{∞} for the polar solutes in the hexadecane solvent.

$$\ln V'_N = \ln \left[\frac{RT}{\gamma_{13}^{\infty} P_1^*} \right] - \left[\frac{(B_{11} - V_1^*)}{RT} \right] P_1^* + \left[\frac{(2B_{12}) P_o}{RT} \right] \quad (5.1.)$$

where

$$V_N = V_N^* + \phi U_o J_3^2 \quad (5.2.)$$

and

$$V_N = (t_r - t_g) U_o J_3^2 \quad (5.3.)$$

where ϕ is a function of net retention volume at infinite diluti, V_N and mean column flowrate, $U_o J_3^2$, t_r^* is the retention time obtained for each sample size and t_r is the infinite dilution retention time obtained from the extrapolation of retention time and solute size data (see Appendix iii), $U_o J_3^2$ is the mean column pressure, V_N is the net retention vomue at zero sample size, V_N^* is the net retention volume at zero sample size and zero mean column flowrate, V_N^o is the molal net retention volume corrected

to zero sample size and zero mean column flowrate, V_N' is the net retention volume corrected to zero sample size, zero mean column flowrate and to infinite solvent coverage. The results showed that V_N was a linear function of a) sample size, b) mean flowrate and c) solvent loading.

5.2. RESULTS

Data were collected for 7 columns at two temperatures, 298.15 K and 303.15 K. Helium was used as the carrier gas and gas retention times, t_g , were determined using air. Equation 5.1. was used to determine γ_{13}^∞ .

For each column loading the flowrate was varied over at least a fivefold range. Hence for each column at a single temperature at worst three runs were obtained. For each system and temperature three columns were packed. Solvent loadings varied from between five to fifteen mass per cent. V_N' was obtained from the extrapolation of the net retention volume, V_N° to infinite solvent coverage ie. W_s approaches zero, where W_s is the mass of celite per mole of solvent. B_{11} and B_{22} data was obtained by extrapolation of values found in the literature⁽³⁶⁾, where B_{11} and B_{22} are the second virial coefficients of the solute and the carrier gas respectively. B_{12} data was calculated from the approximation⁽³⁶⁾ below since no mixed critical constants at the temperatures of this experiment were found in the literature

$$B_{12} = \frac{1}{2}(B_{11} + B_{22}) \quad (5.4.)$$

The results are summarised in numerical and graphical forms. Table 5.1 is a summary of the column specifications. Tables 5.2 to 5.22 gives a summary of the experimentally determined parameters viz. infinite dilution retention time, t_r , retention time of gas, t_g , outlet pressure, P_o , mean column flowrate, $U_o J_3^2$, and net retention volume, V_N . Figures 5.1 to 5.21 are the graphs obtained from the plots of $U_o J_3^2$ versus V_N . Tables 5.23 to 5.25 gives the constants used in equation 5.1. for the calculation of γ_{13}^∞ . Tables 5.1.26 to tables 5.1.28 give a summary of $\text{Log } V_N^*/n_3$

($=\text{Log } V_N^o$) and W_s values for each column at the temperatures 293.15 K and 303.15 K. The graphs are plotted in figures 5.22 and 5.23.

In order to show how the activity coefficients were calculated for the alkanol-hexadecane systems, the results for the methanol - hexadecane system at 293.15 K are described in detail.

RESULTS : SAMPLE CALCULATION OF γ_{13}^∞ FOR THE METHANOL -HEXADECANE SYSTEM AT 293.15 K.

For each column the retention times, t_r^* , were extrapolated to zero sample size. For columns 1, 2, and 3 the graphs obtained from retention time, t_r^* , versus sample size are plotted in figures 1, 4, and 7 (see Appendix iii).

The retention times obtained at infinite dilution are used to calculate the net retention volume, V_N , according to equation

$$V_N = (t_r - t_g) U_o J_3^2 \quad (5.3.)$$

The graphs of mean column flowrate versus net retention volume (corresponding to zero sample size) are given numerically in Tables 5.1.2., 5.1.5. and 5.1.8. and represented graphically in figures 5.1., 5.4. and 5.7. The net retention volume, V_N , was extrapolated to zero mean column pressure, $U_o J_3^2$ to obtain V_N^* . The values for the molal net retention volume, V_N^*/n_3 ($= V_N^o$) together with the mass of celite per mole of solvent loading, W_s , are tabulated in table 5.1.26. and plotted in figure 5.22. to obtain the net retention volume at zero sample size, zero mean column flowrate and infinite solvent coverage, V_N' . The value of V_N' together with the calculated γ_{13}^∞ value is given in Table 5.1.28.

Calculation of γ_{13}^∞ for experiments 5.1.1., 5.1.4. and 5.1.7. on columns 1, 2 and 3 respectively at 293.15 K.

Using equation 5.1. and from table 5.1.28. $\log V_N/n_3$ is 6.38 at 293.15 K.

$$\gamma_{13}^{\infty} = \left[\frac{1}{V_N'} * \frac{RT}{P_1^*} \right] * e^D$$

$$\gamma_{13}^{\infty} = \left[\left(\frac{1}{0.0023988} \right) * \left(\frac{1}{12996} \right) * (8.314) * (293.15) * (0.9385) \right]$$

Hence

$$\gamma_{13}^{\infty} = 73$$

RESULTS : COLUMN SPECIFICATIONS

TABLE 5.1.1. Column Specifications

Column Number	n_3	mass of celite	mass percentage loading [†]	W_s [‡]
	mmol	g	mass %	g mol ⁻¹
1.	1.406	5.3944	5.6	3836
2.	2.227	4.3758	10.3	1964
3.	3.439	4.2268	15.6	1229
4.	1.123	4.1335	5.8	3676
5.	2.326	5.8501	8.3	2515
6.	3.117	5.7116	11.0	1832
7.	5.193	6.6320	15.1	1277

† the percentage loading is given by the mass of solvent divided by the mass of celite and solvent ie. percentage loading = mass of solvent / (mass of solvent and mass of celite) and ‡ W_s is the mass of celite divided by the moles of solvent

RESULTS : COLUMN MEASUREMENTS

Experiment 5.1.1. Column 1 (5%) at 293.15 K

TABLE 5.1.2. Results obtained from column 1 (hexadecane 5%) with methanol as solute at 293.15 K

Run No.	t_r s	t_g s	P_o mmHg	$10^7 \times U_o J_3^2$ $m^3 s^{-1}$	$10^6 \times V_N$ m^3
1.	144.36	109.58	769.90	2.0827	5.6618
2.	57.82	44.18	760.25	5.285	5.8339
3.	45.13	34.38	771.95	6.790	5.9504
4.	27.80	21.38	774.80	11.647	6.2606

Experiment 5.1.2. Column 1 (5%) at 293.15 K

TABLE 5.1.3. Results obtained from column 1 (hexadecane 5%) with ethanol as solute at 293.15 K

Run No.	t_r s	t_g s	P_o mmHg	$10^7 \times U_o J_3^2$ $m^3 s^{-1}$	$10^6 \times V_N$ m^3
5.	105.63	63.54	760.25	3.6787	12.611
6.	57.95	34.38	771.95	6.792	13.176
7.	47.46	27.58	779.95	8.399	13.725
8.	35.82	21.38	774.80	11.741	14.328

Experiment 5.1.3. Column 1 (5%) at 293.15 K

TABLE 5.1.4. Results obtained from column 1 (hexadecane 5%)
with propan-2-ol as solute at 293.15 K

Run No.	t_r s	t_g s	P_o mmHg	$10^7 \times U_o J_3^2$ $m^3 s^{-1}$	$10^5 \times V_N$ m^3
9.	198.28	88.02	767.25	2.648	2.3300
10.	134.40	57.70	766.30	3.939	2.4293
11.	68.31	28.87	763.35	8.284	2.6992

Experiment 5.1.4. Column 2 (10%) at 293.15 K

TABLE 5.1.5. Results obtained from column 2 (hexadecane 10%)
with methanol as solute at 293.15 K

Run No.	t_r s	t_g s	P_o mmHg	$10^7 \times U_o J_3^2$ $m^3 s^{-1}$	$10^6 \times V_N$ m^3
12.	51.08	33.30	773.85	5.652	8.0331
13.	40.78	26.28	759.10	7.251	8.3354
14.	33.68	22.15	760.15	9.563	9.0778
15.	29.48	19.00	767.50	10.779	9.3044

Experiment 5.1.5. Column 2 (10% hexadecane) at 293.15 K

TABLE 5.1.6. Results obtained from column 2 (hexadecane 10%)
with ethanol as solute at 293.15 K

Run No.	t_r s	t_g s	P_o mmHg	$10^7 \times U_o J_3^2$ $m^3 s^{-1}$	$10^5 \times V_N$ m^3
16.	103.22	46.70	758.10	4.014	1.83015
17.	74.63	33.30	773.85	5.652	1.8673
18.	47.56	22.15	760.15	9.563	2.0005
19.	42.14	19.00	767.50	10.779	2.0544

Experiment 5.1.6. Column 2 (10% hexadecane) at 293.15 K

TABLE 5.1.7. Results obtained from column 2 (hexadecane 10%)
with propan-2-ol as solute at 293.15 K

Run No.	t_r s	t_g s	P_o mmHg	$10^7 \times U_o J_3^2$ $m^3 s^{-1}$	$10^6 \times V_N$ m^3
20.	173.94	48.80	765.35	3.762	3.8174
21.	122.21	34.00	768.65	5.408	3.8837
22.	101.73	28.29	772.90	6.836	4.0679
23.	83.91	21.91	757.15	8.520	4.3198
24.	62.49	16.30	770.85	12.178	4.6906

Experiment 5.1.7. Column 3 (15% hexadecane) at 293.15 K

TABLE 5.1.8. Results obtained from column 3 (hexadecane 15%)
with methanol as solute at 293.15 K

Run No.	t_r s	t_g s	P_o mmHg	$10^7 \times U_o J_3^2$ $m^3 s^{-1}$	$10^6 \times V_N$ m^3
25.	46.88	27.29	765.65	6.606	10.532
26.	37.08	22.19	767.75	8.888	10.772
27.	31.73	19.00	768.95	10.513	10.880
28.	23.00	14.01	767.65	15.221	11.447

Experiment 5.1.8. Column 3 (15% hexadecane) at 293.15 K

TABLE 5.1.9. Results obtained from column 3 (hexadecane 15%)
with ethanol as solute at 293.15 K

Run No.	t_r s	t_g s	P_o mmHg	$10^6 \times U_o J_3^2$ $m^3 s^{-1}$	$10^5 \times V_N$ m^3
29.	78.68	30.12	765.65	6.612	2.6102
30.	58.58	21.67	767.75	8.888	2.6673
31.	44.96	17.07	767.65	11.821	2.7206
32.	36.20	14.01	767.65	15.139	2.8073

Experiment 5.1.9. Column 3 at 293.15 K

TABLE 5.1.10. Results obtained from column 3 (hexadecane 15%)
with propan-2-ol as solute at 293.15 K

Run No.	t_r s	t_g s	P_o mmHg	$10^6 \times U_o J_3^2$ $m^3 s^{-1}$	$10^5 \times V_N$ m^3
33.	183.48	37.92	760.40	4.655	5.4292
34.	106.95	22.50	770.90	8.235	5.6128
35.	62.64	13.65	762.10	14.881	6.0395

Experiment 5.1.10. Column 4 (5%) at 303.15 K

TABLE 5.1.11. Results obtained from column 4 (hexadecane 5%) with
methanol as solute at 303.15 K

Run No.	t_r s	t_g s	P_o mmHg	$10^7 \times U_o J_3^2$ $m^3 s^{-1}$	$10^6 \times V_N$ m^3
36.	101.11	80.32	771.70	2.598	4.3325
37.	39.80	30.48	777.45	6.495	5.0180
38.	26.76	20.38	778.10	10.037	5.4195

Experiment 5.1.11. Column 4 at 303.15 K

TABLE 5.1.12. Results obtained from column 4 (hexadecane 5%) with ethanol as solute at 303.15 K

Run No.	t_r s	t_g s	P_o mmHg	$10^7 \times U_o J_3^2$ $m^3 s^{-1}$	$10^6 \times V_N$ m^3
39.	118.49	80.32	777.10	2.598	7.9544
40.	70.10	46.38	775.85	4.297	8.2998
41.	49.84	33.03	764.40	6.115	8.5974
42.	35.94	23.85	776.95	8.922	9.1008

Experiment 5.1.12. Column 4 (5% hexadecane) at 303.15 K

TABLE 5.1.13. Results obtained from column 4 (hexadecane 5%) with propan-1-ol as solute at 303.15 K

Run No.	t_r s	t_g s	P_o mmHg	$10^6 \times U_o J_3^2$ $m^3 s^{-1}$	$10^5 \times V_N$ m^3
43.	293.19	17.674	779.10	3.664	2.7058
44.	294.15	18.650	768.45	4.551	2.7547
45.	295.55	20.316	769.70	6.098	2.9413
46.	296.95	22.110	755.15	12.535	3.6835
47.	296.55	21.583	758.25	13.113	3.7496

Experiment 5.1.13. Column 4 (5% hexadecane) at 303.15 K

TABLE 5.1.14. Results obtained from column 4 (hexadecane 5%)
with propan-2-ol as solute at 303.15 K

Run No.	t_r s	t_g s	P_o mmHg	$10^6 \times U_o J_3^2$ $m^3 s^{-1}$	$10^5 \times V_N$ m^3
48.	120.63	60.38	776.90	3.074	1.4937
49.	85.02	42.28	763.20	4.352	1.5392
50.	62.59	30.08	776.95	6.187	1.6014
51.	46.56	23.85	776.95	8.938	1.7100

Experiment 5.1.14. Column 5 (8% hexadecane) at 303.15 K

TABLE 5.1.15. Results obtained from column 5 (hexadecane 8%)
with propan-1-ol as solute at 303.15 K

Run No.	t_r s	t_g s	P_o mmHg	$10^6 \times U_o J_3^2$ $m^3 s^{-1}$	$10^5 \times V_N$ m^3
52.	164.01	46.28	757.20	5.291	5.0963
53.	95.44	27.46	760.15	9.677	5.5494
54.	74.35	20.56	771.90	13.100	5.9608
55.	69.94	19.38	761.40	13.857	5.9870

Experiment 5.1.15. Column 6 (10% hexadecane) at 303.15 K

TABLE 5.1.16. Results obtained from column 6 (hexadecane 10%) with methanol as solute at 303.15 K

Run No.	t_s s	t_g s	P_o mmHg	$10^7 \times U_o J_3^2$ $m^3 s^{-1}$	$10^6 \times V_N$ m^3
56.	182.68	122.38	771.45	1.551	7.4049
57.	76.98	51.96	773.90	3.692	7.4514
58.	34.68	23.55	763.60	8.266	7.5436

Experiment 5.1.16. Column 6 (10% hexadecane) at 303.15 K

TABLE 5.1.17. Results obtained from column 6 (hexadecane 10%) with ethanol as solute at 303.15 K

Run No.	t_r s	t_g s	P_o mmHg	$10^6 \times U_o J_3^2$ $m^3 s^{-1}$	$10^5 \times V_N$ m^3
59.	152.40	73.08	770.20	2.590	1.6483
60.	107.79	51.96	773.90	3.692	1.6605
61.	66.67	32.37	771.80	5.943	1.6774
62.	34.41	17.29	759.55	11.678	1.7306

Experiment 5.1.17. Column 6 (10% hexadecane) at 303.15 K

TABLE 5.1.18. Results obtained from column 6 (hexadecane 10%)
with propan-1-ol as solute at 303.15 K

Run No.	t_r s	t_g s	P_o mmHg	$10^6 \times U_o J_3^2$ $m^3 s^{-1}$	$10^5 \times V_N$ m^3
63.	347.52	73.08	770.20	2.590	5.6240
64.	151.10	32.37	773.90	5.937	5.7861
65.	106.36	23.11	762.50	8.436	5.9021
66.	85.57	18.77	764.65	10.608	5.9902

Experiment 5.1.18. Column 6 (10% hexadecane) at 303.15 K

TABLE 5.1.19. Results obtained from column 6 (hexadecane 10%)
with propan-2-ol as solute at 303.15 K

Run No.	t_r s	t_g s	P_o mmHg	$10^6 \times U_o J_3^2$ $m^3 s^{-1}$	$10^5 \times V_N$ m^3
67.	224.16	73.08	770.70	2.590	3.1480
68.	79.11	26.67	768.70	7.600	3.3093
69.	58.64	19.38	771.85	10.312	3.4096
70.	51.32	17.29	753.30	11.625	3.4559

Experiment 5.1.19. Column 7 (15% hexadecane) at 303.15 K

TABLE 5.1.20. Results obtained from column 7 (hexadecane 15%)
with methanol as solute at 303.15 K

Run No.	t_r s	t_g s	P_o mmHg	$10^6 \times U_o J_3^2$ $m^3 s^{-1}$	$10^5 \times V_N$ m^3
71.	190.08	112.38	758.40	2.025	1.2570
72.	100.41	62.30	760.20	4.328	1.3285
73.	76.27	47.73	760.20	5.942	1.3786
74.	49.52	30.28	754.30	9.164	1.4671

Experiment 5.1.20. Column 7 (15% hexadecane) at 303.15 K

TABLE 5.1.21. Results obtained from column 7 (hexadecane 15%) with
ethanol as solute at 303.15 K

Run No.	t_r s	t_g s	P_o mmHg	$10^6 \times \bar{U}_o J_3^2$ $m^3 s^{-1}$	$10^5 \times V_N$ m^3
75.	289.12	112.38	754.30	2.027	2.8592
76.	127.45	52.80	772.95	5.226	3.1357
77.	75.76	30.28	754.30	9.164	3.4680

Experiment 5.1.19. Column 7 (15% hexadecane) at 303.15 K

TABLE 5.1.20. Results obtained from column 7 (hexadecane 15%)
with methanol as solute at 303.15 K

Run No.	t_r s	t_g s	P_o mmHg	$10^6 \times U_o J_3^2$ $m^3 s^{-1}$	$10^5 \times V_N$ m^3
71.	190.08	112.38	758.40	2.025	1.2570
72.	100.41	62.30	760.20	4.328	1.3285
73.	76.27	47.73	760.20	5.942	1.3786
74.	49.52	30.28	754.30	9.164	1.4671

Experiment 5.1.20. Column 7 (15% hexadecane) at 303.15 K

TABLE 5.1.21. Results obtained from column 7 (hexadecane 15%) with
ethanol as solute at 303.15 K

Run No.	t_r s	t_g s	P_o mmHg	$10^6 \times \tilde{U}_o J_3^2$ $m^3 s^{-1}$	$10^5 \times V_N$ m^3
75.	289.12	112.38	754.30	2.027	2.8592
76.	127.45	52.80	772.95	5.226	3.1357
77.	75.76	30.28	754.30	9.164	3.4680

Experiment 5.1.21. Column 7 (15% hexadecane) at 303.15 K

TABLE 5.1.22. Results obtained from column 7 (hexadecane 15%) with propan-2-ol as solute at 303.15 K

Run No.	t_r s	t_g s	P_o mmHg	$10^6 \times U_o J_3^2$ $m^3 s^{-1}$	$10^5 \times V_N$ m^3
78.	280.90	73.18	754.30	3.610	6.0604
79.	204.62	52.80	772.95	5.226	6.3772
80.	125.25	30.28	754.30	9.164	7.2419

RESULTS : PERIPHERAL DATA FROM THE LITERATURE

TABLE 5.1.23. Data used in the calculation of γ_{13}^{∞} at 293.15 K, where P_1^* is the vapour pressure of the pure solute, V_1^* is the molar volume of the solute, B_{11} is the second virial coefficient of the solute and B_{12} is the mixed virial coefficient.

Solute	P_1^*	$10^5 \times V_1^*$	$-(10^6 \times B_{11})$	$-(10^6 \times B_{12})$
	Pa	$\text{m}^3 \text{mol}^{-1}$	$\text{m}^3 \text{mol}^{-1}$	$\text{m}^3 \text{mol}^{-1}$
methanol	12996	4.0506	1750	869.5
ethanol	5809	5.8374	4000	1944.5
propan-2-ol	4124	7.6511	2050	1019.6

TABLE 5.1.24. Data used in the calculation of γ_{13}^{∞} at 303.15 K, where P_1^* is the vapour pressure of the pure solute, V_1^* is the molar volume of the solute, B_{11} is the second virial coefficient of the solute and B_{12} is the mixed virial coefficient.

Solute	P_1^*	$10^5 \times V_1^*$	$-(10^6 \times B_{11})$	$-(10^6 \times B_{12})$
	Pa	$\text{m}^3 \text{mol}^{-1}$	$\text{m}^3 \text{mol}^{-1}$	$\text{m}^3 \text{mol}^{-1}$
methanol	21861	4.0996	1640	814.5
ethanol	10420	5.9024	3480	1734.5
propan-1-ol	3772	7.5536	2010	999.5
propan-2-ol	7762	7.7330	1910	949.5

TABLE 5.1.25. Summary of the terms $(B_{11} - V_1^*)(P_1^*/RT)$ and $2B_{12}P_0/RT$ and P_0 for the solute : methanol, ethanol, propan-1-ol and propan-2-ol at 293.15 K and 303.15 K where $A = (B_{11} - V_1^*)(P_1^*/RT)$ and $B = 2B_{12}P_0/RT$.

Solute	T = 293.15 K			T = 303.15 K		
	A	B	P_0 $\frac{\times 10^5}{\text{Pa}}$	A	B	P_0 $\frac{\times 10^5}{\text{Pa}}$
methanol	-0.009547	-0.07298	1.022	-0.01458	-0.0735	1.138
ethanol	-0.009672	-0.1674	1.023	-0.01463	-0.1408	1.023
propan-1-ol	-	-		-0.00312	-0.0809	1.020
propan-2-ol	-0.003598	-0.08529	1.019	-0.00612	-0.0770	1.022

P_0 , the atmospheric pressure was obtained by calculating the average atmospheric pressure for each column and then determining the average atmospheric pressure for all three columns at each temperature.

RESULTS : SUMMARY OF RESULTS RELATING TO EQUATION 5.1.

TABLE 5.1.26. Summary of results obtained at 293.15 K giving the values of $\text{Log } V_N^*/n_3$, and W_s for each column loading.

The table corresponds to figures 5.1.to 5.9.

Column Number	Log V_N^*/n_3	W_s
		g mol ⁻¹
Methanol*		
1	6.59	3836
2	6.47	1964
3	6.45	1229
Ethanol*		
1	6.92	3836
2	6.88	1964
3	6.85	1229
Propan-2-ol*		
1	7.19	3836
2	7.18	1964
3	7.17	1229

* these results have been graphed in figure 5.22.

TABLE 5.1.27. Summary of results obtained at 303.15 K giving the values of $\text{Log } V_N^*/n_3$, and W_s for each column loading.

The table corresponds to figures 5.10. to 5.21.

Column Number	Log V_N^*/n_3	W_s
		g mol ⁻¹
Methanol**		
4	6.55	3676
6	6.37	1832
7	6.36	1277
Ethanol**		
4	6.82	3676
6	6.72	1832
7	6.71	1277
Propan-1-ol**		
4	7.30	3676
5	7.29	2515
6	7.25	1832
Propan-2-ol**		
4	7.09	3676
6	6.99	1832
7	7.01	1277

** These results have been graphed in figure 5.23.

RESULTS : FINAL

Table 5.1.28. Results obtained from figure 5.22. where $\text{Log } V'_N$ corresponds to $W_s = 0$. Equation 5.1. together with data found in table 5.1.22. was used in the calculation of γ_{13}^∞ for the alkanol-hexadecane system at 293.15 K.

Solute	$\text{Log } V'_N$	γ_{13}^∞
Methanol	6.38	73
Ethanol	6.82	54
Propan-2-ol	7.16	38

Table 5.1.29. Results obtained from figure 5.23. where $\text{Log } V'_N$ corresponds to $W_s = 0$. Equation 5.1. together with data found in table 5.1.23. was used in the calculation of γ_{13}^∞ for the alkanol-hexadecane system at 303.15 K.

Solute	$\text{Log } V'_N$	γ_{13}^∞
Methanol	6.24	63
Ethanol	6.64	49
Propan-1-ol	7.21	38
Propan-2-ol	6.93	36

FIG.5.1. Methanol on column 1 at 293.15 K

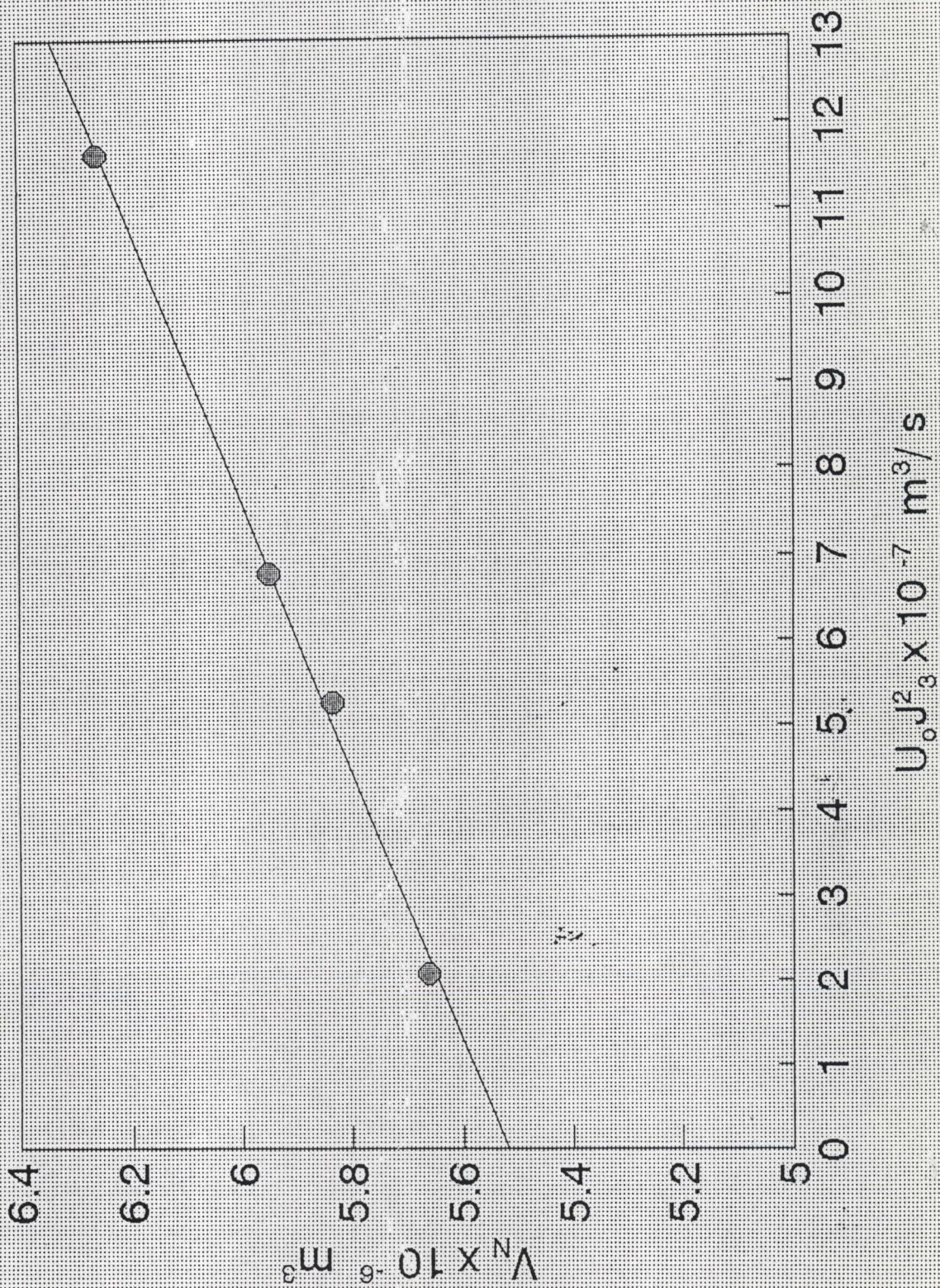


FIG.5.2. Ethanol on column 1 at 293.15 K

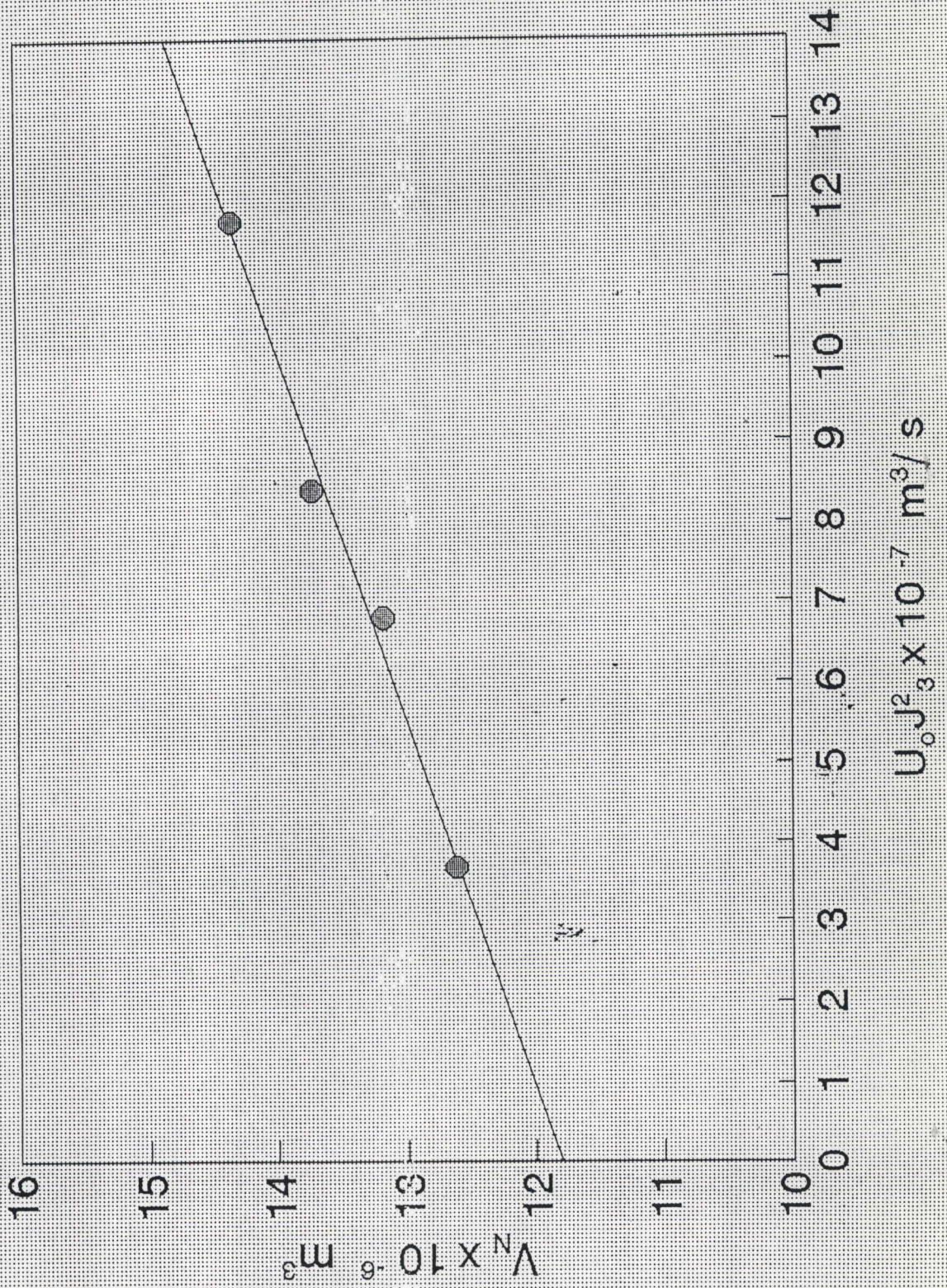


FIG.5.3. Propan-2-öl on column 1 at 293.15 K

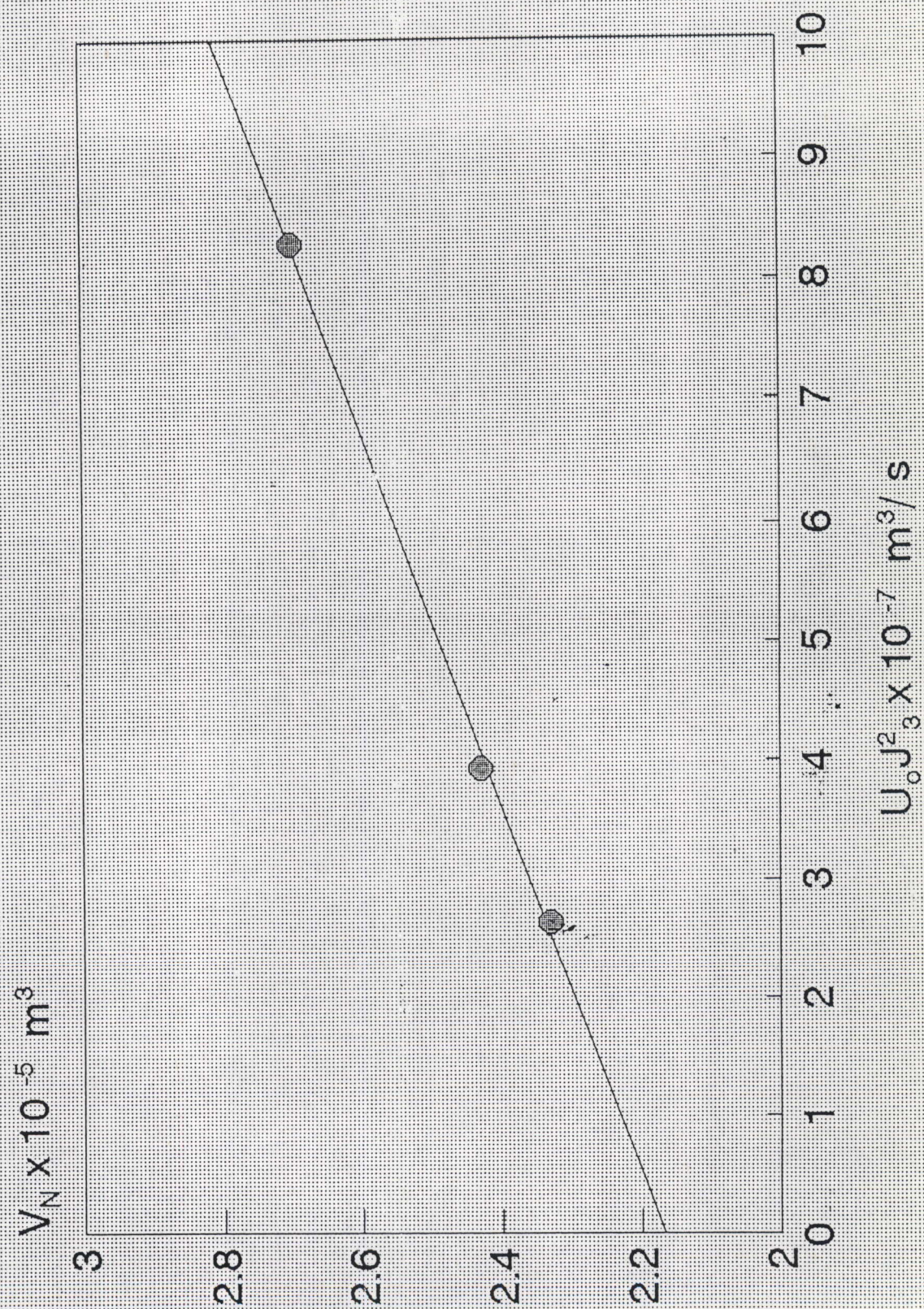


FIG.5.4. Methanol on column 2 at 293.15 K

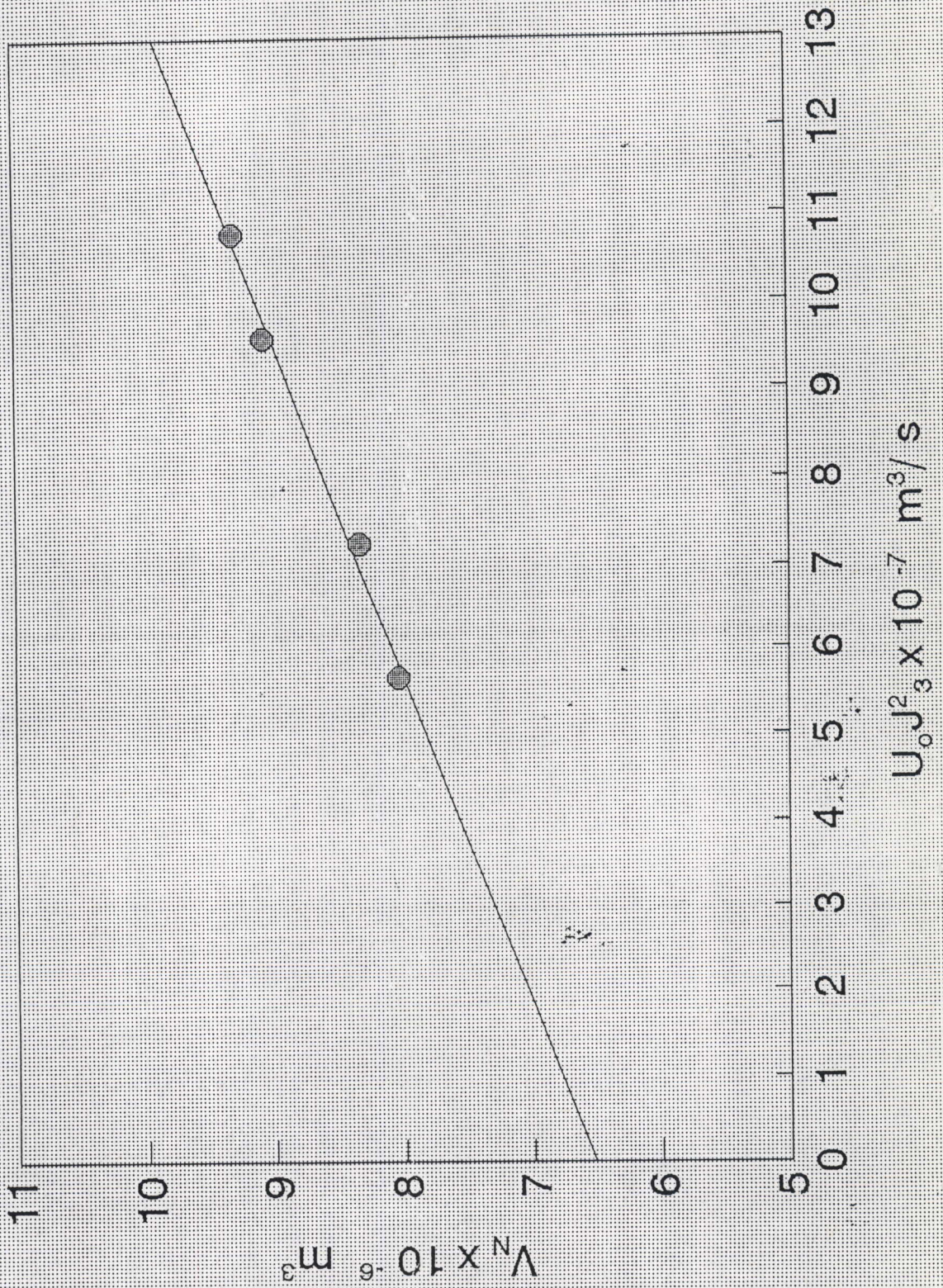


FIG.5.5. Ethanol on column 2 at 293.15 K

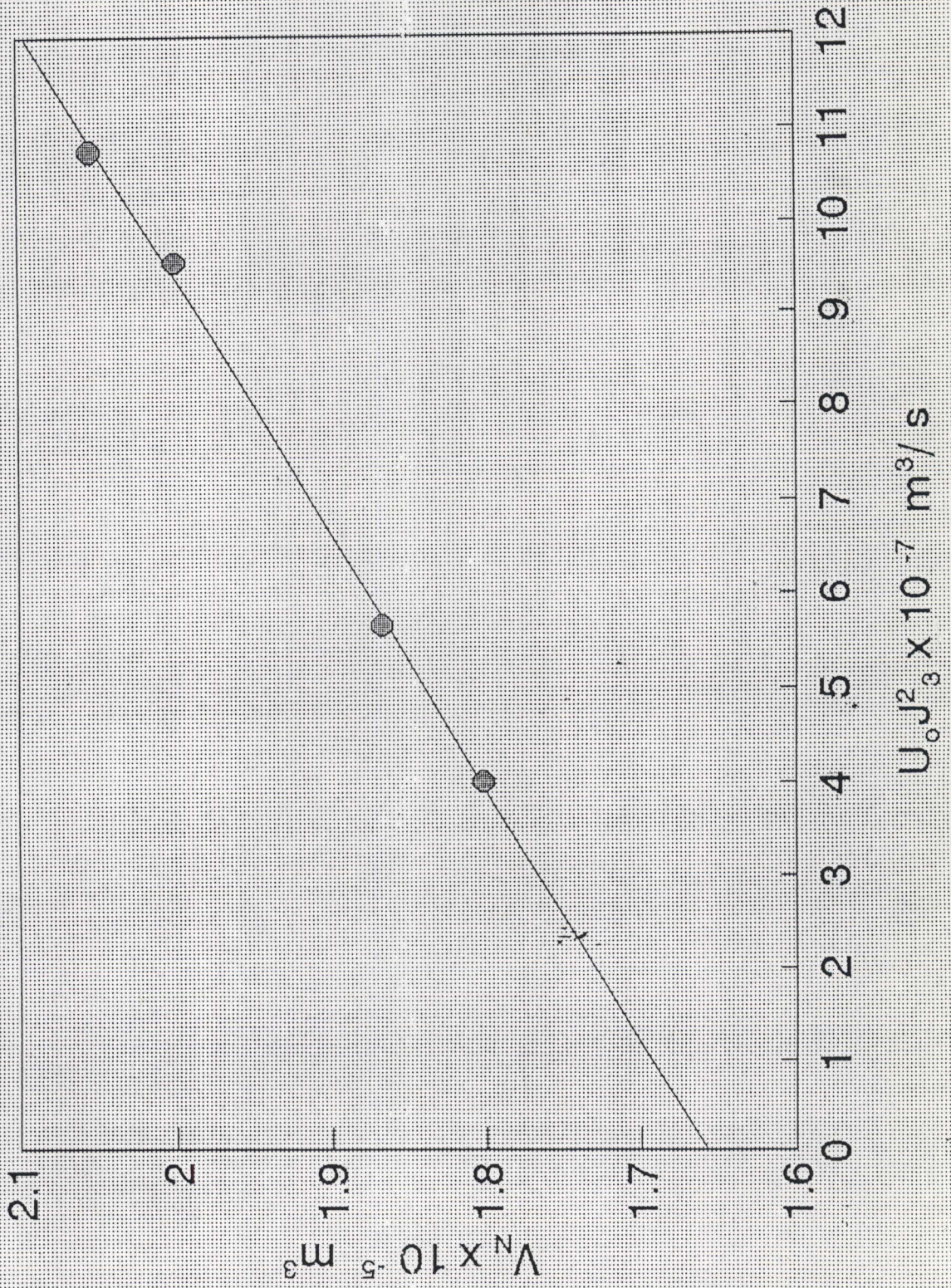


FIG.5.6. Propan-2-ol on column 2 at 293.15 K

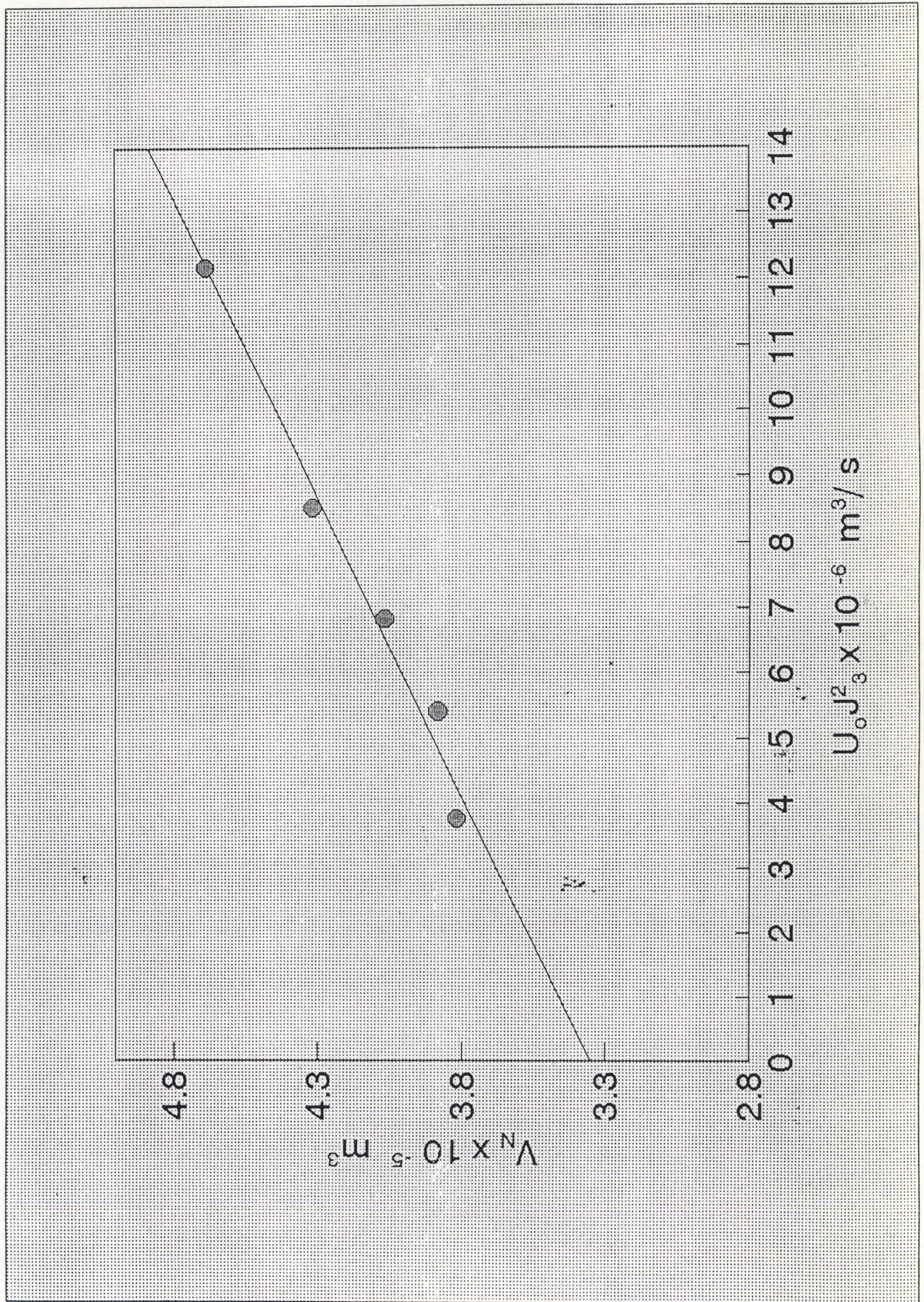


FIG.5.7. Methanol on column 3 at 293.15 K

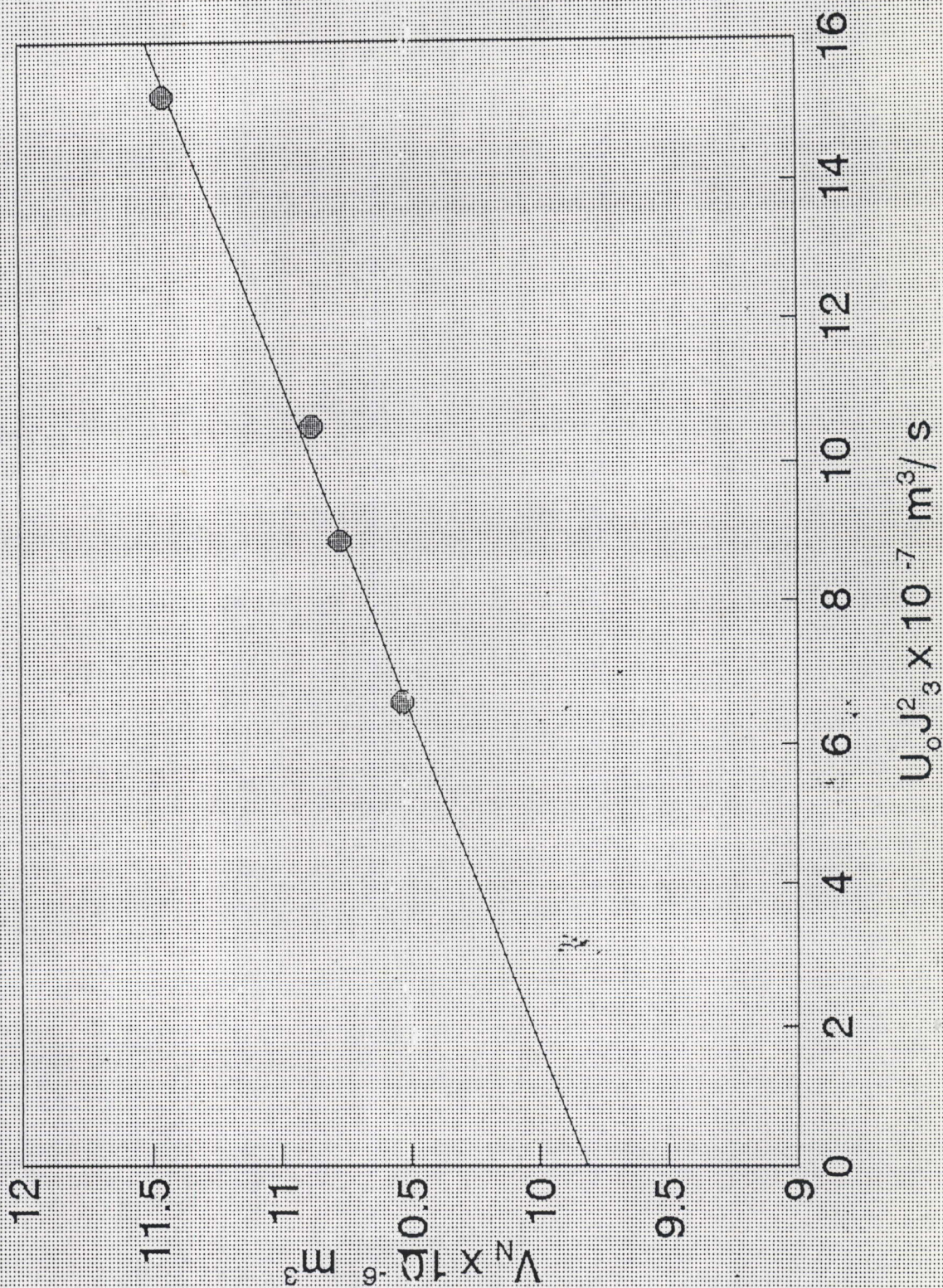


FIG.5.8. Ethanol on column 3 at 293.15 K

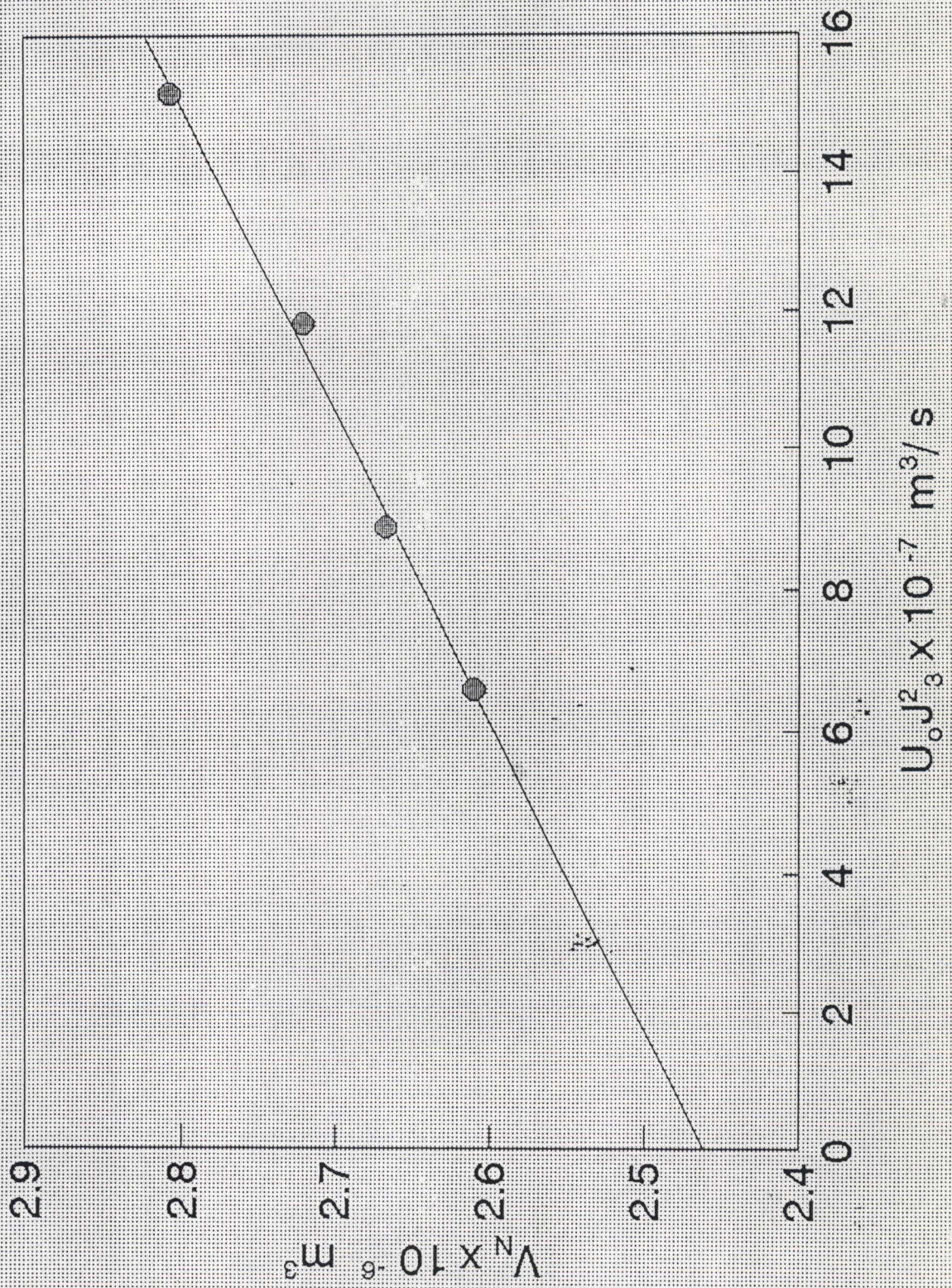


FIG.5.9. Propan-2-ol on column 3 at 293.15 K

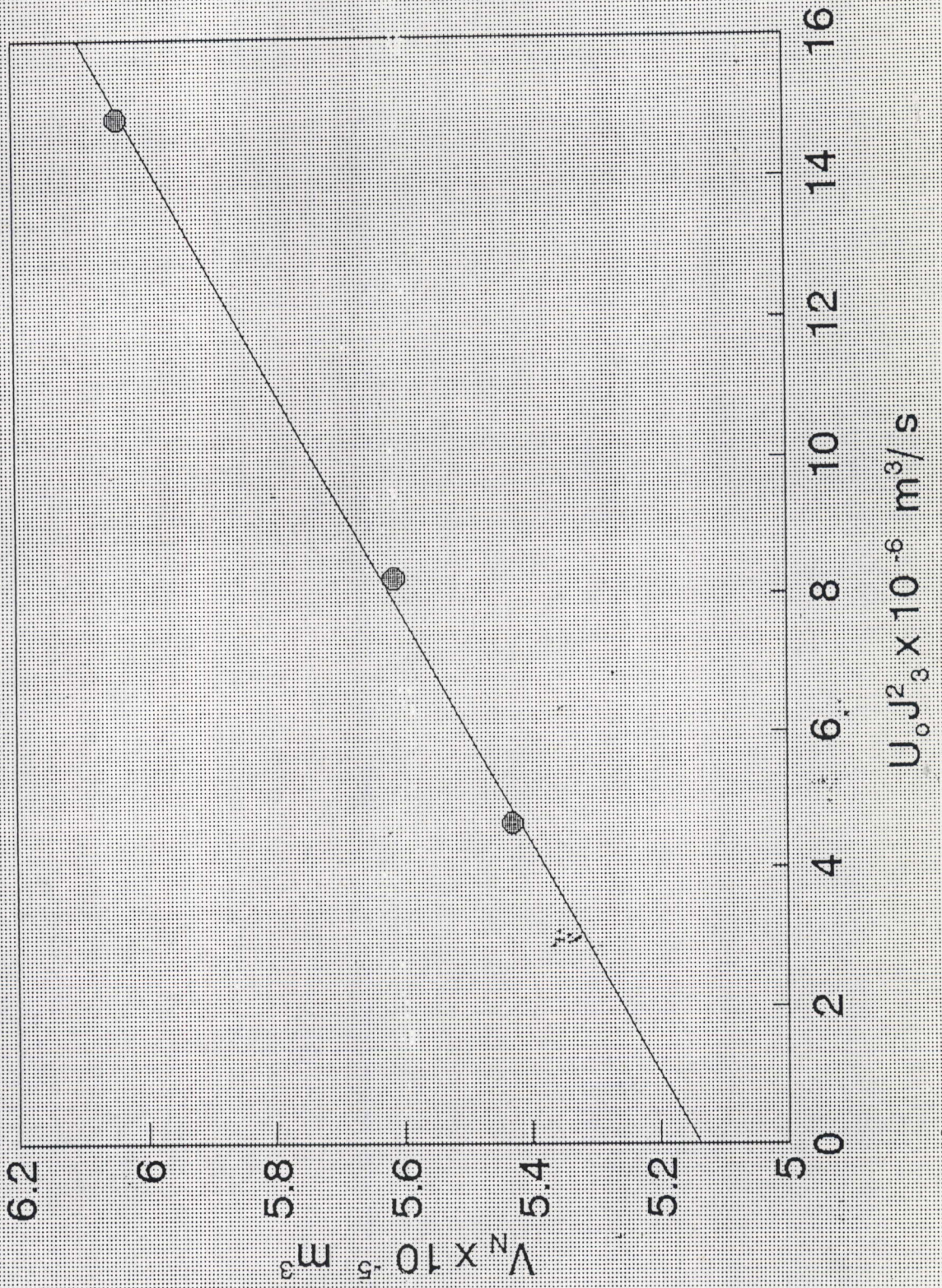


FIG.5.10. Methanol on column 4 at 303.15 K

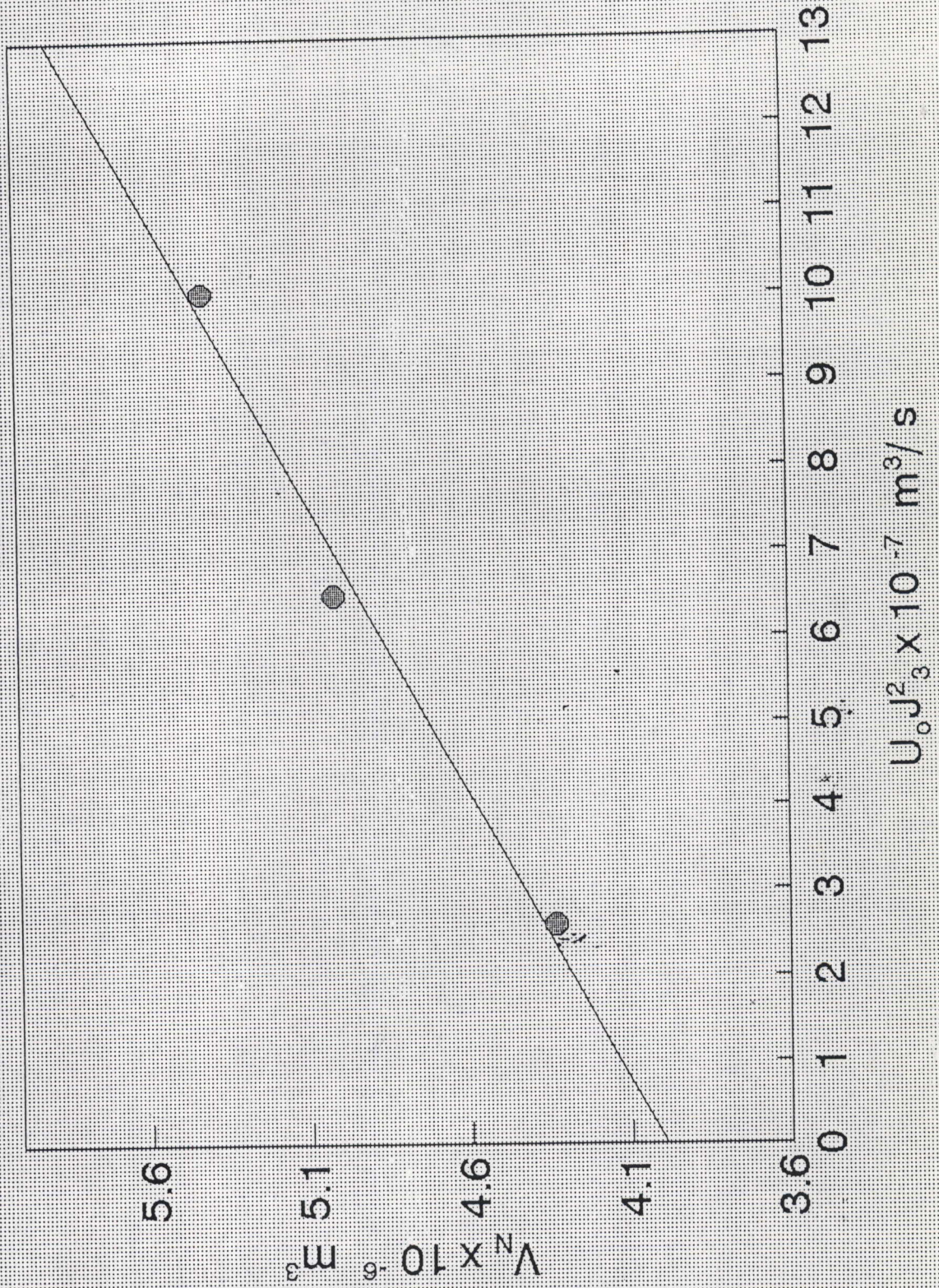


FIG.5.11. Ethanol on column 4 at 303.15 K

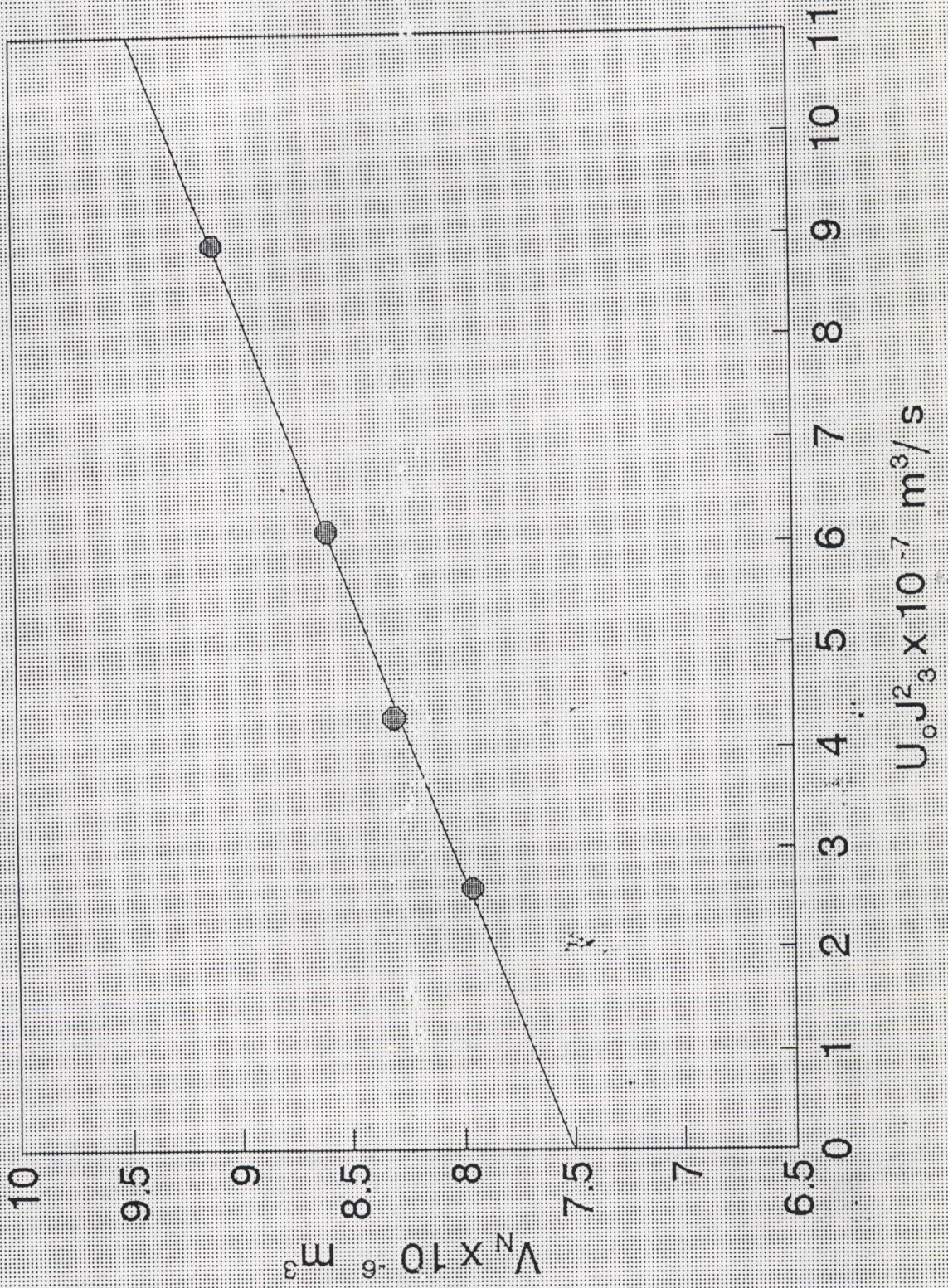


FIG.5.12. Propan-1-ol on column 4 at 303.15 K

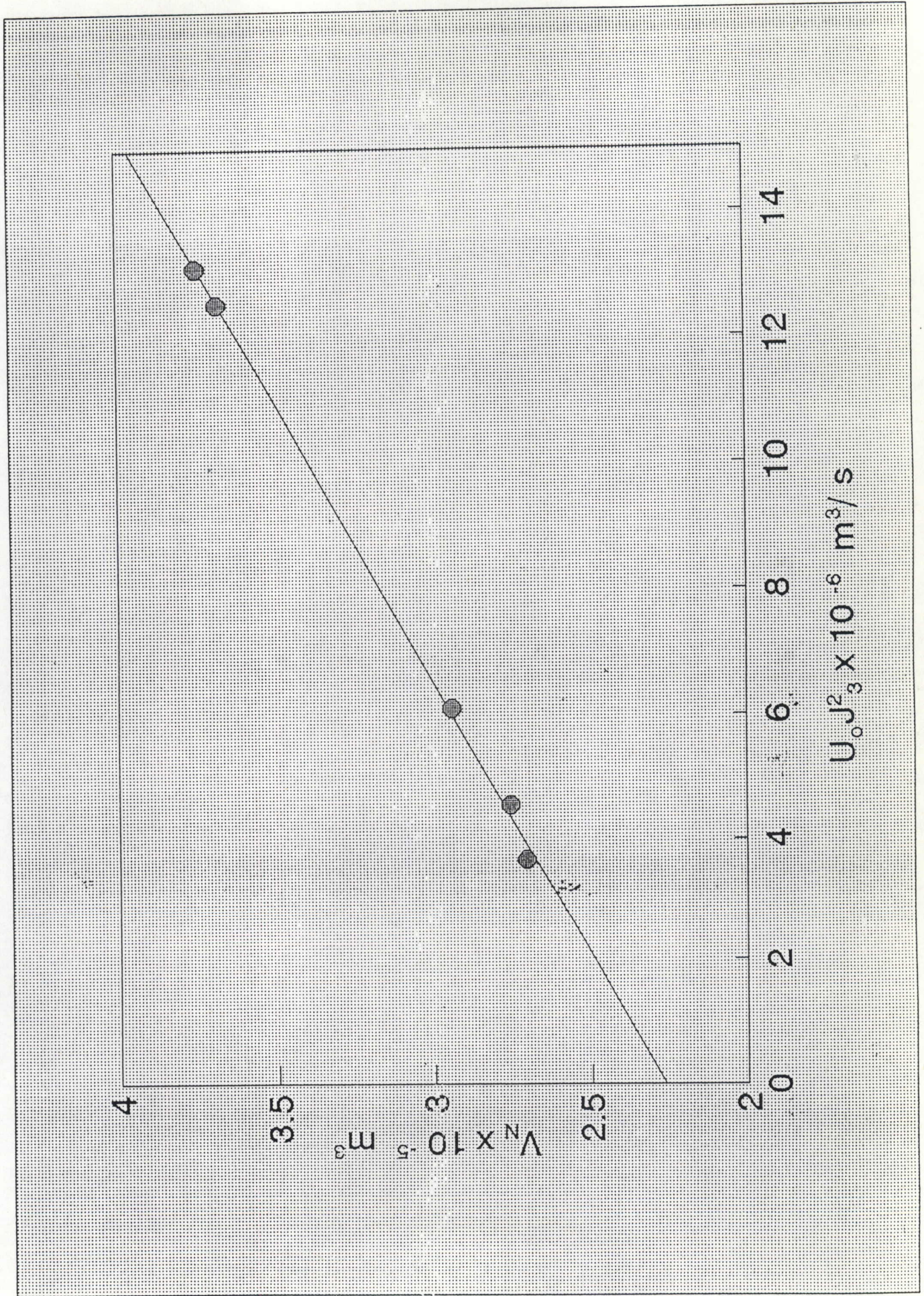


FIG.5.13. Propan-2-ol on column 4 at 303.15 K

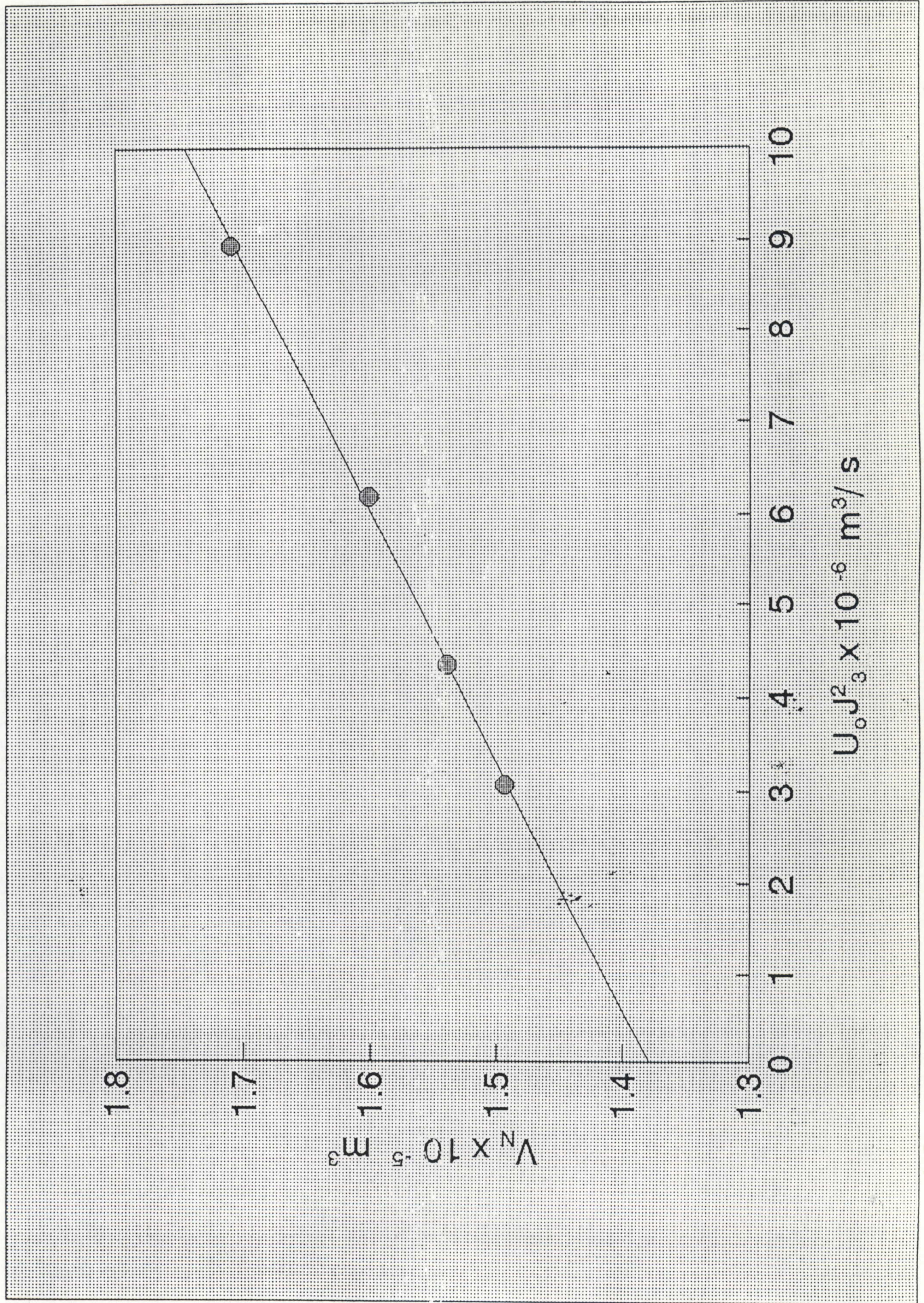


FIG.5.14. Propan-1-ol on column 5 at 303.15 K

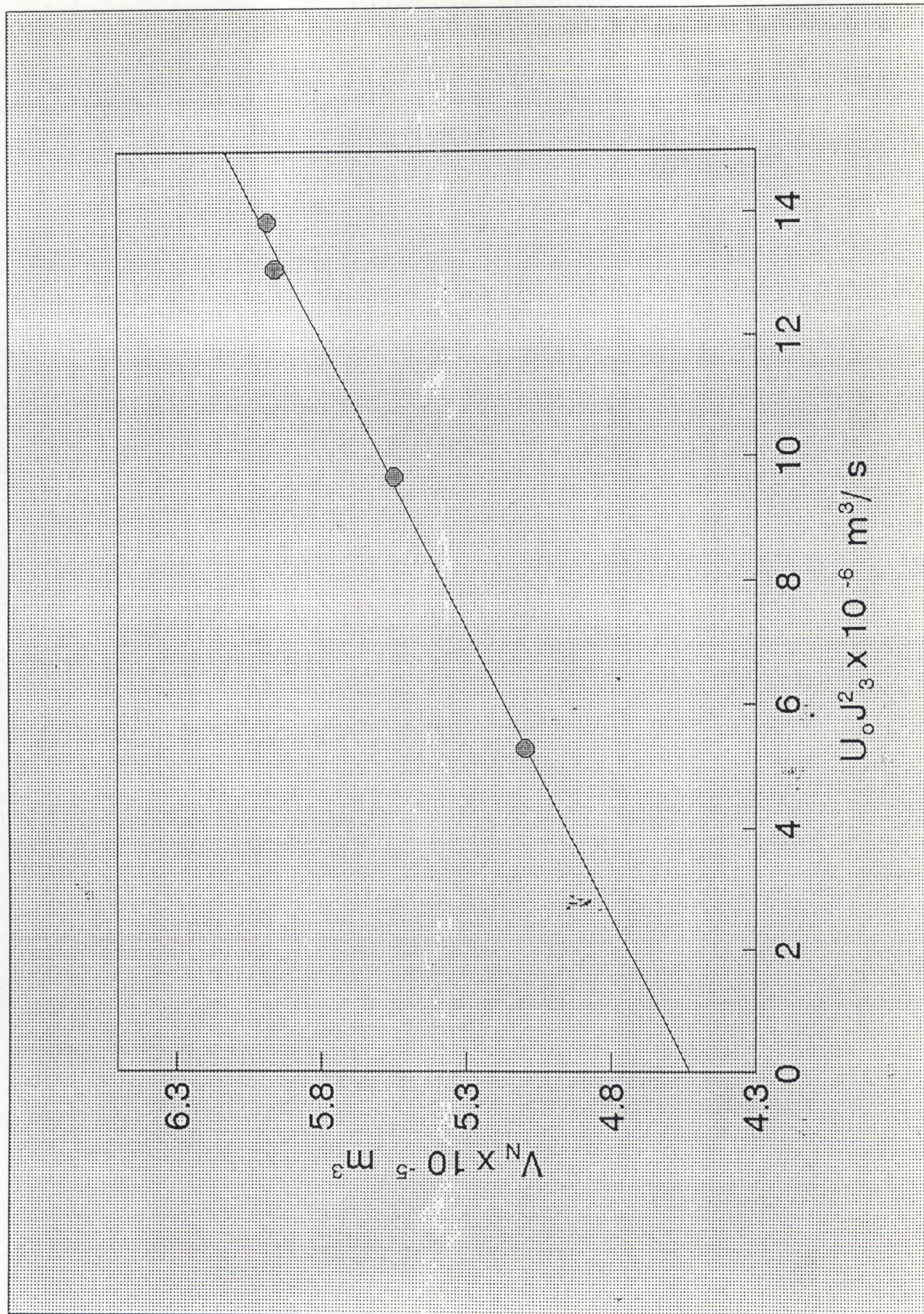


FIG.5.15. Methanol on column 6 at 303.15 K

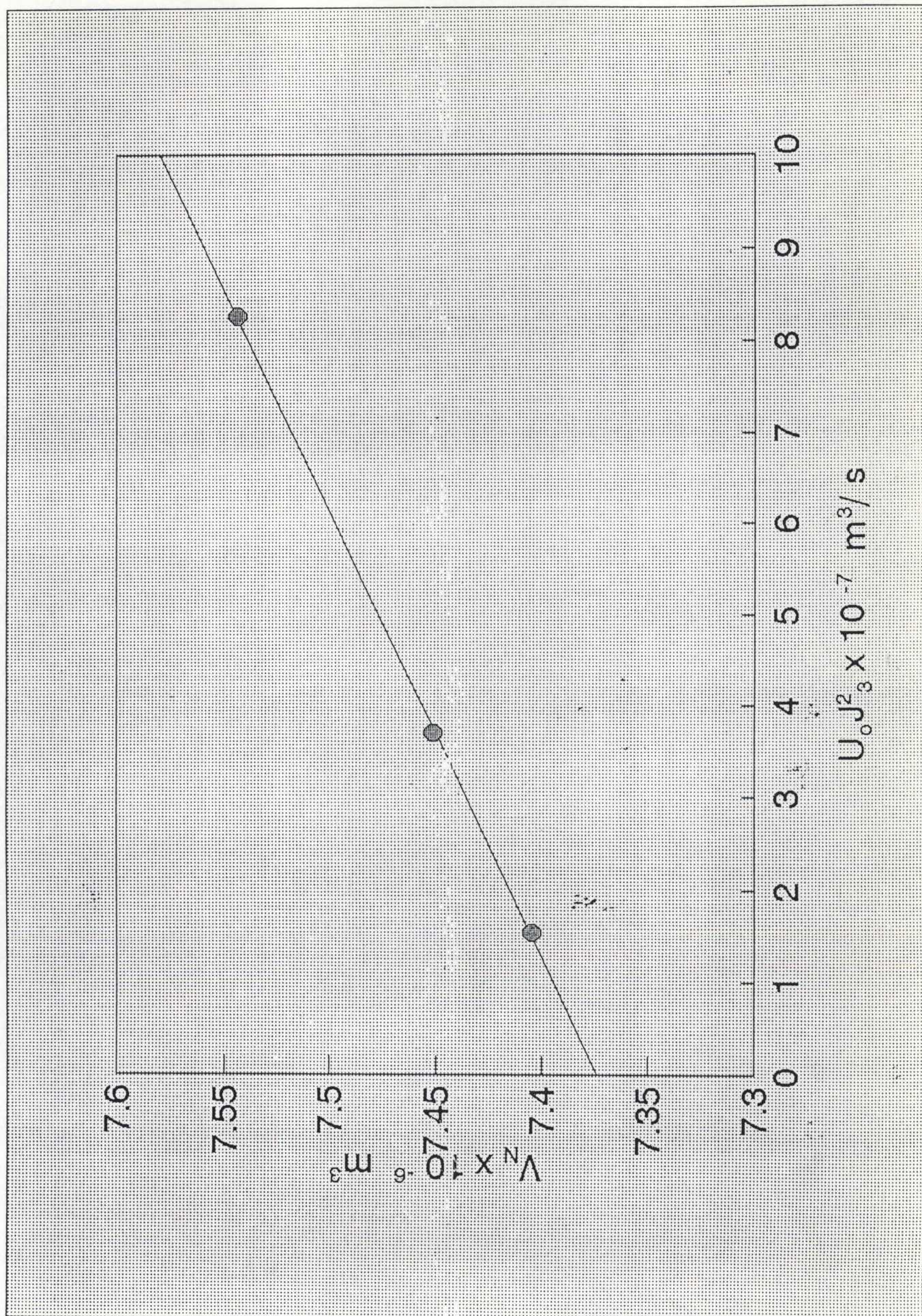


FIG.5.16. Ethanol on column 6 at 303.15 K

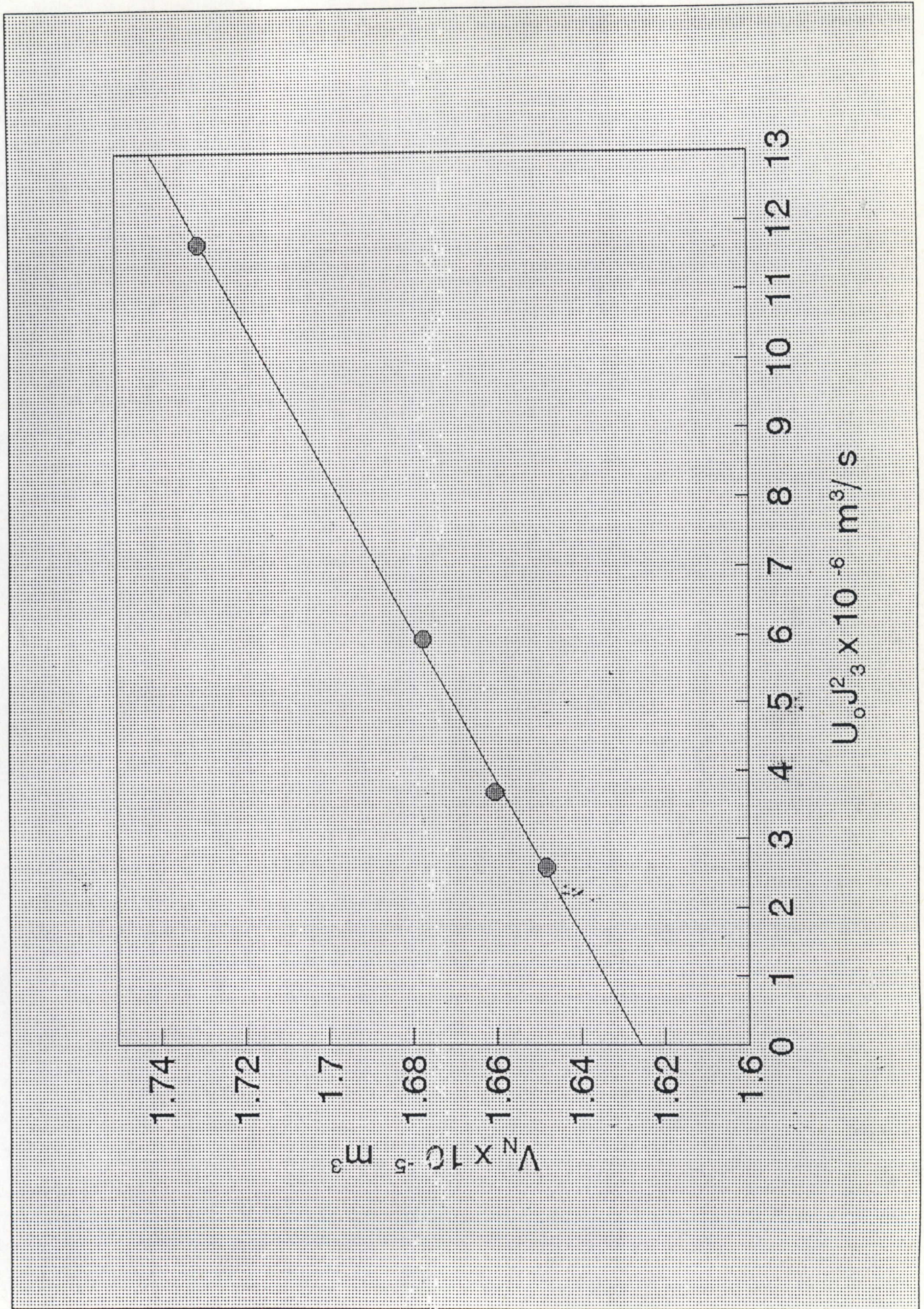


FIG.5.17. Propan-1-ol on column 6 at 303.15 K

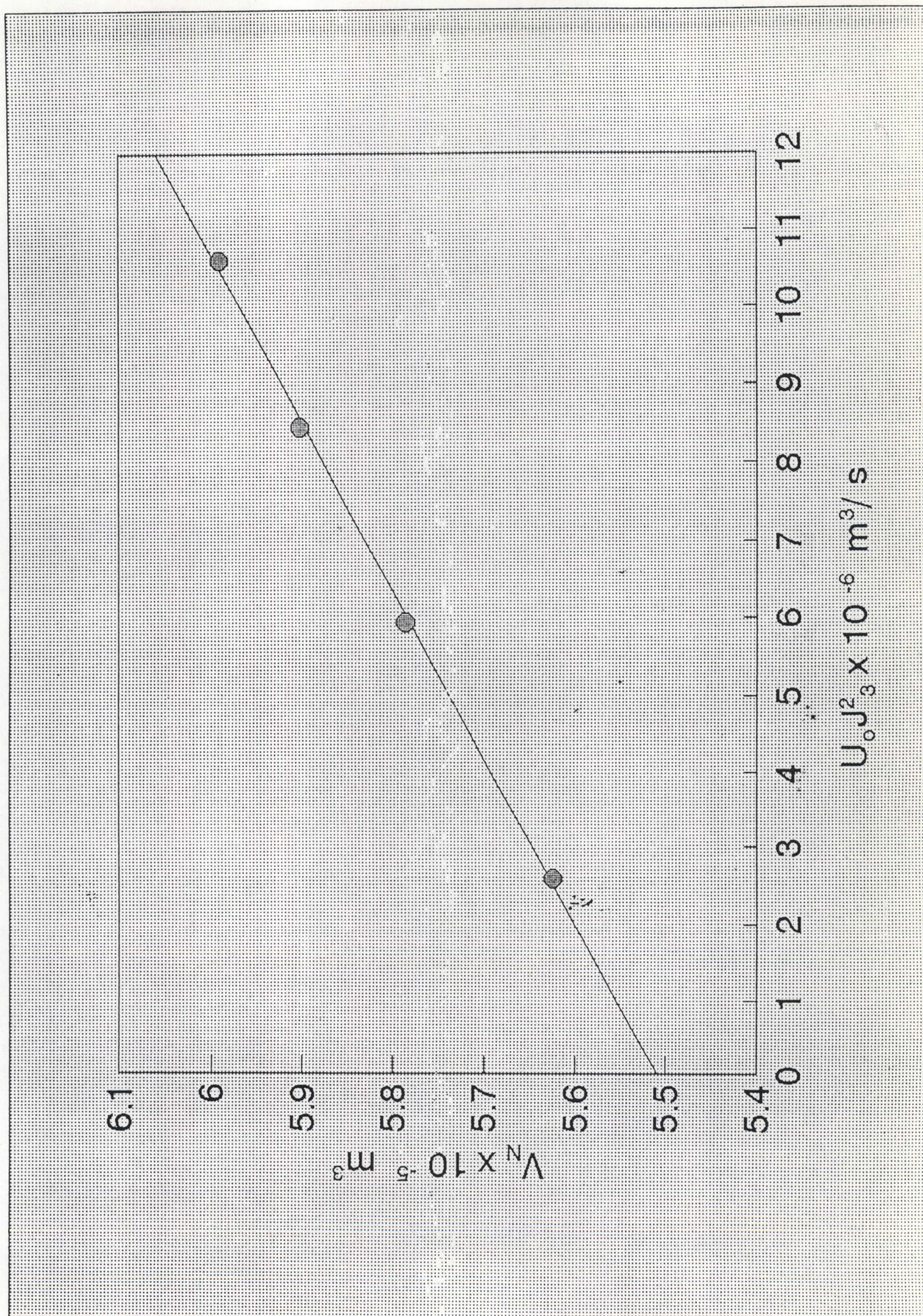


FIG.5.18. Propan-2-ol on column 6 at 303.15 K

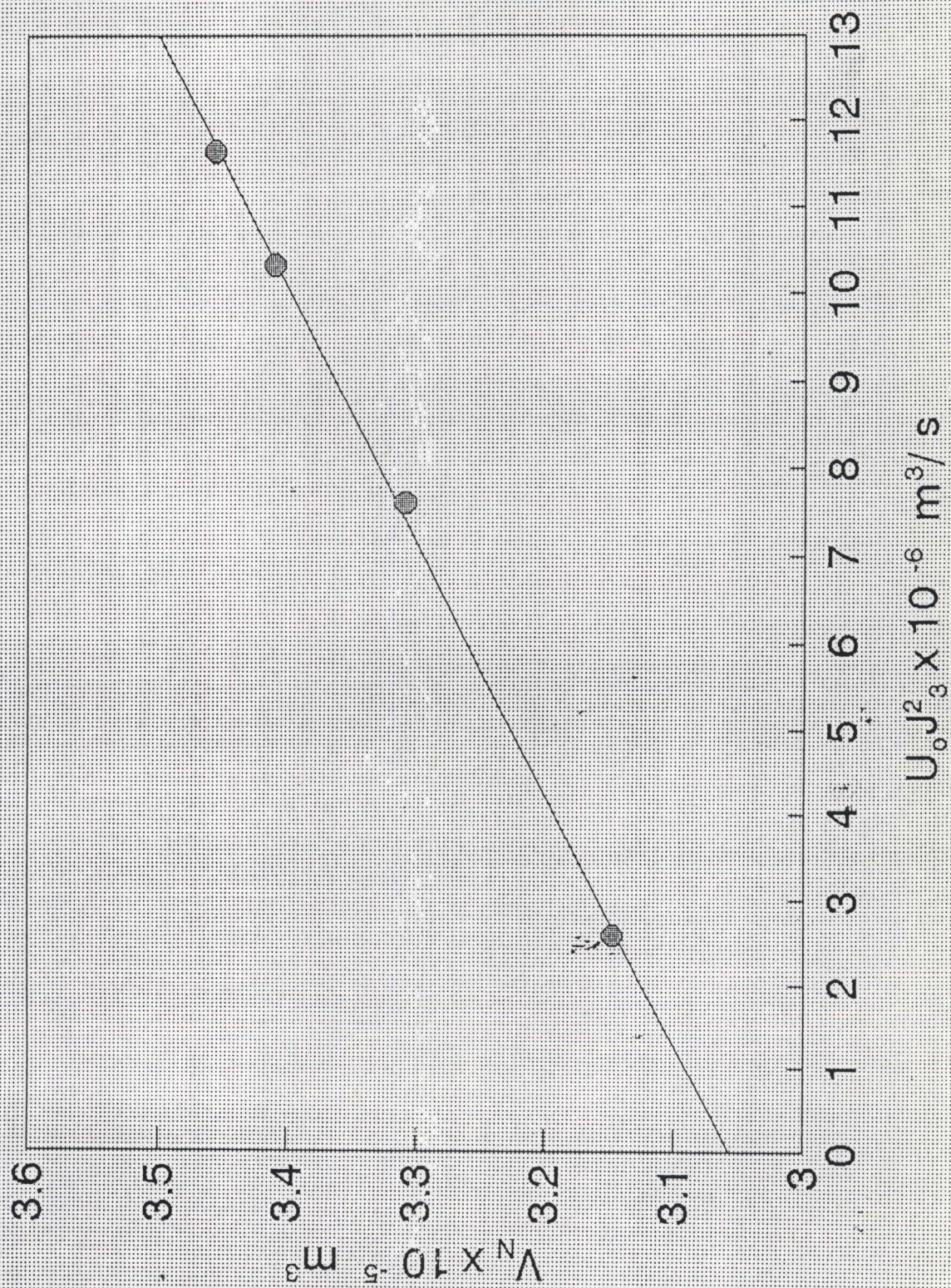


FIG.5.19. Methanol on column 7 at 303.15 K

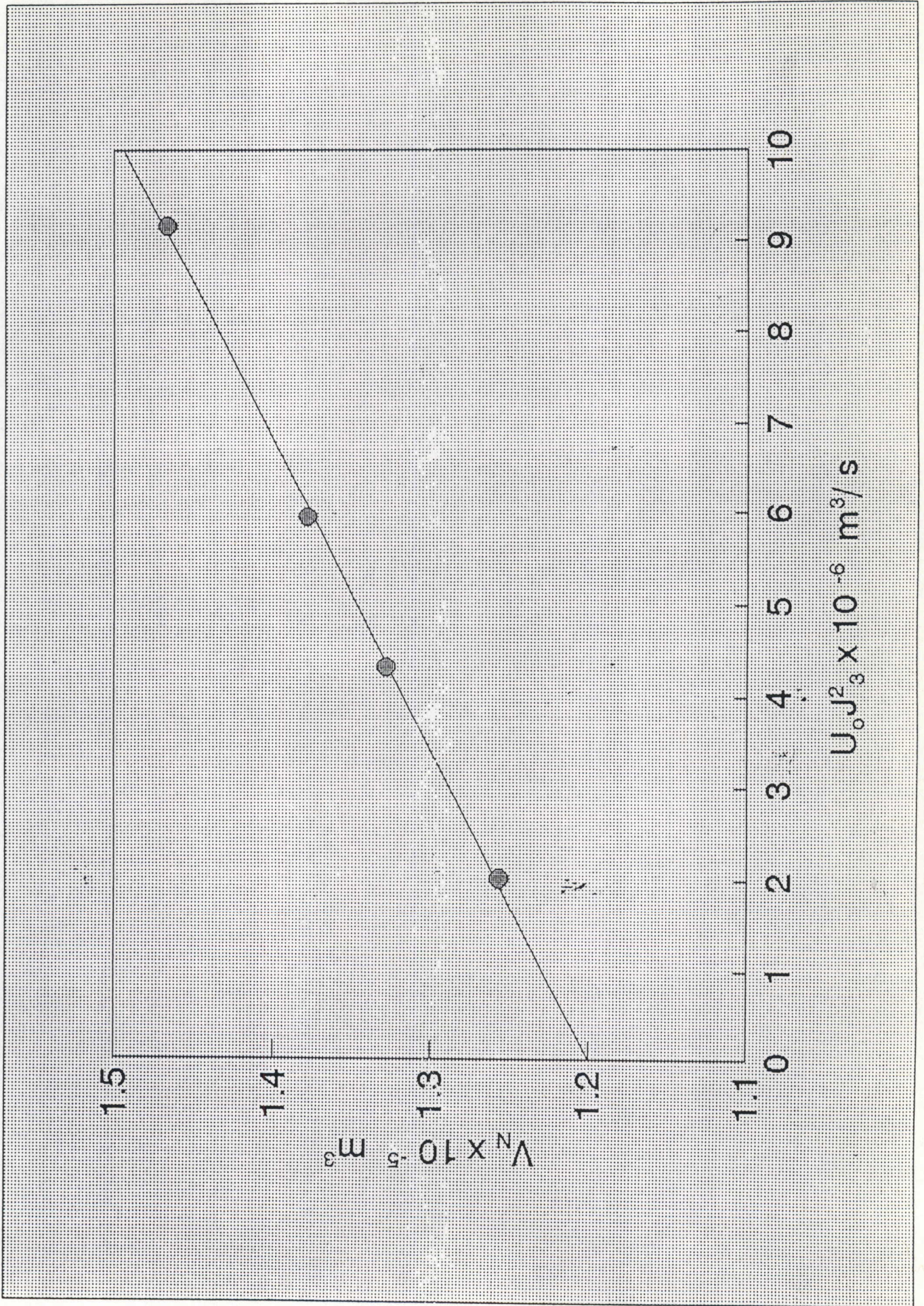


FIG.5.20. Ethanol on column 7 at 303.15 K

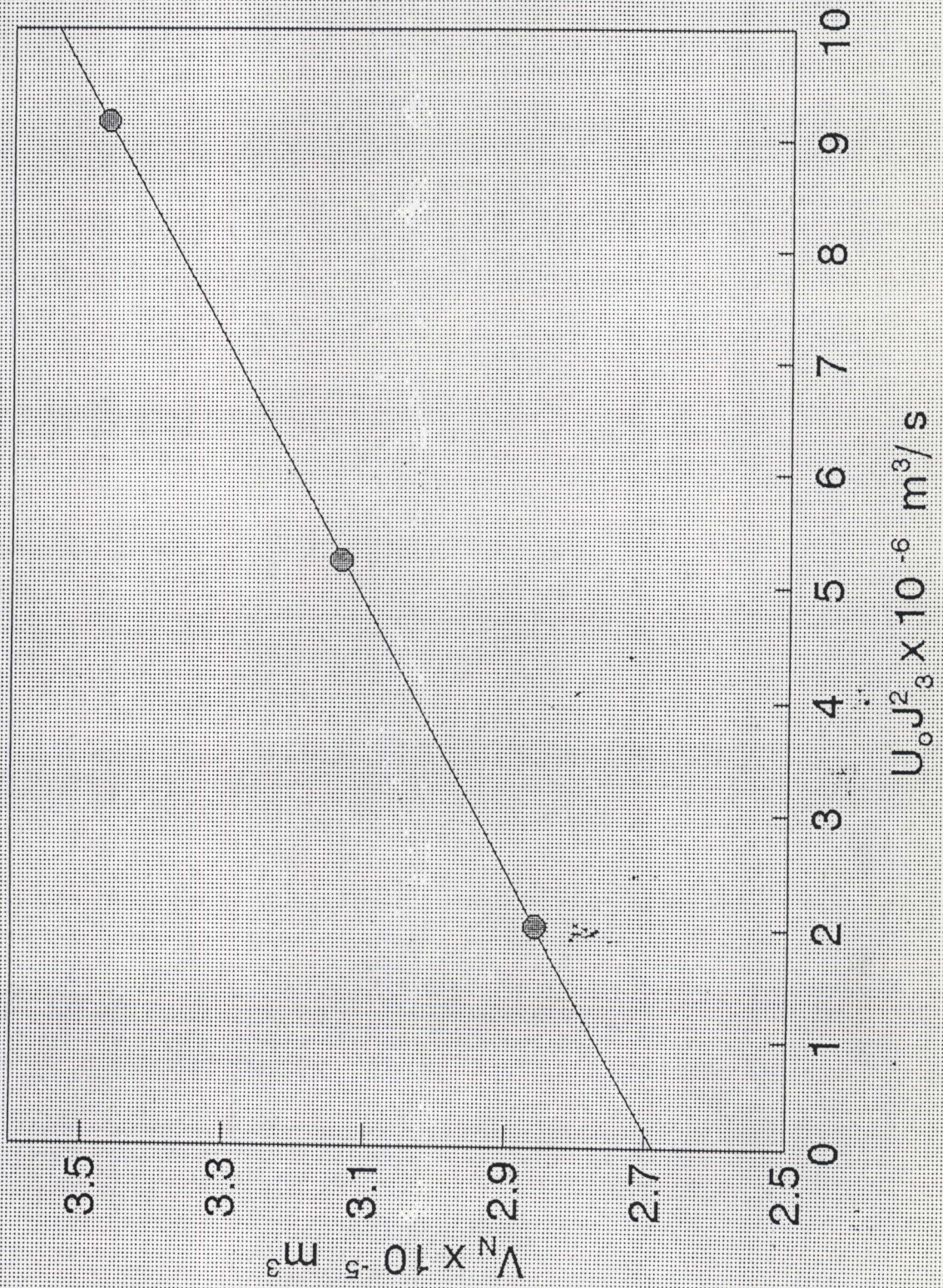


FIG.5.21. Propan-2-ol on column 7 at 303.15 K

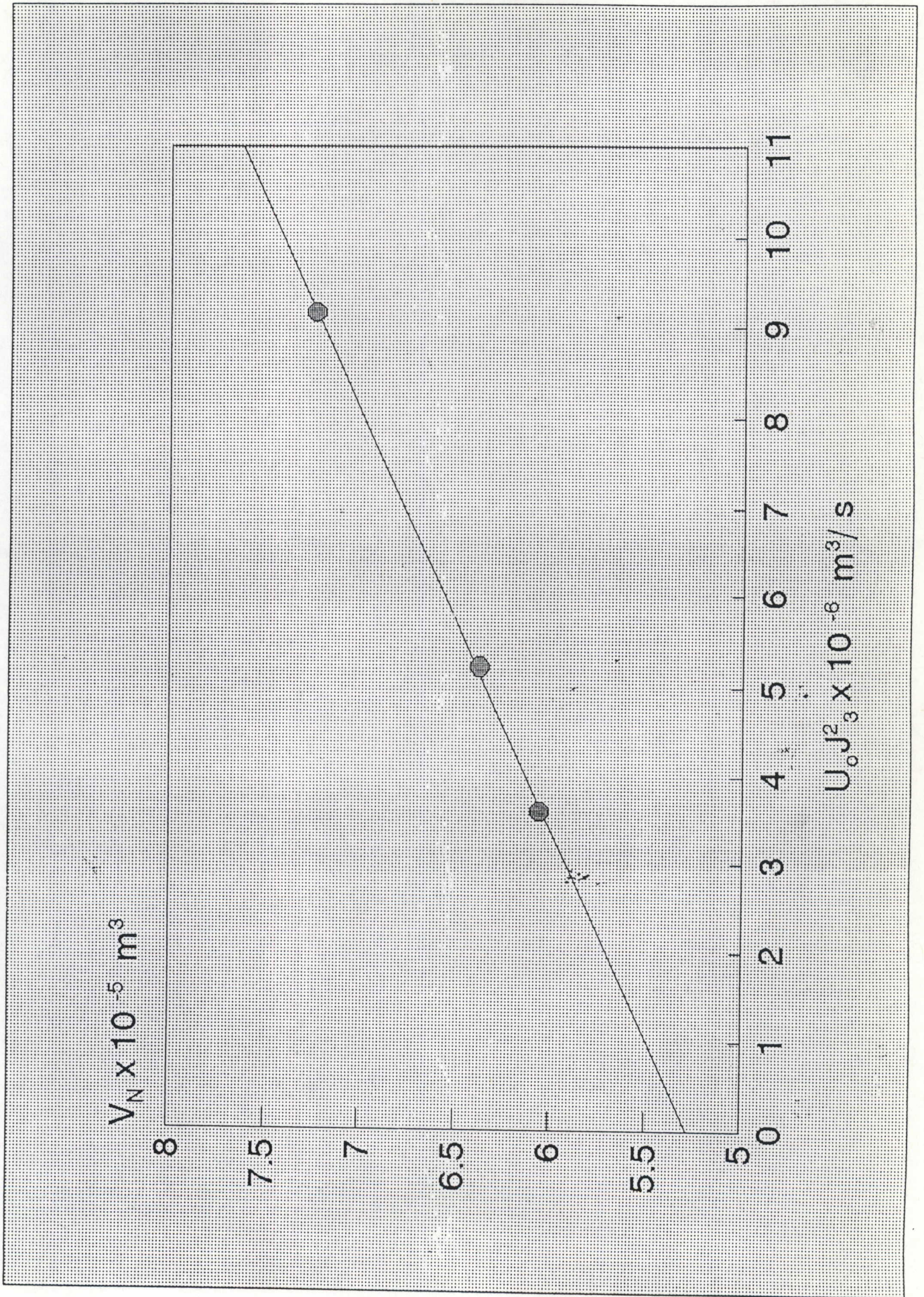


FIG. 5.22. Results for columns 1,2,3 at 293.15 K

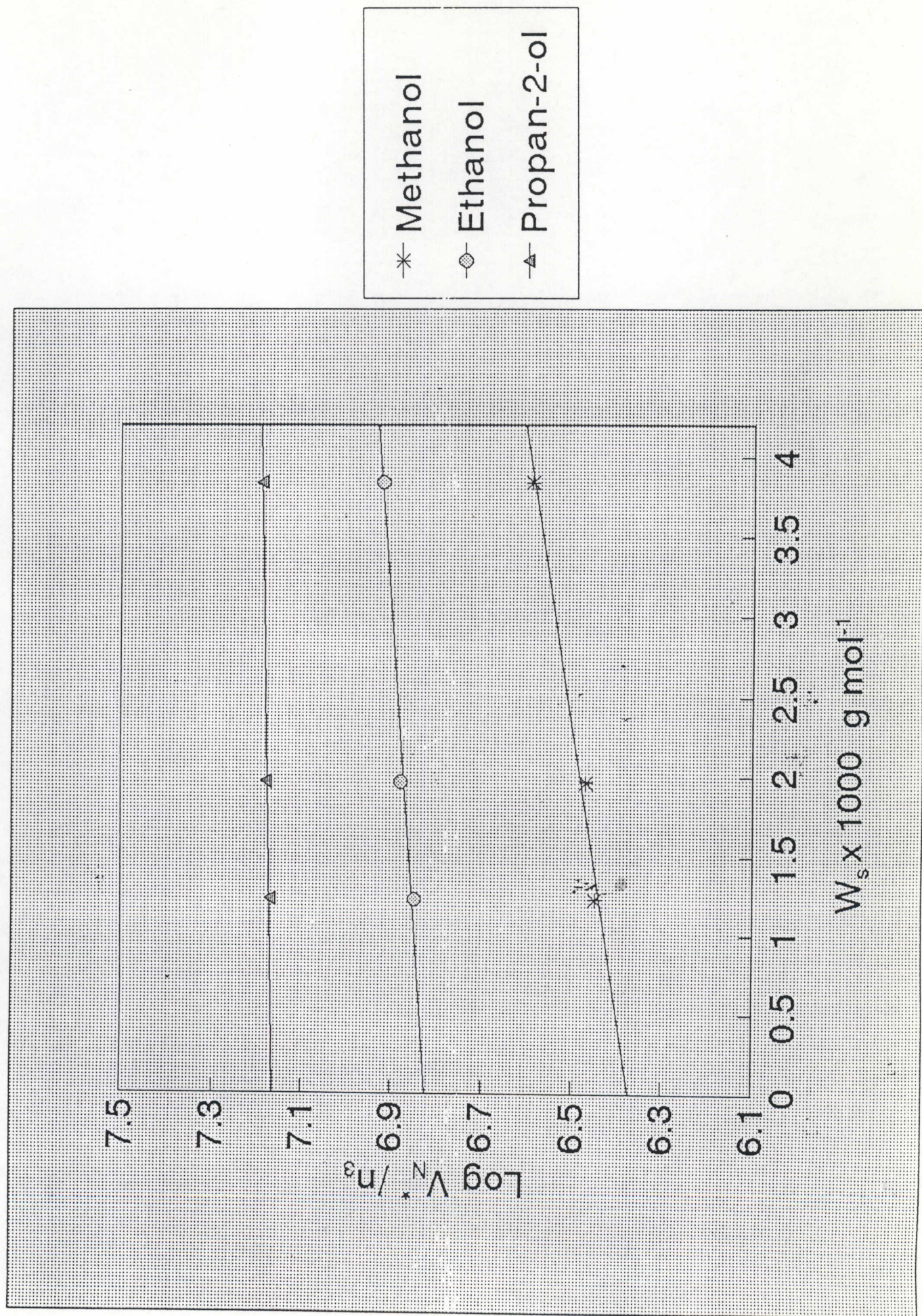
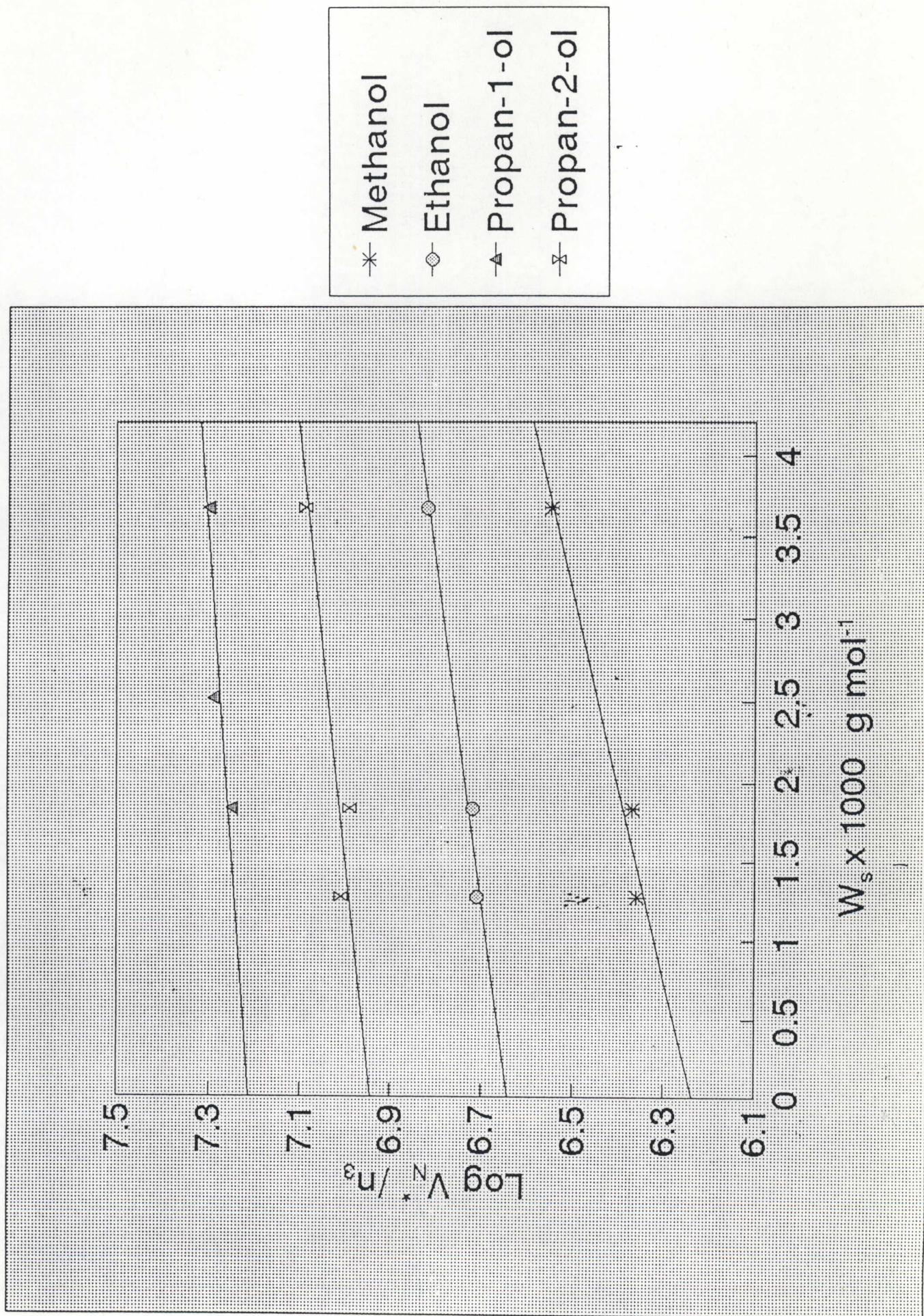


FIG. 5.23. Results for columns 4,5,6 and 7 at 303.15 K



5.3. ERROR ANALYSIS

Determination of the Error in γ_{13}^{∞} for the alkanol-hexadecane systems

The equation for determination of γ_{13}^{∞} is

$$\ln \gamma_{13}^{\infty} = \ln \frac{RT}{V_N' P_1^*} - \left[\frac{(B_{11} - V_1^*)}{RT} \right] P_1^* + \left[\frac{(2B_{12})}{RT} \right] P_o \quad (5.1.)$$

where

$$V_N' = V_N^* + \phi U_o J_3^2 \quad (5.2.)$$

The functional relationship between V_N' and γ_{13}^{∞} can be rewritten as

$$V_N' = \frac{RT}{P_1^* \gamma_{13}^{\infty}} * e^D \quad (5.3.)$$

where

$$V_N' = \frac{V_N^*}{n_3} \quad (5.4)$$

and

$$D = -\left[\frac{B_{11}-V_1^*}{RT}\right]P_1^* + \frac{B_{12}P_o}{RT} \quad (5.5)$$

The standard deviation of any function $x = f(u, v, \dots)$ is given by⁽²²⁾

$$\sigma_x^2 = \sigma_u^2 \left(\frac{\partial x}{\partial u}\right)^2 + \sigma_v^2 \left(\frac{\partial x}{\partial v}\right)^2 + \dots \quad (5.6)$$

Therefore

$$\sigma_{\gamma_{13}}^2 = \left(\frac{\partial \gamma_{13}^\infty}{\partial V_N'}\right)^2 * \sigma_{V_N'}^2 \quad (5.7)$$

$$\sigma_{\gamma_{13}}^2 = \left[\frac{(R^*T)}{P_1^*(V_N')^2} * e^D \right]^2 * \sigma_{V_N'}^2 \quad (5.8)$$

Now the net retention volume, V_N , is given by

$$V_N = (t_r - t_g)U_o J_3^2 \quad (5.9)$$

And

$$\sigma_{V_N}^2 = 2 * \left[\sigma_{U_o}^2 \left(\frac{\partial V_N}{\partial U_o}\right)^2 + \sigma_{t_r}^2 \left(\frac{\partial V_N}{\partial t_r}\right)^2 \right] \quad (5.10)$$

$\sigma_{V_N}^{1/2}$ is approximated to be $(\sigma_{V_N}^2)^{1/2} / 100$ at 293.15 K and $(\sigma_{V_N}^2)^{1/2} / 1000$ at 303.15 K.

Calculation of the Error in γ_{13}^{∞} for methanol in hexadecane at 293.15 K.

From equation 5.10.

$$\sigma_{V_N} = [(4 \cdot 10^{-8})^2 (1 \cdot 145)^2] + [(4)^2 \cdot (15 \cdot 10^{-7})^2] m^3$$

$$\sigma_{V_N} = 6 \cdot 10^{-11} m^3$$

Now from equation 5.8.

$$\sigma_{\gamma_{13}^{\infty}}^2 = \left[\frac{(R \cdot T)}{P_1^* (V_N')^2} \cdot e^D \right]^2 \cdot \sigma_{V_N}^2$$

$$\sigma_{\gamma_{13}^{\infty}} = \pm \sqrt{\left[\frac{(8.314)(293.15)}{(2.3988 \cdot 10^{-3})^2 \cdot (12996)} \cdot 0.94 \right]^2 \cdot 7 \cdot 10^{-8}} = \pm 8$$

5.4. DISCUSSION

The purpose of this work was to obtain a new method for the determination of the activity coefficients at infinite dilution for polar solutes in the solvent hexadecane. This method has actually been attempted once and that was by the Bristol group⁽³⁾. The Bristol group⁽³⁾ studied the benzene/glycerol/carbon dioxide system in which the solvent was polar. Their data treatment involved extrapolation of retention volume to zero mean column flowrate, zero mean column pressure, and to infinite solvent coverage on the packing. In this work our data was extrapolated to zero sample size,

zero mean column pressure, and to infinite solvent coverage on the packing. Another reason for choosing the alkanol-hexadecane systems was the paucity of accurate data in the literature for these mixtures.

5.4.1. Experimental Errors in γ_{13}^{∞} for the Polar Solute in a Non-polar Solvent

γ_{13}^{∞} and $\sigma\gamma_{13}^{\infty}$ for the solutes : methanol, ethanol, propan-1-ol and propan-2-ol in n-hexadecane at 293.15 K and 303.15 K are given in tables 5.4.1. and 5.4.2. The experimental error in γ_{13}^{∞} was determined from equation 5.8.

TABLE 5.4.1. The calculated values of γ_{13}^{∞} for the solutes : methanol, ethanol, and propan-2-ol in n-hexadecane at 293.15 K

Solute	$10^4 \times \sigma V_N^*/n_3$	γ_{13}^{∞}	$\sigma\gamma_{13}^{\infty}$
methanol	5.691	73	± 8
ethanol	6.216	54	± 7
propan-2-ol	3.446	38	± 2

TABLE 5.4.2. The calculated values of γ_{13}^{∞} for the solutes : methanol, ethanol, propan-1-ol and propan-2-ol in n-hexadecane at 303.15 K

Solute	$10^4 \times \sigma V_N^*/n_3$	γ_{13}^{∞}	$\sigma\gamma_{13}^{\infty}$
methanol	7.109	63	± 6
ethanol	5.128	49	± 5
propan-1-ol	11.43	38	± 2
propan-2-ol	13.98	36	± 3

To place the results obtained from this work in perspective with literature values obtained from the glc method, it is necessary to look at the effect of solute size, flowrate and loading on the net retention volume, V_N . Thereafter the techniques used by other workers will be analyzed.

The equation used in calculating γ_{13}^∞ is given by

$$\ln \gamma_{13}^\infty = \ln \frac{RT}{V_N' P_1^*} - \left[\frac{(B_{11} - V_1^*)}{RT} \right] P_1^* + \left[\frac{(2B_{12})}{RT} \right] P_o \quad (5.1.)$$

where

$$V_N = V_N^* + \phi U_o J_3^2 \quad (5.2.)$$

V_N^* is the net retention volume corrected to zero mean flowrate and V_N' is the molal retention volume extrapolated to infinite solvent coverage.

5.4.2. Solute size

The net retention volume V_N is related to the retention time at infinite dilution, t_r , by equation 5.3.

$$V_N = (t_r - t_g) U_o J_3^2 \quad (5.3.)$$

Each retention time, t_r^* , for a particular run was extrapolated to 0 mm³ to obtain the retention time at infinite dilution, t_r . From the tables and graphs given in Appendix iii, retention times decrease with decreasing sample size. The effect is a decrease in the net retention volume, V_N . From equation 5.1. it can be seen that a decrease in V_N results in an increase in γ_{13}^∞ .

$$\ln \gamma_{13}^{\infty} = \ln \frac{n_3 RT}{V_N^o P_1^*} - \left[\frac{(B_{11} - V_1^*)}{RT} \right] P_1^* + \left[\frac{(2B_{12})}{RT} \right] P_o \quad (3.4.)$$

Polar solutes at infinite concentration will tend to associate in non-polar solvents giving large values for the activity coefficient at infinite dilution. Therefore the condition of infinite dilution must be satisfied, especially if γ_{13}^{∞} is large, in order to obtain meaningful results. For example, it is possible that at a solute size of $x_1 = 0.1 \text{ mm}^3$ the activity coefficient could be very different from from $x_1 \rightarrow 0 \text{ mm}^3$. If γ_{13}^{∞} is $\gg 100$ at $x_1 = 0.1 \text{ mm}^3$ then at $x_1 \rightarrow 0 \text{ mm}^3$, γ_{13}^{∞} could be 40. To ensure infinite dilution, retention times were extrapolated to zero injection volume. Furthermore because of the complex process taking place on the column (adsorption and dissolution of the solute) and slowness of the equilibration the retention volume was found to be a function of carrier-gas flowrate. As a result extrapolation to zero flowrate was required.

5.4.3. Flowrate

From equation 5.3. it can be seen that V_N is proportional to the flowrate, U_o . Since retention volumes were extrapolated to zero flowrate and from the graphs of flowrate versus retention volume (figures 5.1. - 5.21.), V_N decreases with decreasing flowrate. The dependence of the net retention volume (at zero solute size) on mean column flowrate was as much as 45% of the extrapolated net retention volume at zero mean column flowrate. The decrease in net retention volume (at zero sample size) translates as an increase in $\ln RT/V_N^o P_o^*$, hence an increase in γ_{13}^{∞} .

5.4.4. Percentage loading

The graphs plotted for $\text{Log } V_N/n_3$ versus W_s , where W_s is the mass of celite per mole of solvent, shows a clear trend. As W_s approaches zero ie. in the limit of infinite coverage $\text{Log } V_N/n_3$ also decreases. The implication is that n_3/V_N

becomes larger, hence γ_{13}^{∞} also becomes larger. The effect of extrapolating the data to infinite solvent coverage in one case was as large as 2.5% expressed as a function of the $\text{Log } V_N^*/n_3$ values.

Since the mixed second virial coefficient is relatively large it was necessary to account for B_{12} in the calculation of γ_{13}^{∞} . In the literature relating to the determination of γ_{13}^{∞} on alkanol-hexadecane systems none of the workers took into account B_{12} values in the calculation of γ_{13}^{∞} . Alessi *et al*⁽⁴⁴⁾ did a series of work on the alkanol-hexadecane systems. Their retention times were corrected to infinite dilution conditions. However their method does not extrapolate to zero mean flowrate and infinite solvent coverage. Their values for γ_{13}^{∞} are smaller than our values probably because the effect of mean column flowrate and solvent coverage on the column was not considered in their data treatment.

Kwantes and Rijnders⁽⁴²⁾ determined the activity coefficient for the polar solutes methanol, ethanol, propan-1-ol, and propan-2-ol in hexadecane by glc. Their work involved the use of fine metal helices to completely eliminate adsorption on the support. The peaks obtained for the polar solute were symmetrical and independent of sample size ensuring infinite dilute conditions.

Park *et al*⁽⁴⁵⁾ used headspace analysis to determine γ_{13}^{∞} for the ethanol-hexadecane system. The analytical measurements were the slope of either the area or the height of the solute peak and mole fraction. The slopes were then used to calculate the apparent Henry's Law constant to ensure infinite dilution conditions. The Henry's Law infinite dilution activity coefficient is used in the calculation of the activity coefficient at infinite dilution. The value of the activity coefficient obtained from the work by Park *et al*⁽⁴⁵⁾ is smaller than ours. This can be due to the fact that for polar solute in nonpolar solvent the partition coefficient depends entirely on the solute-solvent interactions which in turn is dependent on the Henry's law constant. The Henry's Law constants are sensitive to the experimental conditions. Therefore the type of peak obtained and its symmetry will be important in calculating the Henry's Law constant.

In our method the effect of peak asymmetry was taken into effect by extrapolating the net retention volume to zero mean column flowrate.

Our results are higher than the literature values in most cases. This could be due to extrapolation of the net retention volume data to infinite sample size, zero mean column flowrate and to infinite solvent coverage.

Table 5.4.3. is a summary of the activity coefficients at infinite dilution obtained by other workers on similar systems.

TABLE 5.4.3. Comparison of γ_{13}^{∞} with literature values of γ_{13}^{∞}

Solute	Temperature	γ_{13}^{∞}	γ_{13}^{∞}	Author
	K	This work	literature	
Methanol	293.15	73	83.76 ⁽⁴¹⁾	Gritinia
	298.15	-	71.50 ⁽⁴²⁾	Kwantes et al
	303.15	63	58.00 ⁽⁴³⁾	Ignat et al
	312.0	-	21.53 ⁽⁴⁴⁾	Alessi et al
Ethanol	293.15	54	54.65 ⁽⁴¹⁾	Gritinia
	298.15	-	34.75 ⁽⁴²⁾	Kwantes et al
	303.15	49	-	
	312.0	-	20.35 ⁽⁴⁴⁾	Alessi et al
Propan-1-ol	298.15	-	31.50 ⁽⁴²⁾	Kwantes et al
	303.15	38	24.02 ⁽⁴⁵⁾	Park et al
	312.0	-	18.14 ⁽⁴⁴⁾	Alessi et al
Propan-2-ol	293.15	38	-	
	298.15	-	26.50 ⁽⁴²⁾	Kwantes et al
	303.15	36	-	

The technique used is slow and tedious due to slow equilibration of the solute molecules between the gaseous and liquid phases. At lower liquid loadings there is greater adsorption of solute molecules on the column packing resulting in increased peak asymmetry. In some cases the sample retention times decreased from approximately $0.1 \text{ mm}^3 - 1 \text{ mm}^3$ and in other cases there was an increase in retention times from $0.2 \text{ mm}^3 - 0.1 \text{ mm}^3$. Although our data was extrapolated to infinite solute size, it is not possible to tell from this work whether for solute size below 0.1 mm^3 if the retention times will increase or decrease. However, Martire and Riedl⁽⁴¹⁾ explained that at low sample size ($< 0.1 \text{ mm}^3$) there is incomplete saturation of the adsorbing surface resulting in longer retention times with peak trailing. A major problem with small sample sizes is that the detector sensitivity is lessened.

At low liquid loadings as in the case of this work there are greater uncertainties in the retention times. Cruickshank *et al*⁽³⁾ found that when the retention volumes are small, as for methanol, then the experimental uncertainty in $\log V_N^* / n_3$ versus W_s is large. Due to the trailing of some peaks at lower column loadings non-equilibrium effects⁽²²⁾ could have also effected the results. A possible way to improve the method would be to set the outlet pressure and to extrapolate the net retention data (corrected for infinite dilution and to zero mean column flowrate) to zero mean column pressure. before extrapolation of the net retention volume to infinite solvent coverage.

5.5. CONCLUSION

The glc technique is usually a very rapid one but when polar solutes are involved the simple technique has to be altered. The method is time-consuming with peak asymmetry increasing with liquid loadings. To eliminate adsorption a high loading of the solvent should be used to ensure that the support surface is completely covered with solvent. The method used results in large errors in γ_{13}^{∞} due to the number of extrapolations that had to be done. The error in the calculated value of γ_{13}^{∞} ranged between 5 - 10%. Comparison of γ_{13}^{∞} from this work with the literature values indicates that the accuracy of the γ_{13}^{∞} values is not high.

6. NON-POLAR SOLUTES IN DECANE

6.1. INTRODUCTION

The aim of this experiment was to extend the method previously developed by Letcher *et al*⁽⁴⁾ to include a more volatile solvent. Decane was chosen as the "more volatile solvent".

Letcher *et al*⁽⁴⁾ have extended the Everett⁽²⁾ and Cruickshank⁽³⁾ theory to include a moderately volatile solvent by relating the solvent evaporation off the column to its partial pressure (P_3')

$$\frac{V_N}{n_3 e^c} = \frac{RT}{\gamma_{13}^\infty P_1^*} - \frac{U_o t}{n_3} \left[\frac{P_3'}{\gamma_{13}^\infty P_1^*} \right] \quad (6.1.)$$

where

$$C = - \left[\frac{B_{11} - V_1^*}{RT} \right] P_1^* + \left[\frac{2B_{12} - V_1^\infty}{RT} \right] P_o J_2^3 \quad (6.2.)$$

U_o is the volumetric flowrate corrected to column temperature and for the presence of water vapour and t is the time of injection of the solute into the column. B_{11} and B_{12} were calculated from McGlashan and Potter's⁽³⁸⁾ modification of the Beattie - Bridgeman⁽⁴⁷⁾ equation.

Moollan⁽³⁴⁾ used this technique to determine the activity coefficient at infinite dilution for n-alkanes in cis- and trans-decalin.

Other workers have calculated γ_{13}^∞ for volatile solvents using different techniques.

Kwantes and Rijnders⁽⁴²⁾ avoided evaporation of the solvent off the column by the use of a presaturator. Letcher *et al*⁽⁴⁸⁾ monitored the loss of solvent by measuring the retention time of a solute at intervals. Relative gas-liquid chromatography was also used by Letcher⁽⁴⁹⁾ to determine γ_{13}^{∞} values for volatile solvents. In this method one γ^{∞} value must be known for one solvent under the conditions of measurements. γ^{∞} in each of the solvents is then a function of the specific retention volume, V_g° .

6.2. RESULTS

In this work the theory developed by Letcher *et al*⁽⁴⁾ was extended to include a volatile solvent. Data were collected for 8 columns at two temperatures, 278.15 K and 293.15 K. The solutes were pentane, cyclopentane, hexane, cyclohexane and benzene in the solvent decane. Helium was used as the carrier gas and gas retention times, t_g were determined by injecting air into the column. For each column loading the flowrate was kept constant. The solvent loading varied from 0.4% to 4%. A small percentage loading was used at 278.15 K to obtain retention times of a few minutes. It was important in this work to obtain $U_0 t/n_3$ as close to zero, since this indicates retention times in the solvent before any evaporation has occurred. Depending on the column packing the flowrate was set to obtain retention times, t_r of a few minutes. Data was collected for the retention time of the solute, t' , the time of injection of the solute, t , the gas hold-up time, t_g , and the flowrate of the carrier gas, U_0 . Each column was used for between 1 hr. and 1.5 hrs.

Based on equation 6.1. graphs of $U_0 t/n_3$ versus $V_N/n_3 e^C$ were plotted. γ_{13}^{∞} was calculated from the intercept and the partial pressure of the solvent P_3' , was determined from the slopes of the graphs.

The intercept is given by

$$a = \frac{RT}{\gamma_{13}^{\infty} P_1^*} \quad (6.3.)$$

and the slope

$$b = \frac{P'_3}{\gamma_{13}^\infty P_1^*} \quad (6.4.)$$

P'_3 , the partial pressure of the solvent, was obtained by dividing b by a

$$\frac{b}{a} = \frac{P'_3}{RT} \quad (6.5.)$$

Tables 6.1.1. is a summary of the moles of solvent on the column together with the operating conditions for each column. The results obtained from columns 8 -15 are summarised in tables 6.1.2. to 6.1.9. and the graphs obtained for $U_0 t/n_3$ versus $V_N/n_3 e^C$ plots are given in figures 6.1. to 6.10. Table 6.1.12 to 6.1.14. summarises the results obtained for γ_{13}^∞ and P'_3 .

Table 6.1.1. Column Specifications and Operating Conditions

Column No.	n_3 mmol	$10^{-5} \times P_i$ Pa	$10^{-5} \times P_o$ Pa	t_g s	J_3^2	$10^7 \times U_o$ $m^3 s^{-1}$
8	2.184	1.38658	1.08742	25.06	0.874	8.8368
9	3.301	1.36453	1.09243	21.00	0.885	10.708
10	3.121	1.49411	1.08619	19.96	0.834	13.841
11	1.868	1.49521	1.09098	14.73	0.836	15.097
12	6.618	1.47230	1.09439	23.59	0.845	8.837
13	6.739	1.36937	1.09439	26.58	0.884	9.222
14	3.301	1.48918	1.09185	24.39	0.839	11.448
15	2.863	1.45914	1.08619	21.07	0.847	12.113

Experiment 6.1.1. n-Pentane and cyclopentane in decane on Column 8 at 278.15 K

TABLE 6.1.2. Results obtained from column 8 with n-pentane and cyclopentane

run as a mixture at 278.15 K.

Run No.	$10^{-3} \times t$ s	t_r s	$10^5 \times V_N$ m^3	$V_N/n_3 e^e$ $m^3 \text{ mol}^{-1}$	$U_o t/n_3$ $m^3 \text{ mol}^{-1}$
	Solute: Pentane				
1.	1.8003	61.28	1.4239	0.06399	7.284
2.	2.1003	61.60	1.4177	0.06385	8.498
3.	2.4004	59.41	1.3567	0.06110	9.712
4.	3.0005	57.67	1.2995	0.05852	12.140
5.	3.3005	55.28	1.2384	0.05577	13.354
6.	3.8485	55.33	1.1340	0.05107	15.571

	Solute: Cyclopentane				
7.	1.8003	61.28	2.8000	0.1300	7.2843
8.	2.4004	59.41	2.6825	0.1233	9.7123
9.	2.7018	57.41	2.6137	0.1161	10.9321
10.	3.0005	57.67	2.5518	0.1170	12.1407
11.	3.3005	55.28	2.4050	0.1111	13.3543
12.	3.8485	55.33	2.3400	0.1086	15.5717

Experiment 6.1.2. n-Hexane in decane on Column 9 at 278.15 K

TABLE 6.1.3 Results obtained from column 9 with n-hexane as the solute.

Run No.	$\frac{10^{-3} \times t}{s}$	t_r s	$\frac{10^5 \times V_N}{m^3}$	$\frac{V_N/n_3e^c}{m^3 \text{ mol}^{-1}}$	$\frac{U_0t/n_3}{m^3 \text{ mol}^{-1}}$
13.	0.7955	107.00	8.1884	0.2702	2.8358
14.	1.5127	99.92	7.5143	0.2480	5.3924
15.	2.0327	95.21	7.0658	0.2332	7.2462
16.	2.1698	93.52	6.9049	0.2279	7.7347
17.	2.4484	92.23	6.7821	0.2238	8.7279
18.	2.7250	89.17	6.4907	0.2142	9.7139
19.	3.1268	86.09	6.1975	0.2045	11.1461
20.	3.4193	84.20	6.0175	0.1906	13.6168

Experiment 6.1.3. Cyclohexane in decane on Column 10 at 278.15 K

TABLE 6.1.4. Results obtained from column 10 with cyclohexane as the solute.

Run No.	$10^{-3} \times t$ s	t_r s	$10^4 \times V_N$ m^3	V_N/n_3e^c $m^3 \text{ mol}^{-1}$	$U_o t/n_3$ $m^3 \text{ mol}^{-1}$
21.	0.8049	148.14	1.4814	0.4736	3.5699
22.	1.2416	127.62	1.2442	0.3977	5.5069
23.	1.6661	123.54	1.1971	0.3827	7.3895
24.	1.8284	124.00	1.2024	0.3844	8.1094
25.	1.9987	119.88	1.1548	0.3691	8.8647
26.	2.1677	121.00	1.1677	0.3733	9.6142
27.	2.7004	113.53	1.0814	0.3457	11.9766
28.	3.0003	111.17	1.0541	0.3370	13.3067

Experiment 6.1.4. Benzene in decane on Column 11 at 278.15 K

TABLE 6.1.5. Results obtained from column 11 with benzene as the solute.

Run No.	$10^{-3} \times t$ s	t_r s	$10^5 \times V_N$ m^3	V_N/n_3e^c $m^3 \text{ mol}^{-1}$	$U_o t/n_3$ $m^3 \text{ mol}^{-1}$
29.	1.1666	61.60	5.9217	0.3163	9.4286
30.	1.8007	59.44	5.6488	0.3017	14.5537
31.	2.1003	56.41	5.2660	0.2813	16.9751
32.	2.4004	55.39	5.1371	0.2744	19.3999
33.	2.7004	52.69	4.7960	0.2562	21.8248

Experiment 6.1.5. Pentane in decane on Column 12 at 293.15 K

TABLE 6.1.6. Results obtained from column 12 with pentane as the solute.

Run No.	$\frac{10^{-3} \times t}{s}$	$\frac{t_r}{s}$	$\frac{10^4 \times V_N}{m^3}$	$\frac{V_N/n_3e^c}{m^3 \text{ mol}^{-1}}$	$\frac{U_0t/n_3}{m^3 \text{ mol}^{-1}}$
34.	1.8798	231.40	2.0179	0.03140	0.3263
35.	2.3482	233.03	2.0338	0.03164	0.4076
36.	2.7295	191.08	1.6264	0.02531	0.4739
37.	3.1714	194.06	1.6553	0.02576	0.5506
38.	3.9387	161.74	1.3415	0.02087	0.6838
39.	4.7573	112.84	0.8666	0.01348	0.8259

Experiment 6.1.6. Cyclopentane in decane on Column 13 at 293.15 K

TABLE 6.1.7. Results obtained from column 13 with cyclopentane as the solute.

Run No.	$\frac{10^{-3} \times t}{s}$	$\frac{t_r}{s}$	$\frac{10^5 \times V_N}{m^3}$	$\frac{V_N/n_3e^c}{m^3 \text{ mol}^{-1}}$	$\frac{U_0t/n_3}{m^3 \text{ mol}^{-1}}$
40.	0.6032	89.63	5.2154	0.07606	0.8255
41.	0.9027	86.78	4.9225	0.07179	1.2354
42.	1.2003	83.74	4.8254	0.07038	1.6427
43.	1.5110	83.24	4.6230	0.06743	2.0678
44.	1.8003	80.58	4.4060	0.06426	2.4638
45.	2.1003	79.48	4.3162	0.06295	2.8743
46.	2.4009	75.98	4.0307	0.05879	3.2856
47.	2.7003	74.74	3.9295	0.05731	3.6955

Experiment 6.1.7. n-hexane and cyclohexane in decane on Column 14 at 293.15 K

TABLE 6.1.8. Results obtained from column 14 with n-hexane and cyclohexane

Run No.	$\frac{10^{-3} \times t}{s}$	t_r s	$\frac{10^5 \times V_N}{m^3}$	$\frac{V_N/n_3 e^c}{m^3 \text{ mol}^{-1}}$	$\frac{U_o t/n_3}{m^3 \text{ mol}^{-1}}$
Solute: Hexane					
48.	0.6239	72.96	4.6700	0.1399	2.1636
49.	1.1611	64.90	3.8927	0.1167	4.0266
50.	1.3772	61.06	3.5227	0.1056	4.7759
51.	1.5009	60.39	3.4593	0.1037	5.2049
52.	1.7806	56.74	3.1086	0.09321	6.1749
53.	2.2517	52.16	2.6685	0.08001	7.8085
54.	2.5612	50.02	2.4628	0.07305	8.8818
55.	2.7005	48.25	2.2928	0.06875	9.3649
56.	3.0003	43.81	1.8661	0.05596	10.4047
57.	3.3222	41.84	1.6768	0.05028	11.5210
58.	3.6003	38.42	1.3482	0.04042	12.4851
Solute: Cyclohexane					
59.	0.6239	100.76	7.3387	0.2209	2.1636
60.	1.1611	89.76	6.2816	0.1890	4.0266
61.	1.3772	84.73	5.7983	0.1745	4.7759
62.	1.5009	83.96	5.7243	0.1723	5.2049
63.	1.7806	76.32	4.9901	0.1502	6.1749
64.	2.2517	70.45	4.4261	0.1332	7.8085
65.	2.5612	68.20	4.2098	0.1267	8.8818
66.	2.7005	63.34	3.7428	0.1126	9.3649
67.	3.0003	55.82	3.0202	0.09091	10.4047
68.	3.3222	53.17	2.7655	0.08324	11.5210
69.	3.6003	46.39	2.1140	0.0636	12.4851

Experiment 6.1.8. Benzene in decane on Column 15 at 293.15 K

TABLE 6.1.9. Results obtained from column 15 with benzene as the solute.

Run No.	$\frac{10^{-3} \times t}{s}$	$\frac{t_r}{s}$	$\frac{10^5 \times V_N}{m^3}$	$\frac{V_N/n_3 e^c}{m^3 \text{ mol}^{-1}}$	$\frac{U_o t/n_3}{m^3 \text{ mol}^{-1}}$
70.	0.6125	70.64	4.7034	0.1632	2.5912
71.	1.2004	60.66	3.9869	0.1384	5.0777
72.	1.5513	56.06	3.4305	0.1190	6.5622
73.	1.8004	51.81	3.0620	0.1091	7.6158
74.	2.1003	46.65	2.6565	0.09222	8.8843
75.	2.4004	43.75	2.3281	0.08082	10.1537
76.	2.7122	38.59	1.7984	0.06243	11.4727

Table 6.1.10. Data used in the calculation of V_N from equation 4.4. where P_1^* is the vapour pressure of the pure solute, V_1^* is the molar volume of the solute, B_{12} is the mixed virial coefficient and B_{11} is the second virial coefficient of the solute at 278.15 K.

Solute	$\frac{P_1^*}{\text{Pa}}$	$\frac{10^6 \times V_1^*}{m^3 \text{ mol}^{-1}}$	$\frac{10^6 \times B_{12}}{m^3 \text{ mol}^{-1}}$	$\frac{-(10^6 \times B_{11})}{m^3 \text{ mol}^{-1}}$
n-pentane	30555.66	112.4	23	1.642
cyclopentane	18012.7	92.24	19	1.527
n-hexane	7865.59	128.06	28	2.334
cyclohexane	4876.14	106.17	23	2.550
benzene	4803.57	87.31	19	2.241

Table 6.1.11. Data used in the calculation of V_N from equation 4.4. where P_1^* is the vapour pressure of the pure solute, V_1^* is the molar volume of the solute, B_{12} is the mixed virial coefficient and B_{11} is the second virial coefficient of the solute at 293.15 K.

Solute	P_1^*	$10^6 \times B_{12}$	$-10^6 \times B_{11}$
	Pa	$\text{m}^3 \text{mol}^{-1}$	$\text{m}^3 \text{mol}^{-1}$
n-pentane	56559.51	24	1.222
cyclopentane	34599	20	1.317
n-hexane	16182.49	29	1.995
cyclohexane	10337.59	24	2.154
benzene	10330.06	20	1.901

TABLE 6.1.12. The critical constants and ionization energies, I , used in the calculation of the mixed second virial coefficient, B_{12} at 278.15 K and 293.15 K

Solute	V_c^*	T_c	I
	$\text{m}^3 \text{mol}^{-1}$	K	kJ mol^{-1}
pentane	304.0	496.65	0.9937
cyclopentane	260.0	511.61	1.0139
hexane	370.0	507.68	0.9822
cyclohexane	309.7	553.64	0.9431
benzene	259.4	562.1	0.9242
helium	5.2	57.8	5.428

TABLE 6.1.13. Results obtained from figures 6.1. to 6.5. together with the calculated values for γ_{13}^{∞} and P_3' for solutes : pentane, cyclopentane, hexane, cyclohexane and benzene at 278.15 K using the equations $a = RT/(P_1^* \gamma_{13}^{\infty})$ and $b/a = P_3'/RT$ where a is the intercept and b the slope.

Figure	Solute	a	γ_{13}^{∞}	b	P_3'
		$m^3 \text{ mol}^{-1}$		$m^3 \text{ mol}^{-1}$	Pa
6.1.	pentane	0.07651	0.99	0.001574	48
6.2.	cyclopentane	0.1461	0.88	0.002564	41
6.3.	hexane	0.2898	1.01	0.007663	61
6.4.	cyclohexane	0.4858	0.98	0.01204	57
6.5.	benzene	0.3656	1.32	0.004844	31

TABLE 6.1.14. Results obtained from figures 6.6. to 6.10. together with the calculated values for γ_{13}^{∞} for solutes : pentane, cyclopentane, hexane, cyclohexane and benzene at 293.15 K using the equations $a = RT/(P_1^* \gamma_{13}^{\infty})$ and $b/a = P_3'/RT$ where a is the intercept and b the slope.

Figure	Solute	a	γ_{13}^{∞}	b	P_3'
		$m^3 \text{ mol}^{-1}$		$m^3 \text{ mol}^{-1}$	Pa
6.7.	cyclopentane	0.08068	0.87	0.06439	195
6.8.	hexane	0.1533	0.98	0.009157	146
6.9.	cyclohexane	0.2479	0.95	0.01461	144
6.10.	benzene	0.1917	1.23	0.01090	139

FIG. 6.1. Pentane in decane on column 8 at 278.15 K

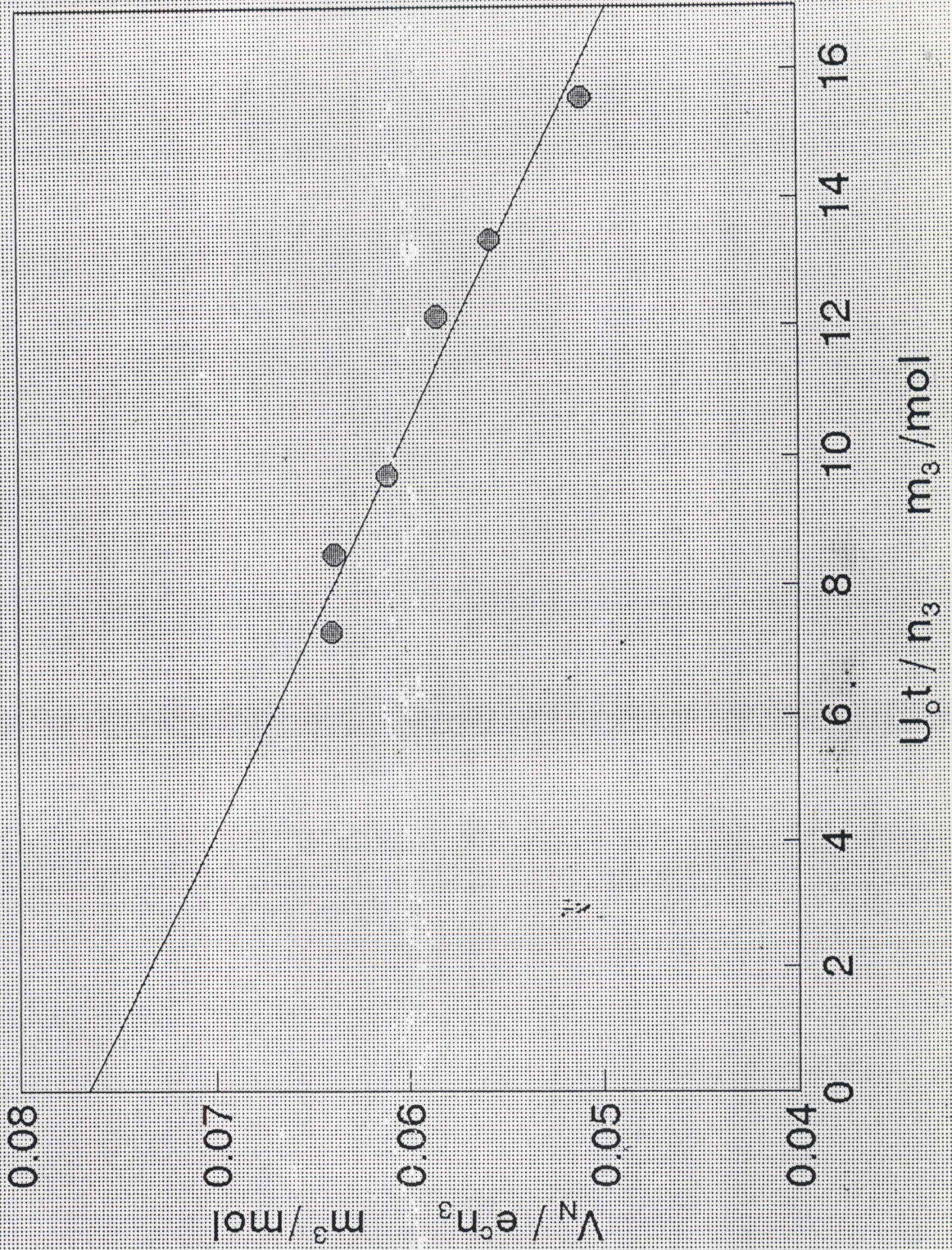


FIG. 6.2. Cyclopentane in decane on column 8 at 278.15 K

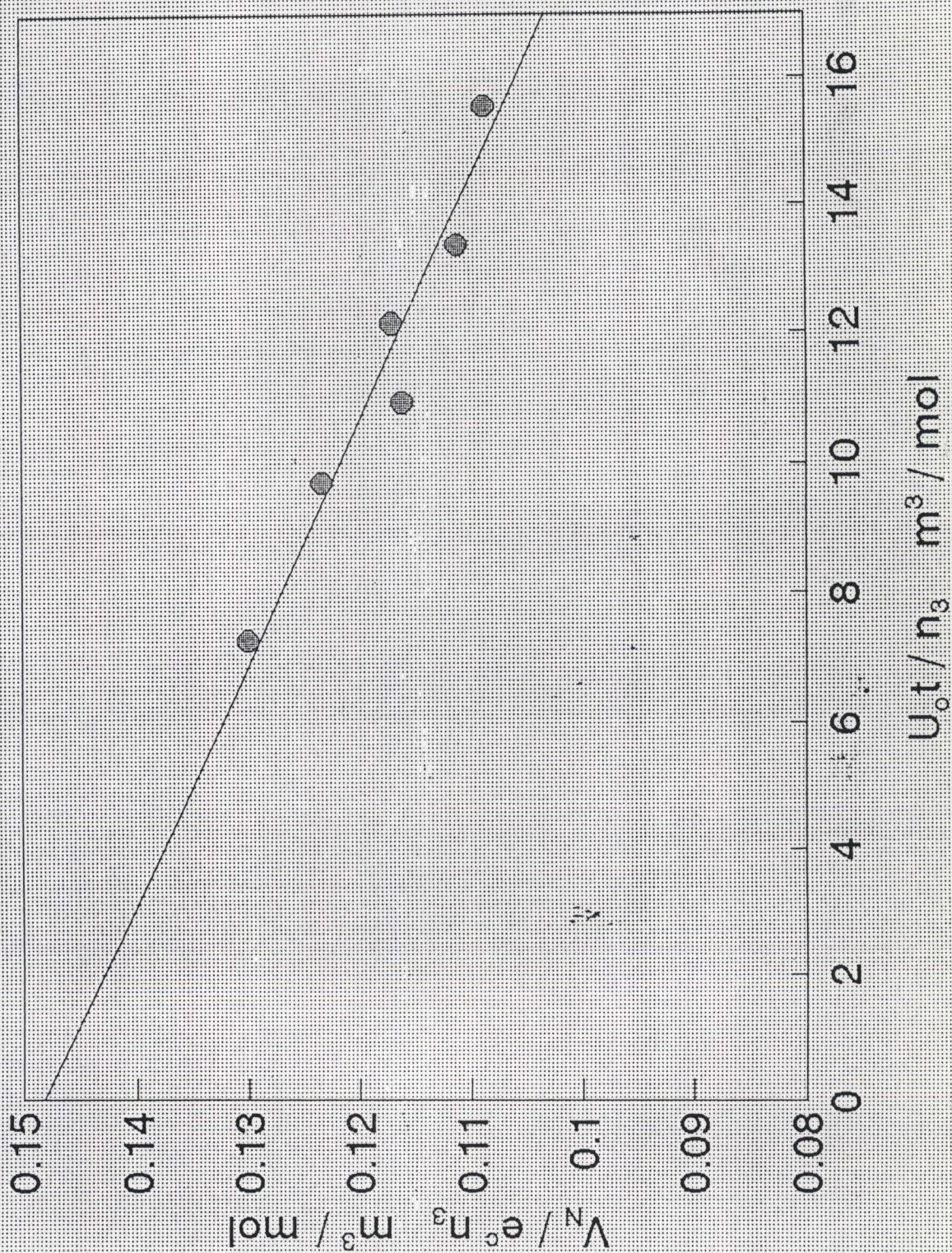


FIG. 6.3. Hexane in decane on column 9 at 278.15 K

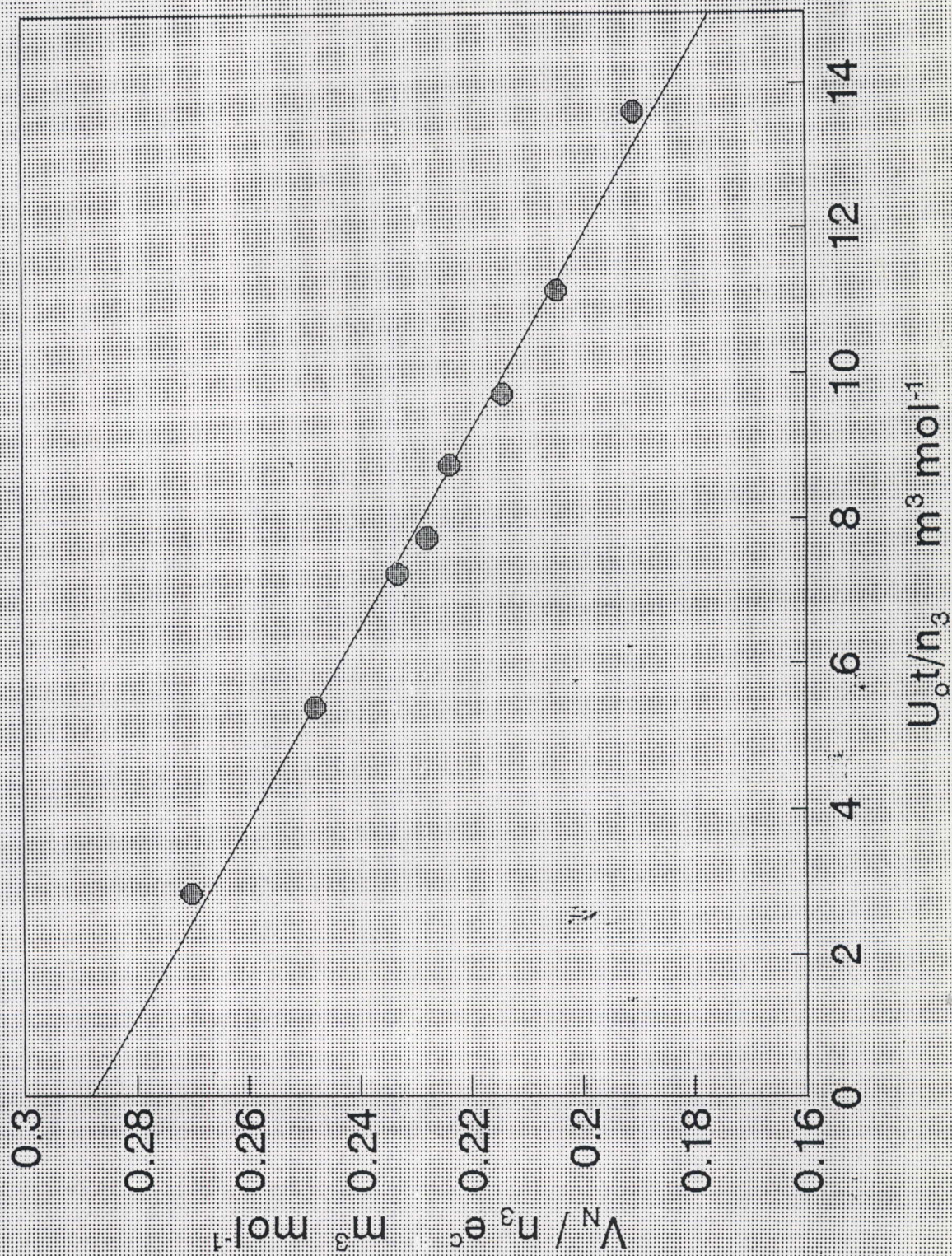


FIG. 6.4. Cyclohexane in decane on column 10 at 278.15 K

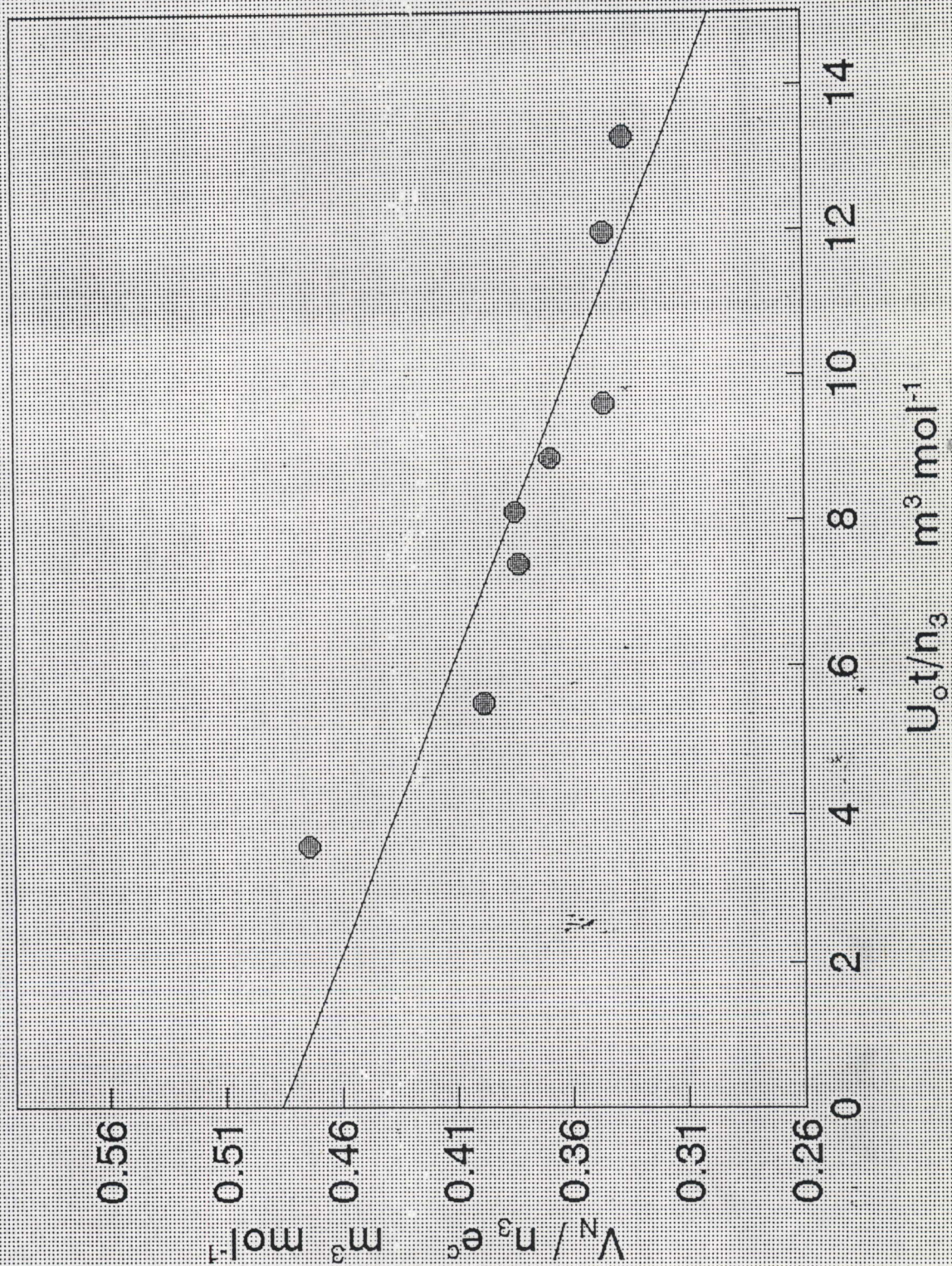


FIG. 6.5. Benzene in decane on column 11 at 278.15 K

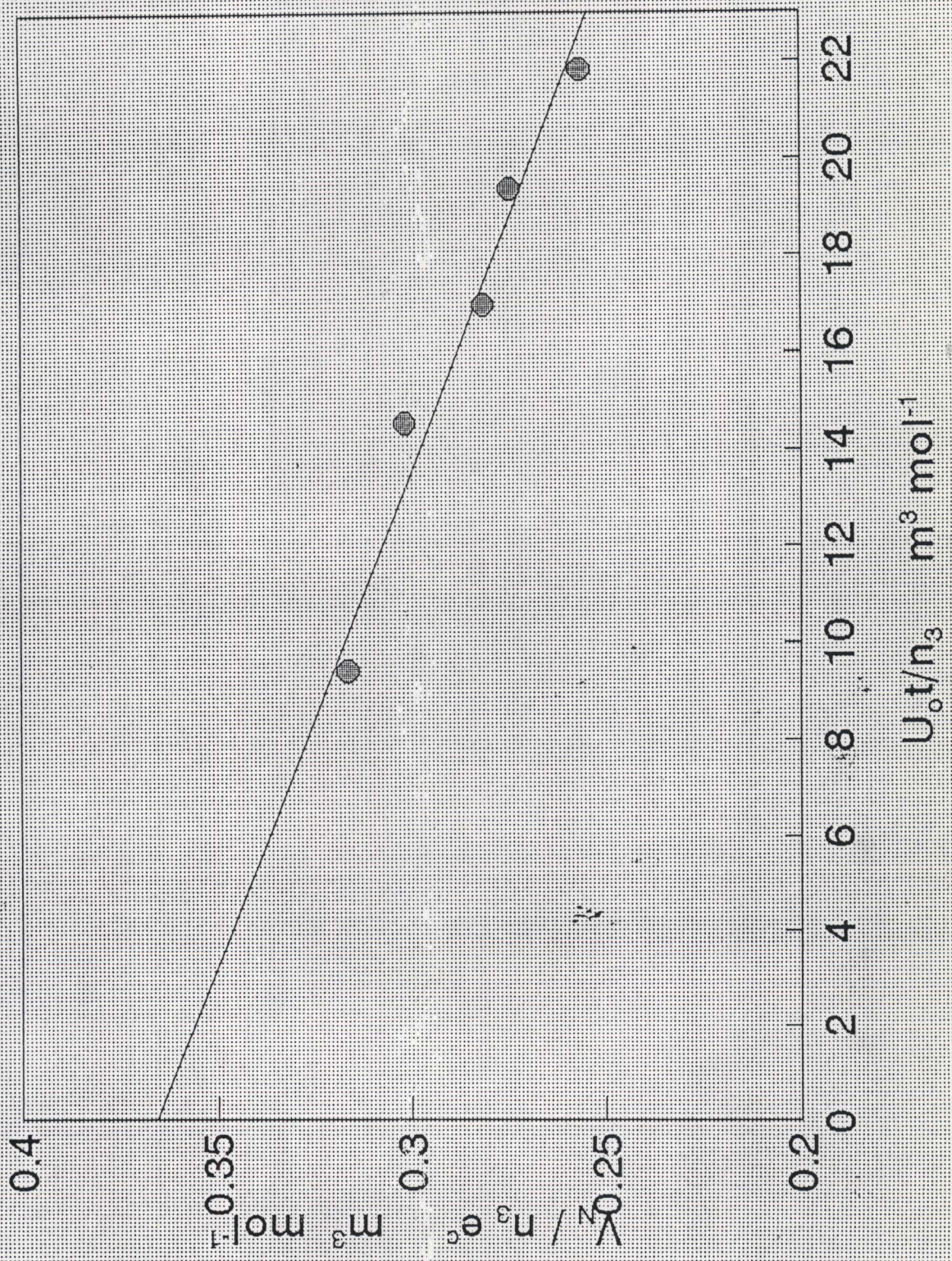


FIG. 6.6. Pentane in decane on column 12 at 293.15 K

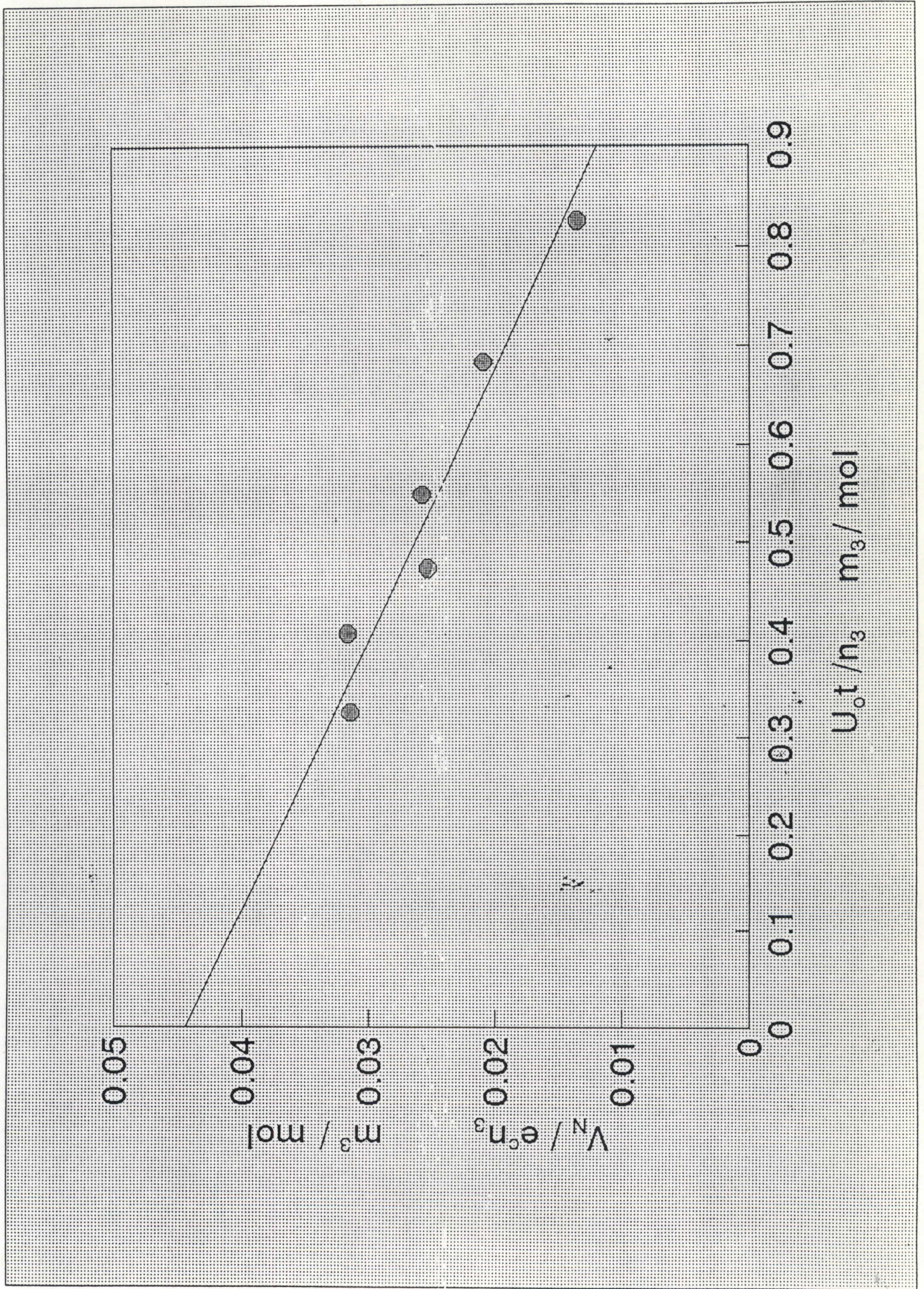


FIG. 6.7. Cyclopentane in decane on column 13 at 293.15 K

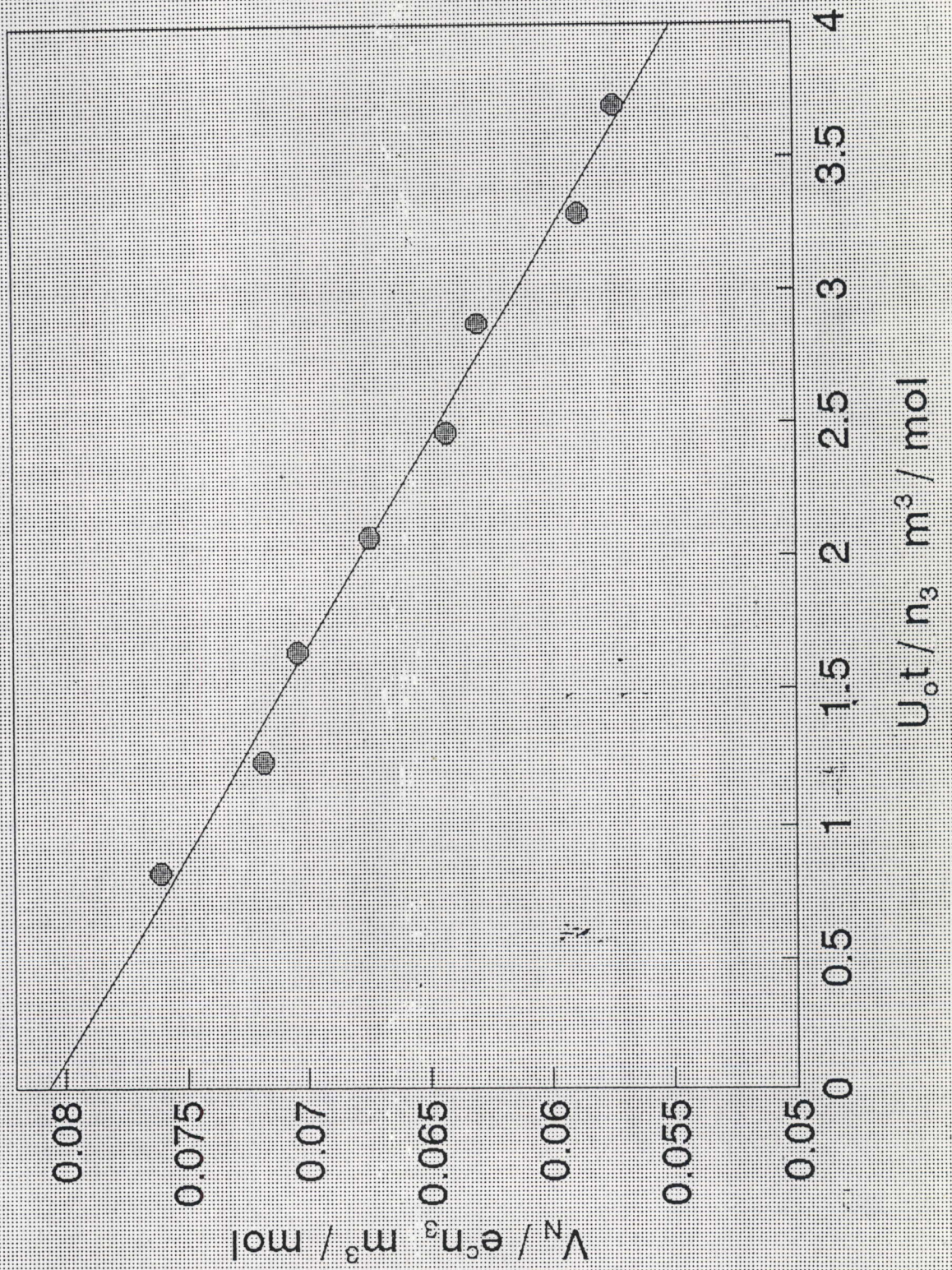


FIG. 6.8. Hexanè in decane on column 14 at 293.15 K

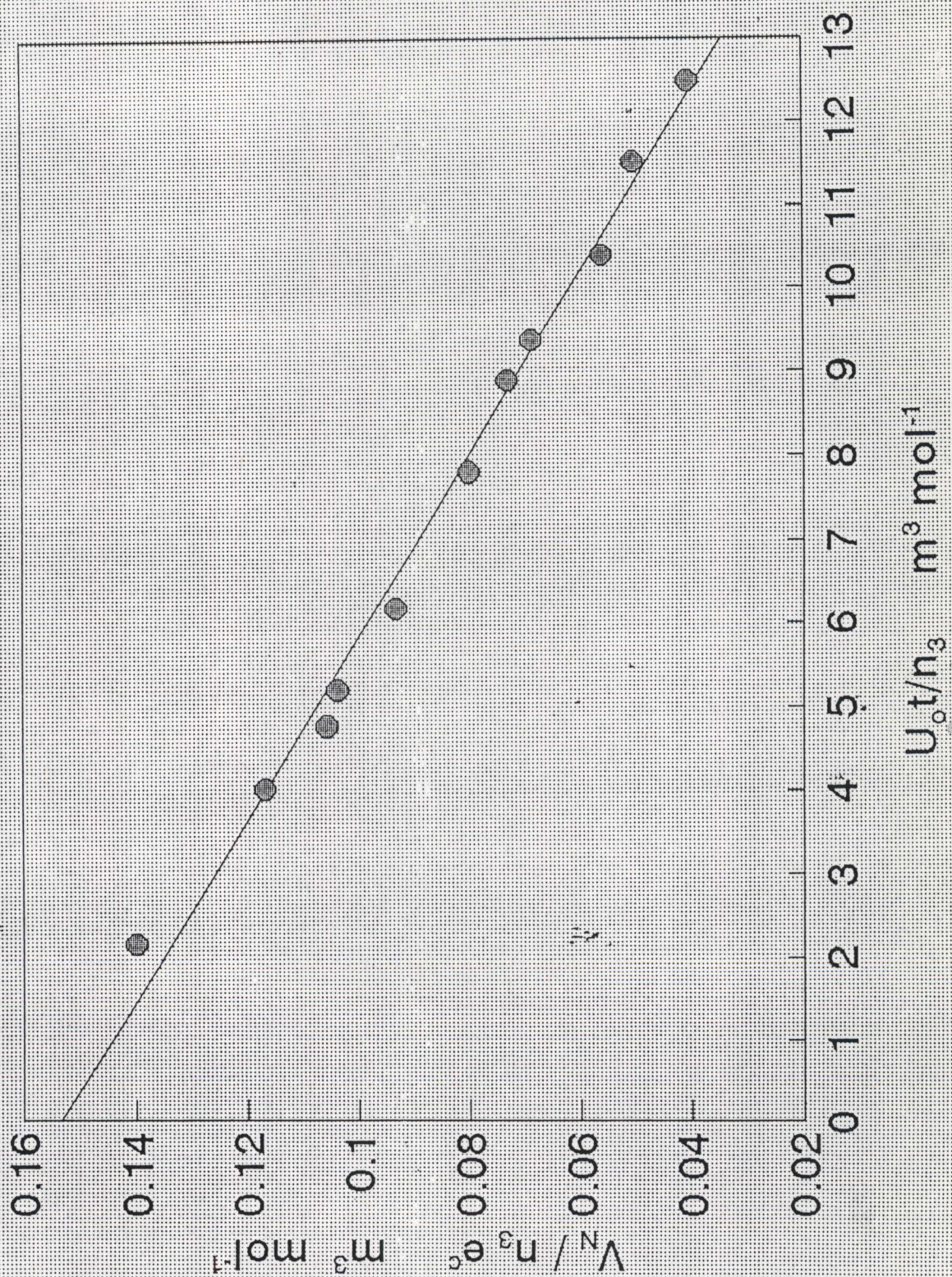


FIG. 6.9. Cyclohexane in decane on column 14 at 293.15 K

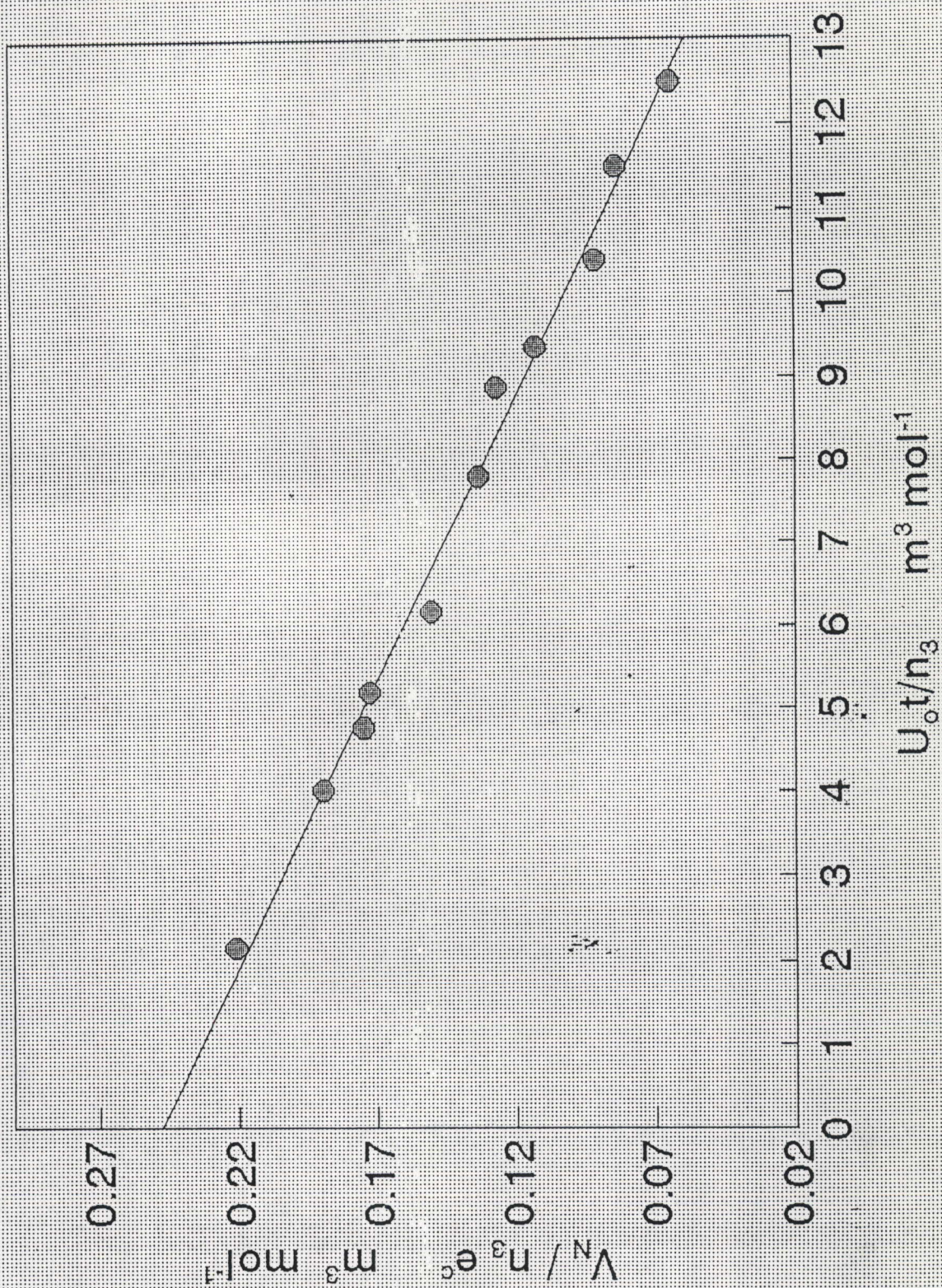
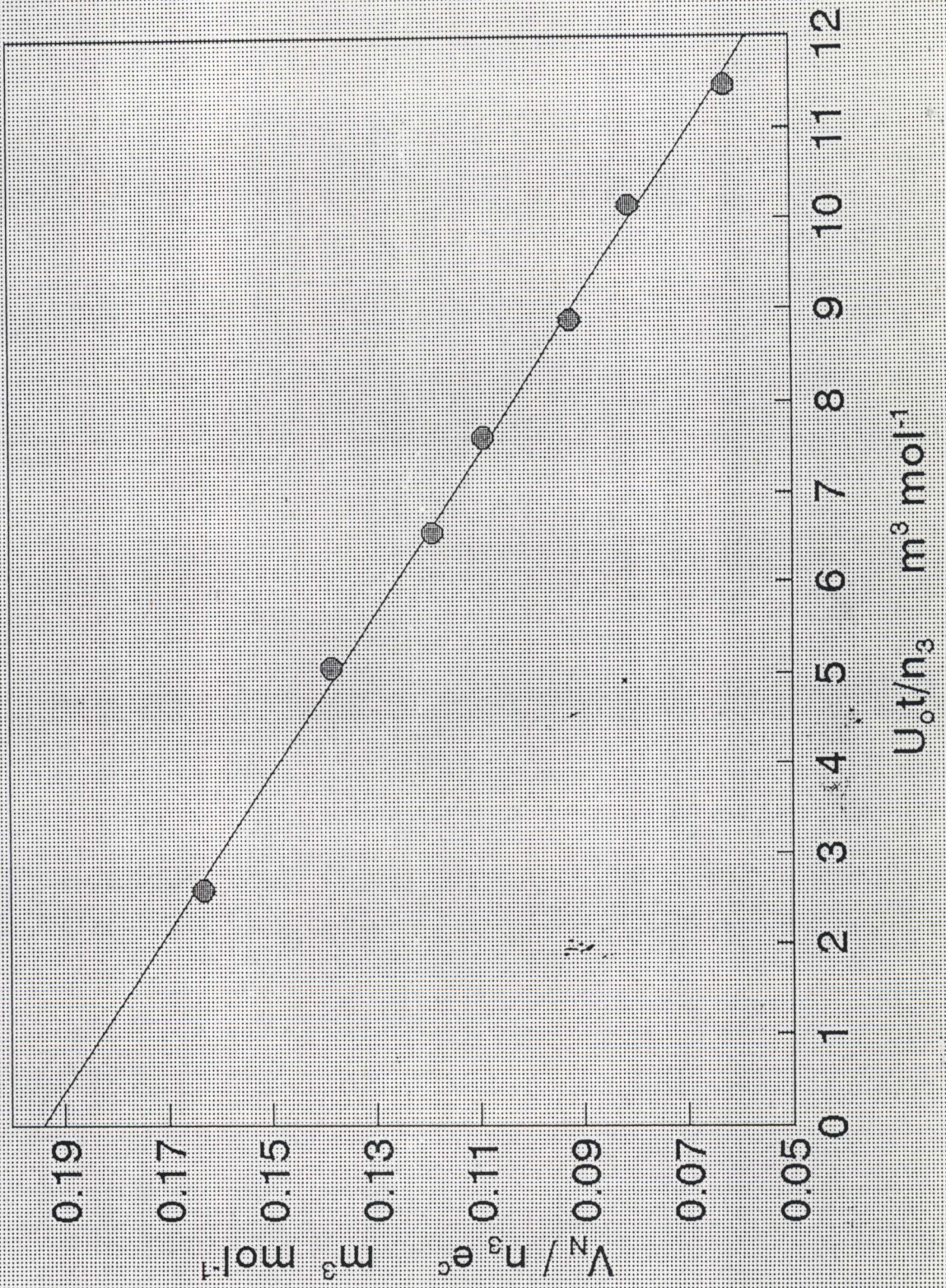


FIG. 6.10. Benzene in decane on column 15 at 293.15 K



6.3 ERROR ANALYSIS

6.3.1. Determination of the Error in γ_{13}^{∞} for a Volatile Solvent

The equation for the determination of γ_{13}^{∞} is

$$\frac{V_n}{n_3 e^C} = \frac{RT}{\gamma_{13}^{\infty} P_1^*} - \frac{U_o t}{n_3} \left[\frac{P_3'}{\gamma_{13}^{\infty} P_1^*} \right] = a - b \left[\frac{U_o t}{n_3} \right] \quad (6.1.)$$

where

$$C = \left[\frac{B_{11} - V_1^*}{RT} \right] P_1^* + \left[\frac{2B_{12} - V_1^{\infty}}{RT} \right] P_o J_3^2 \quad (6.2.)$$

γ_{13}^{∞} is obtained from the intercept of the graph of $V_N / n_3 e^C$ against $U_o t / n_3$.

from the relation

$$a = \frac{RT}{\gamma_{13}^{\infty} P_1^*} \quad (6.3.)$$

Since $a = f(\gamma_{13}^{\infty})$

$$\sigma_a^2 = \sigma_{\gamma_{13}^{\infty}}^2 \left(\frac{\partial a}{\partial \gamma_{13}^{\infty}} \right)^2 \quad (6.6.)$$

But

$$\frac{\partial a}{\partial \gamma_{13}^{\infty}} = \frac{RT}{\gamma_{13}^{\infty 2} P_1^*} \quad (6.7.)$$

Substituting eq. 6.7. into 6.6.

$$\sigma_{\gamma_{13}^{\infty}} = \frac{\sigma_a \gamma_{13}^{\infty 2} P_1^*}{RT} \quad (6.8.)$$

and

$$\sigma_a^2 = \frac{\sigma^2 \sum x_i^2}{N \sum x_i^2 - (\sum x_i)^2} \quad (6.9.)$$

$$\sigma^2 = \frac{1}{N-2} \sum (y_i - a - bx_i)^2 \quad (6.10.)$$

6.3.2. Determination of the error in P_3'

From equation 6.4. P_3' is obtained from the slope

$$b = \frac{P_3'}{\gamma_{13}^{\infty} P_1^*} \quad (6.4.)$$

$$\sigma_b^2 = \left(\frac{\partial b}{\partial P_3'} \right)^2 \sigma_{P_3'}^2 + \left(\frac{\partial b}{\partial \gamma_{13}^{\infty}} \right)^2 \sigma_{\gamma_{13}^{\infty}}^2 \quad (6.11.)$$

$$\Rightarrow \sigma_b^2 = \left(\frac{\sigma_{P_3'}}{\gamma_{13}^{\infty} P_1^*} \right)^2 + \left(\frac{P_3'}{\gamma_{13}^{\infty 2} P_1^*} \right)^2 \sigma_{\gamma_{13}^{\infty}}^2 \quad (6.12.)$$

where

$$\sigma_b^2 = \frac{N \sigma^2}{N \sum x_i^2 - (\sum x_i)^2} \quad (6.13.)$$

6.3.3. Determination of the Error in the Partial Molar Enthalpy

The partial molar enthalpy of mixing at infinite dilution is given by

$$\frac{R}{\frac{1}{T_1} - \frac{1}{T_2}} [\ln \gamma_{13(T_1)}^\infty - \ln \gamma_{13(T_2)}^\infty] = H_1^{E^\infty} \quad (6.14.)$$

Let

$$X = \frac{R}{\frac{1}{T_1} - \frac{1}{T_2}} \quad (6.15.)$$

then

$$\sigma_{H_1^{E^\infty}}^2 = X^2 [\sigma_{\ln \gamma_{13(T_1)}^\infty}^2 - \sigma_{\ln \gamma_{13(T_2)}^\infty}^2] \quad (6.16.)$$

ie.

$$\sigma_{H_1^{E^\infty}}^2 = X^2 \left[\frac{\sigma_{\gamma_{13(T_2)}^\infty}^2}{(\gamma_{13(T_2)}^\infty)^2} - \frac{\sigma_{\gamma_{13(T_1)}^\infty}^2}{(\gamma_{13(T_1)}^\infty)^2} \right] \quad (6.17.)$$

6.4. SAMPLE CALCULATIONS

6.4.1. Calculation of γ_{13}^{∞}

From equation 6.3. and figure 6.1

$$a = \frac{RT}{\gamma_{13}^{\infty} P_1^*} \quad (6.3.)$$

$$\gamma_{13}^{\infty} = \frac{(8.314)(278.15)}{(30555.66) * (0.07651)} = 0.99$$

6.4.2. Calculation of the error in γ_{13}^{∞}

Using equation 6.8. and $\sigma_a = 0.002$

$$\sigma_{\gamma_{13}^{\infty}} = \frac{\sigma_a \gamma_{13}^{\infty 2} P_1^*}{RT} \quad (6.8.)$$

$$\sigma_{\gamma_{13}^{\infty}} = \frac{(0.002)(0.99)^2(30555.66)}{(8.314)(278.15)} = \pm 0.03$$

6.4.3. Calculation of P_3'

From equation 6.5. and at the temperature 278.15 K

$$\frac{b}{a} = \frac{P_3'}{RT} \quad (6.5.)$$

$$P'_3 = \frac{(8.314)(278.15)8(0.001574)}{0.076551} = 48 \text{ Pa}$$

6.4.4. Calculation of $\sigma_{P'_3}$

From equation 6.12. and at 293.15 K

$$\Rightarrow \sigma_b^2 = \left(\frac{\sigma_{P'_3}^2}{\gamma_{13}^\infty P_1^*} \right)^2 + \left(\frac{P'_3}{\gamma_{13}^\infty P_1^*} \right)^2 \sigma_{\gamma_{13}}^2 \quad (6.12.)$$

$$\sigma_{P'_3} = 0.99 * 30555.66 \sqrt{(0.0003469)^2 - \left[\frac{(47.57)}{(0.99)^2 (30555.66)} \right]^2 (0.03)^2} = \pm 10 \text{ Pa}$$

6.4.5. Determination of $H_1^{E\infty}$

The calculated values for γ_{13}^∞ at 278.15 K and 193.15 K are used to determine $H_1^{E\infty}$ from equation 6.14.

$$\frac{R}{\frac{1}{T_1} - \frac{1}{T_2}} [\ln \gamma_{13(T_1)}^\infty - \ln \gamma_{13(T_2)}^\infty] = H_1^{E\infty} \quad (6.14.)$$

$$\frac{8.314}{\frac{1}{278.15} - \frac{1}{293.15}} [(\ln 0.99) - \ln(0.97)] = 900 \text{ J mol}^{-1}$$

6.4.6. Determination of $\sigma H_1^{E\infty}$

$\sigma H_1^{E\infty}$ is determined from equation 6.17.

$$\sigma_{H_1^{E\infty}}^2 = X^2 \left[\frac{\sigma_{\gamma_{13}(T_2)}^2}{(\gamma_{13(T_2)}^\infty)^2} - \frac{\sigma_{\gamma_{13}(T_1)}^2}{(\gamma_{13(T_1)}^\infty)^2} \right] \quad (6.17.)$$

$$\sigma_{H_1^{E\infty}} = \sqrt{\left(\frac{8.314}{\frac{1}{278.15} - \frac{1}{293.15}} \right)^2 \left[\frac{0.04^2}{0.99^2} - \frac{0.03^2}{0.97^2} \right]} = 1 \text{ 000 } Jmol^{-1}$$

6.5. DISCUSSION

The literature values for γ_{13}^{∞} by other workers were done at higher temperatures than in this work and our results fit in with the expected trend. γ_{13}^{∞} for pentane varies to a greater extent with temperature than that for hexane. The method devised by Letcher *et al*⁽⁴⁾ is a quick, easy and reliable method for obtaining γ_{13}^{∞} . This method eliminates the use of a pre-column saturator⁽⁴⁸⁾ and of a reference solvent (Letcher⁽⁴⁹⁾).

6.5.1. Experimental Error in γ_{13}^{∞} and P_3' for non-polar solutes in a volatile solvent

Table 6.5.1. Table of the intercept, a , and the error in a , σa , for solutes: pentane, cyclopentane, hexane, cyclohexane and benzene at 278.15 K and 293.15 K.

Solute	T = 278.15 K		T = 293.15 K	
	a	σa	a	σa
pentane	0.07651	± 0.00162	0.04427	± 0.00243
cyclopentane	0.1461	± 0.0053	0.08068	± 0.00102
hexane	0.2898	± 0.0019	0.1533	± 0.0036
cyclohexane	0.4858	± 0.0019	0.2479	± 0.0055
benzene	0.3656	± 0.0027	0.03076	± 0.00191

Table 6.5.2. Table of the slope, b , and the error in b , σb , for solutes : pentane, cyclopentane, hexane, cyclohexane and benzene at 278.15 K and 293.15 K.

Solute	T = 278.15 K		T = 293.15 K	
	b	σb	b	σb
pentane	0.001574	± 0.000347	-	-
cyclopentane	0.002564	± 0.001155	0.006439	± 0.001172
hexane	0.007663	± 0.000638	0.009157	± 0.001514
cyclohexane	0.01204	± 0.00059	0.01461	± 0.00228
benzene	0.004844	± 0.000193	0.01090	± 0.00063

Table 6.5.3. Table of γ_{13}^{∞} and the error in γ_{13}^{∞} , $\sigma\gamma_{13}^{\infty}$; for solutes : pentane, cyclopentane, hexane, cyclohexane and benzene at 278.15 K and 293.15 K.

Solute	T = 278.15 K		T = 293.15 K	
	γ_{13}^{∞}	$\sigma\gamma_{13}^{\infty}$	γ_{13}^{∞}	$\sigma\gamma_{13}^{\infty}$
pentane	0.99	± 0.03	0.97	± 0.04
cyclopentane	0.88	± 0.03	0.87	± 0.01
hexane	1.01	± 0.01	0.98	± 0.03
cyclohexane	0.98	± 0.04	0.95	± 0.02
benzene	1.32	± 0.01	1.23	± 0.01

TABLE 6.5.4. Literature values⁽⁵⁰⁾ of γ_{13}^{∞} obtained by other workers together with the results from this work

Solute	Temperature				
	278.15 K	293.15 K	303.15 K	333.15 K	343.15 K
	γ_{13}^{∞}	γ_{13}^{∞}	γ_{13}^{∞}	γ_{13}^{∞}	γ_{13}^{∞}
Pentane	0.99	0.97	0.97	0.94	0.93
Cyclopentane	0.88	0.87	0.87	-	-
Hexane	1.01	0.98	0.96	0.97	0.96
Cyclohexane	0.98	0.95	0.93	-	-
Benzene	1.32	1.23	1.21	-	-

TABLE 6.5.5. Table of P_3' and the error in P_3' , $\sigma P_3'$ at 278.15 K and 293.15 K.

Solute	T = 278.15 K		T = 293.15 K	
	P_3'	$\sigma P_3'$	P_3'	$\sigma P_3'$
	Pa	Pa	Pa	Pa
pentane	48	± 10	-	-
cyclopentane	41	± 18	195	± 35
hexane	61	± 5	146	± 24
cyclohexane	57	± 2	144	± 22
benzene	31	± 1	139	± 8

TABLE 6.5.6. Experimental and Literature Values of the Average P'_3 at temperatures 278.15 K and 293.15 K.

	T = 278.15 K	T = 293.15 K
	P'_3	P'_3
	Pa	Pa
Experimental Value	48 ± 18	156 ± 35
Literature Value	$33^{(\dagger)(51)}$	$172^{(52)}$

(†) the value of the vapour pressure was calculated at 277.50 K.

Carruth and Kobayashi⁽⁵¹⁾ reported data for vapour pressure of decane from the temperature range 243.50 K - 310.60 K. Within the experimental error the value for the vapour pressure of decane at 278.15 K correlates well with the literature value. This is probably due to the fact that at 278.15 K equilibrium is better established⁽³⁴⁾ and that the solvent evaporates off the column much more slowly. The value for the vapour pressure of decane at 293.15 K is smaller than the value of the literature value at 304.60 K. At a higher temperature the solvent evaporates off the column at a faster rate. Also at a higher temperature there is more difficulty in obtaining data points close to the x-axis, resulting in larger uncertainty in determining the correct slope⁽³⁴⁾. This method is a good one for determining the vapour pressures of moderately volatile solvents at low temperatures.

Table 6.5.7. Table of $H_1^{E\infty}$ and $\sigma H_1^{E\infty}$ for solute : pentane, cyclopentane, hexane, cyclohexane and benzene at 278.15 K and 293.15 K. Literature values are also given where available. $H_1^{E\infty}$ was calculated from equation 4.16. and $\sigma H_1^{E\infty}$ was calculated from equation 6.19.

Solute	$H_1^{E\infty}$	$\sigma H_1^{E\infty}$	$H_1^{E\infty}$ (lit.) †
	J mol ⁻¹	J mol ⁻¹	J mol ⁻¹
pentane	900	1170	120 ⁽⁴⁹⁾
cyclopentane	500	1450	
hexane	1360	1300	80 ⁽⁴⁹⁾
cyclohexane	1400	1600	1440 ⁽⁴⁹⁾
benzene	3200	1300	3100 ⁽⁴⁹⁾

† $H_1^{E\infty}$ (lit.) were obtained from extrapolation of finite concentration data. The values $H_1^{E\infty}$ obtained for cyclohexane and benzene are favourable compared to literature values. The large discrepancies between the literature and calculated values for pentane and hexane could be due to the greater error in obtaining the correct slope for γ_{13}^∞ and hence a larger error in $H_1^{E\infty}$. Except for benzene, the $\sigma H_1^{E\infty}$ values obtained are greater than the calculated values of $H_1^{E\infty}$. Due to the errors in obtaining γ_{13}^∞ from glc the propagated errors makes $\sigma H_1^{E\infty}$ also large. The glc method for obtaining γ_{13}^∞ gives good results but calculation of $H_1^{E\infty}$ from glc determined γ_{13}^∞ gives poor results.

6.6. CONCLUSION

The method developed by Letcher *et al*⁽⁴⁾ is a quick and reliable method for the determination of γ_{13}^{∞} . However, as the volatility of the solvent increases, the evaporation of the solvent off the column increases resulting in greater difficulty in obtaining data points close to the zero value of the U_0t/n_3 axis. Also, for a greater volatility of solvent the moles of solvent will have to be increased to ensure that the column has a lifespan of about 1 hour. This method can be used for other solvents of similar volatilities as decane. The method is easy and produces errors that are small between 3 - 5%. The results obtained at the two temperatures fit in well with those obtained by other workers. Provided that equilibrium is established this method is useful for calculating P'_3 . The error obtained in P'_3 are large because of the difficulty in obtaining the correct slope. In future work other more volatile solvents such as octane and nonane can be investigated using the same technique.

APPENDIX i

```

program Calculation;

uses Crt,Dos;

const
  nk = 2;
  maxn = 20;

type
  lkey = array[1..2] of Char;
  String40 = string[40];
  nrkey = array[1..nk] of byte;
const
  n1 = 7.1273;
  cat = '';
  tk = 273.15;
  npts =11;
  { nptmax = 3;}
  r = 8.314;
  keys:lkey=('Y','N');

var
x,y,Vn,Tr,y1,y2,y3,Ti,Tis,TIME: array[1..npts] of real;
d,e,f,g,h,i,l,m,z,T1,tg,Tf,Po1,n3,Tmf,H1,H2,Pww,Uo,U1: real;
Pw,U2,A,A1,J,C,Pi,Po,k1,k2,k3,k4,B11,B12,V,T,P,A3: real;
flag:nrkey;
filein, fileout, filegroup:text;
key:char;
Firsttime:boolean;
name:array[1..maxn] of string [20];

{$I inoutlib.pas}

  {-----ReadDataFile-----}

Procedure ReadDataFile;

const
  maxcode = 1;
var
  i: integer;
  s: real;

  begin
    Readln(filein,name[i]);
    Readln(filein,t);
    t:= t + tk;
    i:=0;
    Readln(filein,V);
    Readln(filein,P);
    Readln(filein,B11);
    Readln(filein,B12);
    Readln(filein,Pw);
    Readln(filein,Tg);
    Readln(filein,tF);
    Readln(filein,h1);
    Readln(filein,h2);
  
```

```

    Readln(filein,Tmf);
    Readln(filein,n3);
    Readln(filein,Po1);

Repeat
    Inc(i);
    s:=0;

    begin
        Readln(filein,Tr[i]);
        s:=s + Tr[i];
    end;
    begin
        Readln(filein,Ti[i]);
        s:=s + Ti[i];
    end;
    { begin
        Readln(filein,Tis[i]);
        s:=s + Tis[i];
    end; }

Until Eof(filein);
end;
{-----end if ReadDataFile-----}

{-----FlowRate Correction-----}

Procedure FlowRate;
Begin
    U1:= 100/TF;
    U2:= U1/1000000;
    Pw:= (101325*Pw)/(760);
    Uo:= U2*(T/Tmf)*((Po - Pw)/(Po));
end;

{ - - - - - E n d   F l o w R a t e
Correction-----}

{-----OutletPressure-----}

Procedure Pressure;
begin
{
    Writeln('Input Outlet Pressure,Po1');
    Readln(Po1);
    Po:= (110325*Po1)/(760);
    Pi:= (13.5951)*10*(9.80665)*(H1 - H2) + Po;
end;

{ - - - - - E n d   O u t l e t
Pressure-----}

{-----CorrectionFactor-----}

Procedure CorrectionFac;
Begin
    A:=(Pi/Po);
    A1:=(A)*(A)*(A);
    J:= (3/2)*((sqr(A)-1)/(A1 - 1));

```

```

end;

{-----End of CorrectionFactor-----}

{-----Retention
Volume-----}

Procedure Retention;

var
  i : integer;
Begin
  for i:=1 to npts do begin
    Vn[i] := Uo*(Tr[i] - Tg)*J;
  end;
end;

{-----End of Retention
Volume-----}

{-----Regression
Parameters-----}

{Procedure Parameters;
var
i: integer;
  Begin
    for i :+ 1 to npts do begin
      Vx[i] := Vn[i] - (Uo*J)/n3}
{-----WriteOut File-----}

Procedure WriteOut;

var
  k:integer;

Begin
  Write(fileout,' ', name[k]);
  Writeln(fileout);
  Writeln(fileout,' t = ',20 + tk:5:2,Char(248));
  Writeln(fileout);
  Writeln('Corretion Factor = ',J:7:3);
  Writeln('Flowrate = ',Uo,7:7);
  Writeln('k1 = ',k1,7:7);
  Writeln('k2 = ',k2,7:7);
  Writeln('k3 = ',k3,7:7);
  Writeln('k4 = ',k4,7:7);

  Writeln(fileout,'          Vn          Uo          ');

  for k:= 1 to npts do begin
    Writeln(fileout,i:2,' ', Vn[k]:7:7,' ',Uo:6:10,'
',x[k]:6:5,' ',y[k]:6:5);
  end;
end;

{-----End of WriteOut-----}

var

```

```

k:integer;

Begin
  ClrScr;
  PrepIn(filein,cat);
  PrepOut(fileout,cat);
  Repeat
    ReadDataFile;
    Writeln ('Calculation of Activity coefficients at Infinite
Dilution Using G.L.C. ');
    { Writeln ('Input the Retention time of Unretained Gas, Tg
');
    Readln(Tg);
    Writeln('Input Atm. Pressure mmHg, Po');
    Readln(Po);
    Writeln ('Input Flow Time, Tf');
    Readln (Tf);
    Writeln('Input H1');
    Readln (H1);
    Writeln ('Input H2 ');
    Readln (H2);
    Writeln ('Input Outside Temperature ,Tmf');
    Readln(Tmf);
    {Writeln ('Input Temperature ,Tf');
    Readln(Tf);
    Writeln('Input moles of Solvent, n3');
    Readln(n3);}
    Pressure;
    CorrectionFac;
    FlowRate;
    Retention;
    {CALCULATION OF C}
    z:=R*T;
    d:= - (B11-V); {}/z)*P + (((2*B12)-V)/z)*(1/J)*Po;
    e:= (d)/z;
    f:= e*P;
    g:=2*B12;
    h:=g-V;
    l:= h/z;
    m:= l * (Po/J);
    C:= f + m;

    for k:=1 to npts do begin
      x[k]:=Vn[k]*exp(-C)/n3;
      y[k]:=(Uo*Ti[k])/n3;
      TIME[k] := Ti[k]*60 + Tis[k];
      { y1[k]:=(Uo*(Ti[k]*60+ Tis[k]));
      y2[k] := Vn[k]/n3 * 1000000000;
      y3[k] := ln(y2[k]){/2.303
      k4 := n1/n3;
      k1 := (R*T*(exp(C)))/P;
      k2 := Uo*exp(C)*P/n3;
      k3 := Uo/J/n3;
      }
    end;
    WriteOut;
    Choose('Do you want to continue?(Y/N)',nk,keys,flag);
    Reset(filein);

```

```
Until flag[2] = 1;  
  Close(filein);  
  Close(fileout);  
end.
```

APPENDIX ii

```
program Calculation;
```

```
uses Crt,Dos;
```

```
const
```

```
  nk = 2;
```

```
  maxn =15; {THIS IS THE NUMBER OF POINTS YOU WISH TO CALCULATE,  
            ' MUST BE EQUAL TO OR MORE THAN THE DATA POINTS YOU  
            HAVE, MUST BE PUT IN BY YOU}
```

```
type
```

```
  lkey = array[1..2] of Char;
```

```
  String40 = string[40];
```

```
  nrkey = array[1..nk] of byte;
```

```
const
```

```
  cat = '';
```

```
  tk = 273.15;
```

```
  npts =8; {NUMBER OF DATA POINTS};
```

```
  { nptma
```

```
  x = 3;}
```

```
  r = 8.314;
```

```
  keys:lkey=('Y','N');
```

```
{Tmf=27.8; {THE TEMPERATURE OF THE FLOWMETER, ROOM 11 11 [1111  
11 [1
```

```
          TEMPERATURE}
```

```
  n3=0.003287;{THE NUMBER OF MOLES OF SOLVENT ON THE COLUMN}
```

```
var
```

```
Tmf,Pw,Vmm,Vn1,Uo,Uf,Po1,x,y,C,Uo1,m,Vn,U2,Pi,Tr,Ti,h1,h2,u1,T  
g,J,A,A1,Tf,gamma: array[1..npts] of real;
```

```
d,e,f,g,h,i,l,z,T1,Pww: real;
```

```
Po,B11,B12,V,T,P,A3: real;
```

```
flag:nrkey;
```

```
filein, fileout, filegroup:text;
```

```
key:char;
```

```
Firsttime:boolean;
```

```
name:array[1..maxn] of string [20];
```

```
 {$I inoutlib.pas}
```

```
{THIS PROCEDURE READS THE DATA FROM YOUR DATA FILE, WHICH IS  
ALL YOUR DATA, eg. RETENTION TIME ETC}
```

```
{-----ReadDataFile-----}
```

```
Procedure ReadDataFile;
```

```
const
```

```
  maxcode = 1;
```

```
var
```

```
  i: integer;
```

```
  s: real;
```

```

begin
  Readln(filein,name[i]);{ GIVE YOUR DATA FILE A NAME,
                           eg.SULPHOLANE. DAT}
                           Readln(filein,t);
                           t:= t + tk;
                           i:=0;
  Readln(filein,V);      {MOLAR VOLUME, OF THE SOLUTE, BY
DENITY}
  Readln(filein,P);      {VAPOUR PRESSURE OF SOLUTE, CALCULATED
BY
                           +B/C+t EQUATION}
  Readln(filein,B11);{SECOND VIRIAL COEFFICIENT, SOLUTE}
  {  Readln(filein,B12); {MIXED VIRIAL COEFFICIENT, SOLUTE
AND GAS}
  {  Readln(filein,Pw);   {SATURATED VAPOUR PRESSURE OF
WATER}
  {  Readln(filein, Pol); {Atmospheric Pressure}
  Repeat
    Inc(i);
    s:=0;

    begin
      Readln(filein,Tr[i]); {RETENTION TIME OF THE SOULTE}
      s:=s + Tr[i];
    end;
  begin
    Readln(filein,Tg[i]); {RETENTION TIME OF GAS}
    s:=s + Tg[i];

end;

begin
  Readln(filein,Tf[i]);{TIME FOR BUBBLE TO MOVE 100 cm}
  s:=s + Tf[i];
end;
begin
  Readln(filein,H1[i]); {VALUE OF Hg IN HIGHER ARM}
  s:=s + H1[i];

end;

begin
  Readln(filein,H1[i]);
  s:=s + H1[i];
end;

begin
  Readln(filein,tmf[i]);{VALUE OF Hg IN LOWER ARM}
  s:=s + Tmf[i];
end;
begin
  Readln(filein,Pw[i]);{VALUE OF Hg IN LOWER ARM}
  s:=s + Pw[i];
end;
begin
  Readln(filein,Pol[i]);{VALUE OF Hg IN LOWER ARM}
  s:=s + Pol[i];

end;

Until Eof(filein);

```

```
end;
```

```
{-----end if ReadDataFile-----}
```

```
{-----FlowRate Correction-----}
```

```
Procedure FlowRate;
```

```
var
```

```
  i:integer;
```

```
Begin
```

```
  for i:= 1 to npts do begin
```

```
    U1[i]:= 100/tf[i];
```

```
    U2[i]:= U1[i]/1000000;
```

```
    Pww:=(110325*Pw[i])/(760);
```

```
    Uo[i]:= U2[i]*(T/Tmf[i])*((Po - Pww)/(Po));
```

```
    Uf[i]:= J[i]*Uo[i]*1000000000;
```

```
  end;
```

```
end;
```

```
{-----End FlowRate  
Correction-----}
```

```
{-----OutletPressure-----}
```

```
Procedure Pressure;
```

```
var
```

```
  i:integer;
```

```
begin
```

```
{  Writeln('Input Outlet Pressure,Po1');
```

```
  Readln(Po1);}
```

```
  for i:= 1 to npts do begin
```

```
    Po:= (110325*Po1[i])/(760);
```

```
    Pi[i]:= (13.5951)*10*(9.80665)*(H1[i] - H2[i]) + Po;
```

```
  end;
```

```
end;
```

```
{-----End Outlet Pressure-----}
```

```
{-----CorrectionFactor-----}
```

```
Procedure CorrectionFac;
```

```
var
```

```
  i:integer;
```

```
Begin
```

```
  for i := 1 to npts do begin
```

```
    A[i]:= (Pi[i]/Po);
```

```
    A1[i]:= (A[i])*(A[i])*(A[i]);
```

```
    J[i]:= (3/2)*((sqr(A[i])-1)/(A1[i] - 1));
```

```
  end;
```

```

end;
{-----End of CorrectionFactor-----}

{-----Retention
Volume-----}

Procedure Retention;

var
  i : integer;
Begin
  for i:=1 to npts do begin
    Vn[i] := Uo[i]*(Tr[i] - Tg[i])*J[i];
    Vmm[i]:=Vn[i]*1000000000;
    Vn1[i] := ln(Vmm[i])/2.303;

    end;
  end;
{-----End of Retention
Volume-----}

{-----WriteOut File-----}

Procedure WriteOut;

var
  k:integer;

Begin
  Write(fileout,' ', name[k]);
  Writeln(fileout);
  Writeln(fileout,' t = ',30+ tk:5:2,Char(248));
  Writeln(fileout);
  Writeln(fileout,'
J      UoJ      ln Vn')          Vn      gamma      Uo

  for k:= 1 to npts do begin
    Writeln(fileout,i:2,'
',gamma[k]:6:5,'
',Uf[k]:6:5,'
',Vn1[k]:6:5);
    Vn[k]:10:10,'
',Uo[k]:10:10,'
',J[k]:6:5,'
');
    end;
  end;

{-----End of WriteOut-----}

var
  k:integer;

Begin
  ClrScr;
  PrepIn(filein,cat);
  PrepOut(fileout,cat);
  Repeat
    ReadDataFile;

```

```

WriteLn ('Calculation of Activity coefficients at Infinite
Dilution Using G.L.C. ');
Pressure;
CorrectionFac;
FlowRate;
Retention;
  z:=R*T;
  d:= - B11+V; {} /z)*P + ((2*B12)-V)/z)*(1/J)*Po;}
  e:= -(d)/z;
  f:= e*P;
  g:=2*B12;
  h:=g-V;
  l:= h/z;
for k := 1 to npts do begin
  m[k]:= l * (Po/J[k]);
  C[k]:= f + m[k];
end;

for k:=1 to npts do begin

  gamma[k]:=((n3*R*T)/(Vn[k]*P)) + exp(C[k]);
end;
WriteOut;
Choose('Do you want to continue?(Y/N)',nk,keys,flag);
Reset(filein);
Until flag[2] = 1;
Close(filein);
Close(fileout);
end.

```

APPENDIX iii

TABLE 1. Retention times obtained for different sample sizes for methanol on column 1 at 293.15 K.

Solute Size	Run Number			
	1.	2.	3.	4.
	t_r^*	t_r^*	t_r^*	t_r^*
mm ³	s	s	s	s
0.1	-	58.73	-	28.50
0.2	146.73	60.39	47.11	-
0.7	-	65.44	51.63	32.28
0.9	155.08	68.06	-	-
1.0	156.18	-	54.78	34.78
Extrapolated to 0 mm ³	144.36	57.82	45.13	27.80

TABLE 2. Retention times obtained for different sample sizes for ethanol on column 1 at 293.15 K.

Solute size	Run Number			
	5.	6.	7.	8.
	t_r^*	t_r^*	t_r^*	t_r^*
mm ³	s	s	s	s
0.1	110.12	60.48	49.18	37.78
0.2	-	63.38	52.38	38.08
0.5	126.36	72.89	60.38	-
0.7	135.70	-	64.38	46.38
0.9	143.37	84.08	69.38	48.78
1.0	148.57	86.88	70.68	-
Extrapolated to 0 mm ³	105.63	57.95	47.46	35.82

TABLE 3. Retention times obtained for different sample sizes for propan-2-ol as solute on column 1 at 293.15 K.

Solute Size	Run number		
	9.	10.	11.
t_r^*	t_r^*	t_r^*	t_r^*
mm ³	s	s	s
0.2	-	141.95	75.55
0.5	-	-	86.99
0.7	221.36	163.82	-
0.9	225.18	169.22	101.40
1.0	231.62	-	-
Extrapolated to 0 mm ³	198.28	134.40	68.31

TABLE 4. Retention times obtained for different sample sizes for methanol column 2 at 293.15 K.

Solute Size	Run Number			
	12.	13.	14.	15.
t_r^*	t_r^*	t_r^*	t_r^*	t_r^*
mm ³	s	s	s	s
0.1	51.81	-	34.21	-
0.2	-	-	-	29.68
0.5	-	43.12	-	29.89
0.9	57.08	45.18	38.57	-
1.0	58.29	45.40	38.98	30.38
Extrapolated to 0mm ³	51.08	40.78	33.68	29.48

TABLE 5. Retention times obtained for different sample sizes for ethanol as solute on column 2 at 293.15 K.

Solute size	Run Number			
	16.	17.	18.	19.
	t_r^*	t_r^*	t_r^*	t_r^*
mm ³	s	s	s	s
0.1	107.46	78.35	50.60	43.35
0.2	-	-	52.87	45.46
0.5	125.19	90.28	58.58	49.34
0.7	134.87	97.09	63.77	-
0.9	142.30	104.68	-	55.48
1.0	-	-	73.08	-
Extrapolated to 0 mm ³	103.22	74.63	47.56	42.14

TABLE 6. Retention times obtained for different sample sizes for propan-2-ol as solute on column 2 at 293.15 K.

Solute size	Run Number				
	20.	21.	22.	23.	24.
	t_r^*	t_r^*	t_r^*	t_r^*	t_r^*
mm ³	s	s	s	s	s
0.2	-	131.90	105.08	86.51	63.59
0.5	212.32	140.81	-	90.15	64.30
0.7	217.72	-	113.06	-	-
0.9	240.68	160.85	116.68	96.63	66.60
Extrapolated to 0 mm ³	173.94	122.21	101.73	83.91	62.49

TABLE 7. Retention times obtained for different sample sizes for methanol as solute on column 3 at 293.15 K.

Solute Size	Run number			
	25.	26.	27.	28.
	t_r^*	t_r^*	t_r^*	t_r^*
mm ³	s	s	s	s
0.1	48.55	37.74	32.27	23.22
0.5	50.26	-	-	23.82
0.7	-	39.62	35.26	-
0.9	56.61	-	36.42	24.64
1.0	56.29	40.48	-	-
Extrapolated to 0 mm ³	46.88	37.08	31.73	23.00

TABLE 8. Retention times obtained for different sample sizes for ethanol as solute on column 3 at 293.15 K.

Solute Size	Run number			
	29.	30.	31.	32.
	t_r^*	t_r^*	t_r^*	t_r^*
mm ³	s	s	s	s
0.1	83.79	60.58	-	-
0.2	83.93	63.79	49.08	39.39
0.5	96.10	72.73	-	44.09
0.7	101.96	77.08	58.99	47.05
0.9	109.18	82.09	-	50.48
1.0	114.14	84.18	63.29	-
Extrapolated to 0 mm ³	78.68	58.58	44.96	36.20

TABLE 9. Retention times obtained for different sample sizes for propan-2-ol as solute on column 3 at 293.15 K.

Solute Size <hr/> mm ³	Run number		
	33.	34.	35.
	t_r^* <hr/> s	t_r^* <hr/> s	t_r^* <hr/> s
0.2	197.90	114.89	67.88
0.5	211.31	131.57	-
0.7	220.46	139.27	81.82
0.9	234.40	147.04	-
1.0	-	-	89.28
Extrapolated to 0 mm ³	183.45	106.95	62.64

TABLE 10. Retention times obtained for different sample sizes for methanol column 1 at 303.15 K.

Solute Size <hr/> mm ³	Run Number		
	36.	37.	38.
	t_r^* <hr/> s	t_r^* <hr/> s	t_r^* <hr/> s
0.1	-	-	28.38
0.2	102.28	42.67	-
0.5	-	-	33.41
0.7	104.47	49.48	37.16
1.0	105.98	53.95	-
Extrapolated to 0 mm ³	101.33	39.80	26.76

TABLE 11. Retention times obtained for different sample sizes for ethanol as solute on column 4 at 303.15 K.

Run				
Solute Size	39.	40.	41.	42.
<u>mm³</u>	<u>t_r[*]</u>	<u>t_r[*]</u>	<u>t_r[*]</u>	<u>t_r[*]</u>
	s	s	s	s
0.2	127.18	74.38	52.98	37.38
0.5	136.48	-	55.97	39.38
0.7	145.89	-	-	40.30
0.9	154.30	84.38	-	-
1.0	-	92.30	66.01	42.88
Extrapolated to 0 mm ³	118.49	70.10	49.64	35.94

TABLE 12. Retention times obtained for different sample sizes for propan-1-ol solute on column 4 at 303.15 K.

Run Number					
Solute Size	43.	44.	45.	46.	47.
<u>mm³</u>	<u>t_r[*]</u>	<u>t_r[*]</u>	<u>t_r[*]</u>	<u>t_r[*]</u>	<u>t_r[*]</u>
	s	s	s	s	s
0.1	153.58	120.48	-	-	-
0.2	159.38	129.38	101.48	56.95	52.47
0.5	186.48	151.18	-	-	59.41
0.7	-	164.28	126.74	69.13	62.72
0.9	216.08	-	137.24	76.20	-
1.0	225.38	173.98	141.00	-	67.63
Extrapolated to 0 mm ³	144.91	117.45	91.60	51.28	49.27

TABLE 13. Retention times obtained for different sample sizes for propan-2-ol as solute on column 4 at 303.15 K.

Solute Size <hr/> mm ³	Run Number			
	48.	49.	50.	51.
	$\frac{t_r^*}{s}$	$\frac{t_r^*}{s}$	$\frac{t_r^*}{s}$	$\frac{t_r^*}{s}$
0.1	-	-	-	46.80
0.2	126.30	90.38	65.78	-
0.5	-	-	68.28	47.38
0.7	141.58	105.38	73.58	-
0.9	-	109.58	-	48.28
1.0	149.58	-	76.38	48.38
Extrapolated to 0 mm ³	120.63	85.02	62.59	46.56

TABLE 14. Retention times obtained for different sample sizes for propan-1-ol as solute on column 5 (hexadecane 8%) at 303.15 K.

Solute Size <hr/> mm ³	Run Number			
	52.	53.	54.	55.
	$\frac{t_r^*}{s}$	$\frac{t_r^*}{s}$	$\frac{t_r^*}{s}$	$\frac{t_r^*}{s}$
0.1	-	98.38	-	-
0.2	176.58	99.88	80.89	75.03
0.5	202.18	-	85.59	79.87
0.7	216.88	106.29	-	-
0.9	226.38	-	96.50	-
1.0	-	-	102.35	92.38
Extrapolated to 0 mm ³	164.01	96.14	74.35	69.94

TABLE 15. Retention times obtained for different sample sizes for methanol as solute on column 6 (hexadecane 10%) at 303.15 K.

Solute Size <hr/> mm ³	Run number		
	56.	57.	58.
	t_r^* <hr/> s	t_r^* <hr/> s	t_r^* <hr/> s
0.1	-	77.16	34.92
0.2	186.00	-	-
0.9	197.47	78.08	37.10
1.0	199.28	78.65	37.09
Extrapolated to 0 mm ³	182.68	76.98	34.68

TABLE 16. Retention times obtained for different sample sizes for ethanol as solute on column 6 (10% hexadecane) at 303.15 K.

Solute Size <hr/> mm ³	Run Number			
	59.	60.	61.	62.
	t_r^* <hr/> s	t_r^* <hr/> s	t_r^* <hr/> s	t_r^* <hr/> s
0.1	154.95	109.72	-	-
0.2	-	-	68.62	36.72
0.5	162.05	-	74.28	38.25
0.7	168.33	-	74.58	39.12
0.9	-	125.18	-	-
1.0	-	127.08	-	43.60
Extrapolated to 0 mm ³	152.40	107.79	66.67	34.41

TABLE 17. Retention times obtained for different sample sizes for propan-1-ol as solute on column 6 at 303.15 K.

Solute Size <hr/> mm ³	Run			
	63.	64.	65.	66.
	t_r^* <hr/> s	t_r^* <hr/> s	t_r^* <hr/> s	t_r^* <hr/> s
0.2	-	-	113.91	92.32
0.5	394.18	173.68	125.89	102.72
0.7	417.56	182.00	-	109.72
0.9	433.98	-	140.27	-
1.0	446.38	195.95	145.16	-
Extrapolated to 0 mm ³	344.14	151.10	106.36	85.35

TABLE 18. Retention times obtained for different sample sizes for propan-2-ol as solute on column 6 at 303.15 K.

Solute Size <hr/> mm ³	Run Number			
	67.	68.	69.	70.
	t_r^* <hr/> s	t_r^* <hr/> s	t_r^* <hr/> s	t_r^* <hr/> s
0.1	-	81.03	60.81	-
0.2	231.28	-	61.56	53.98
0.5	246.57	92.49	66.69	59.73
0.7	-	96.60	70.37	62.07
0.9	261.50	-	73.81	-
1.0	-	100.70	-	66.49
Extrapolated to 0 mm ³	224.16	79.11	58.64	51.32

TABLE 19. Retention times obtained for different sample sizes for methanol as solute on column 7 (hexadecane 15%) at 303.15 K.

Solute Size <hr/> mm ³	Run Number			
	71.	72.	73.	74.
	t_r^* <hr/> s	t_r^* <hr/> s	t_r^* <hr/> s	t_r^* <hr/> s
0.1	192.20	-	-	-
0.2	-	100.43	77.57	50.64
0.5	-	-	-	51.78
0.7	-	100.44	80.00	53.21
0.9	210.48	-	81.86	-
1.0	211.38	100.48	-	-
Extrapolated to 0 mm ³	190.08	100.41	76.27	49.52

TABLE 20. Retention times obtained for different sample sizes for ethanol as solute on column 7 at 303.15 K.

Solute Size <hr/> mm ³	Run number		
	75.	76.	77.
	t_r^* <hr/> s	t_r^* <hr/> s	t_r^* <hr/> s
0.2	292.19	131.66	78.34
0.5	295.58	133.04	83.48
0.7	-	133.81	85.28
0.9	301.85	-	-
Extrapolated to 0 mm ³	289.12	130.81	75.76

FIG.1. Methanol on column 1 at 293.15 K

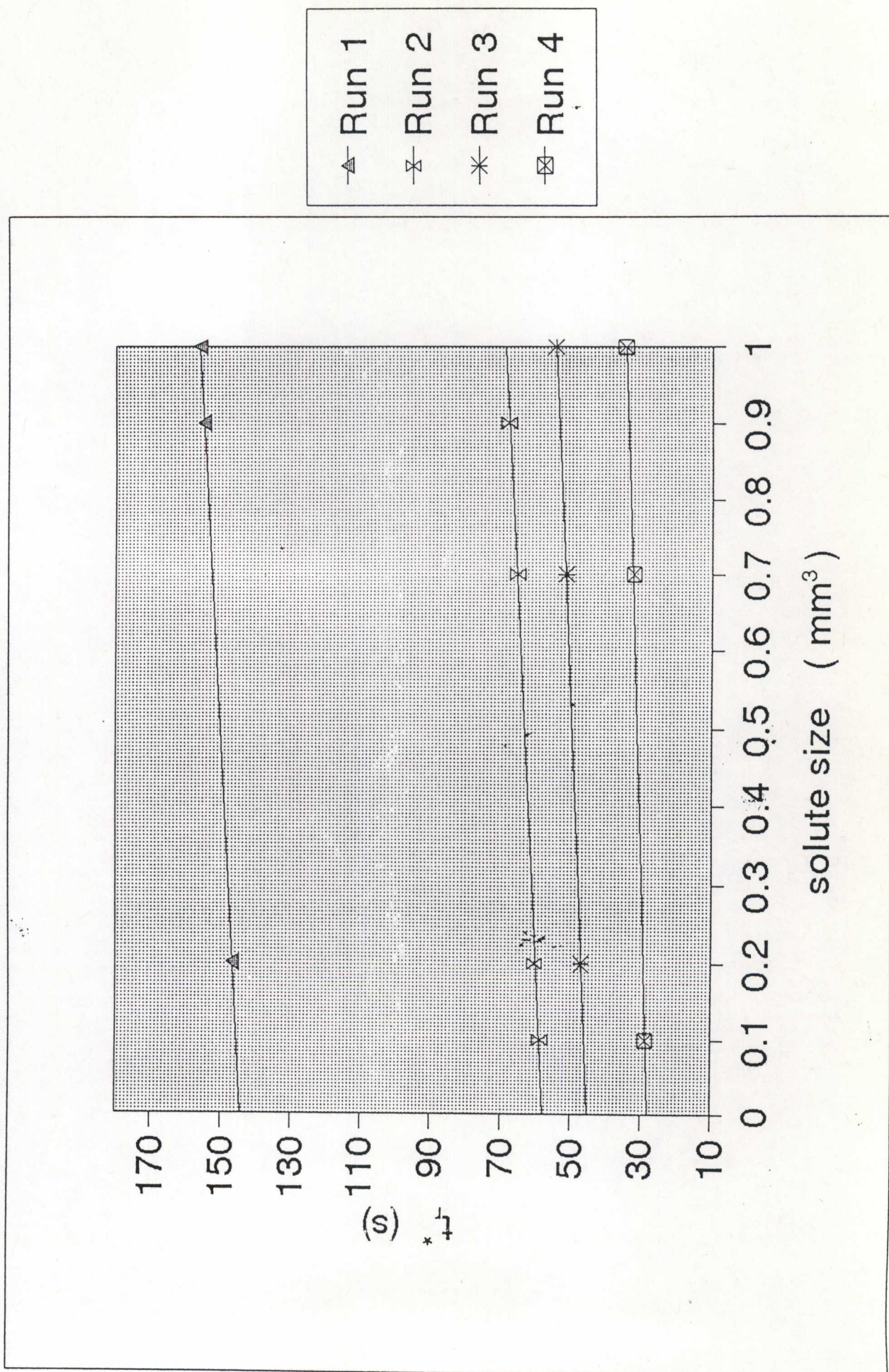


FIG.2. Ethanol on column 1 at 293.15 K

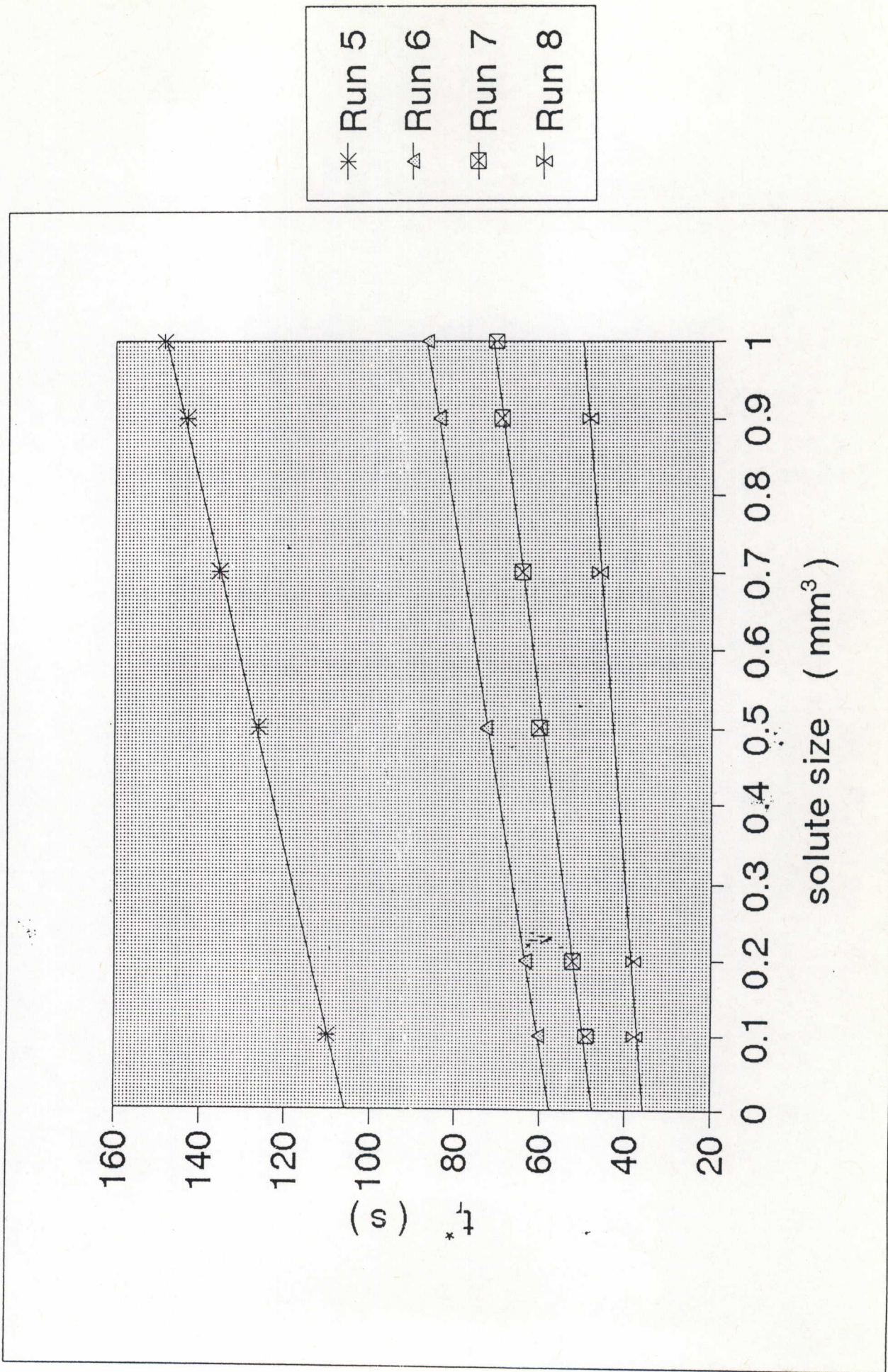


FIG.3. Propan-2-ol on column 1 at 293.15 K

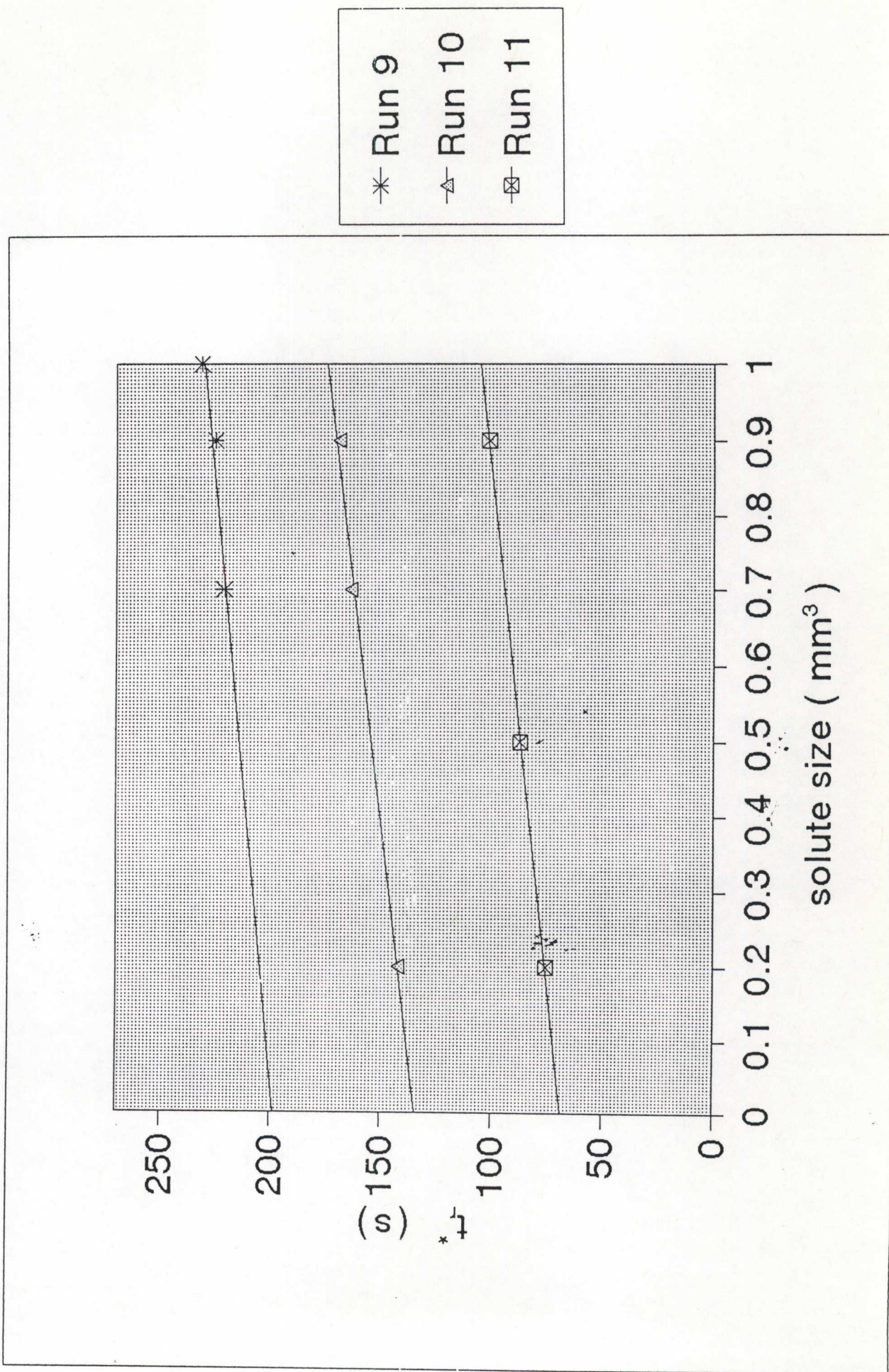


FIG. 4. Methanol on column 2 at 293.15 K

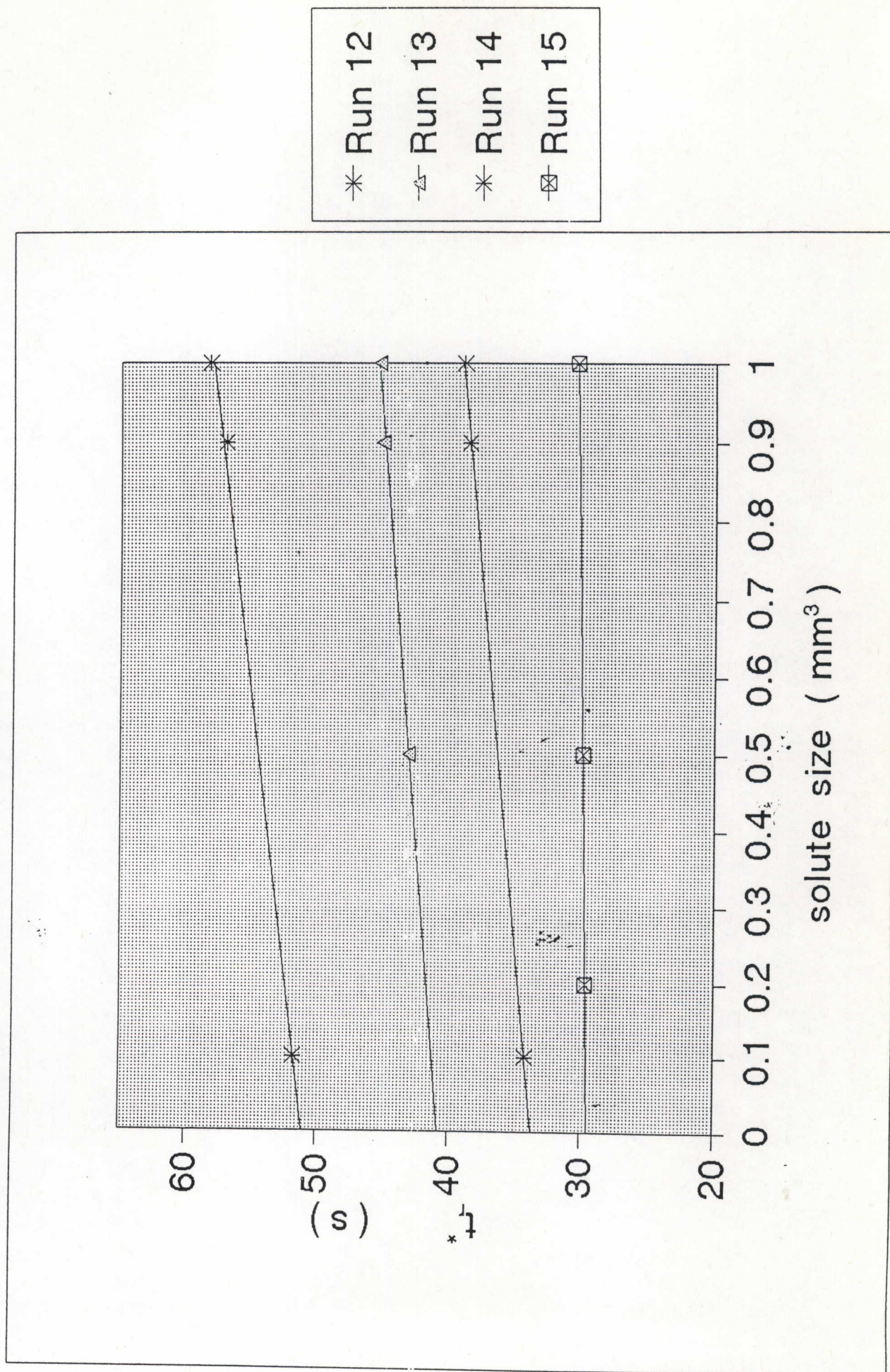


FIG.5. Ethanol on column 2 at 293.15 K

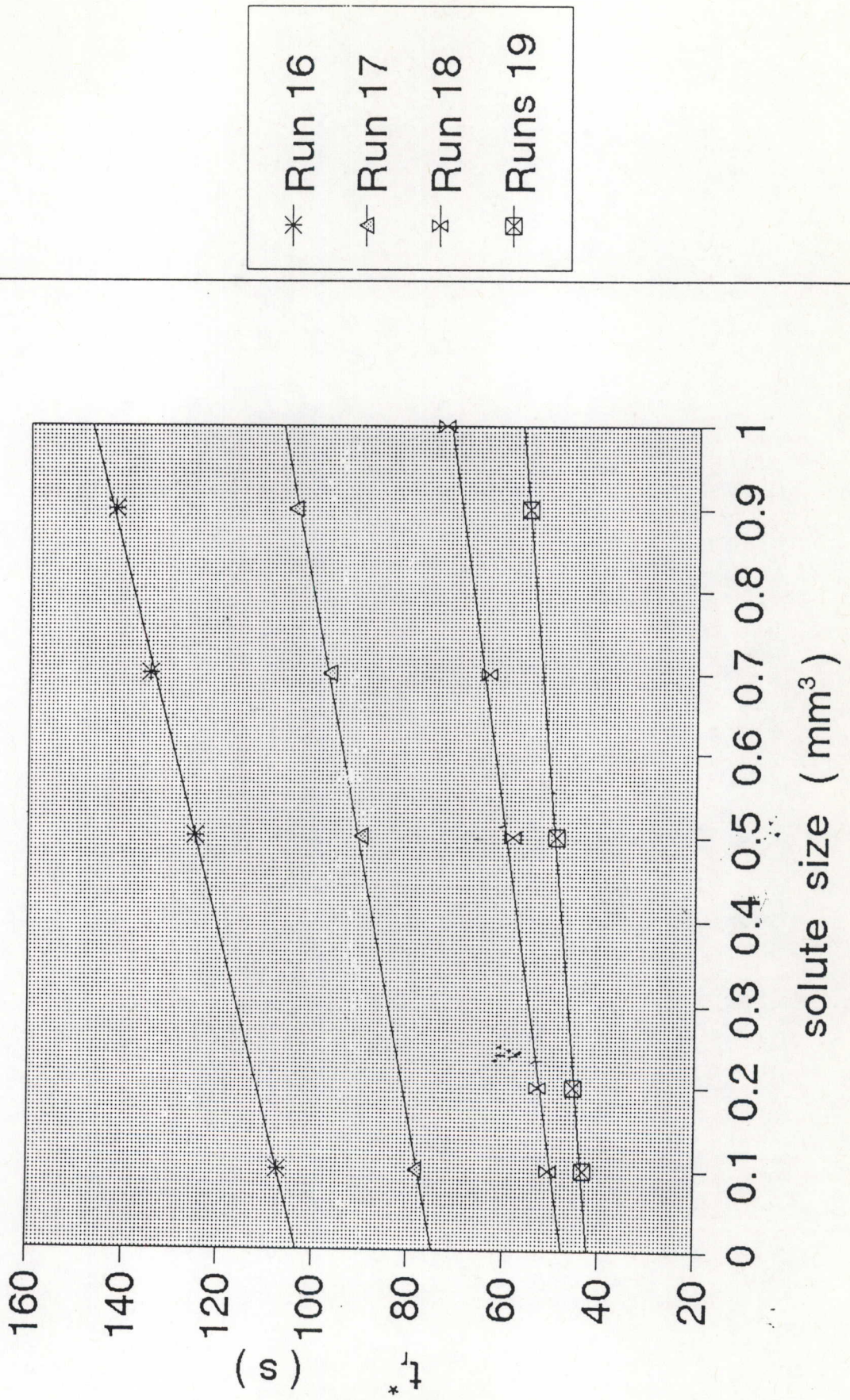


FIG.6. Propan-2-ol on column 2 at 293.15 K

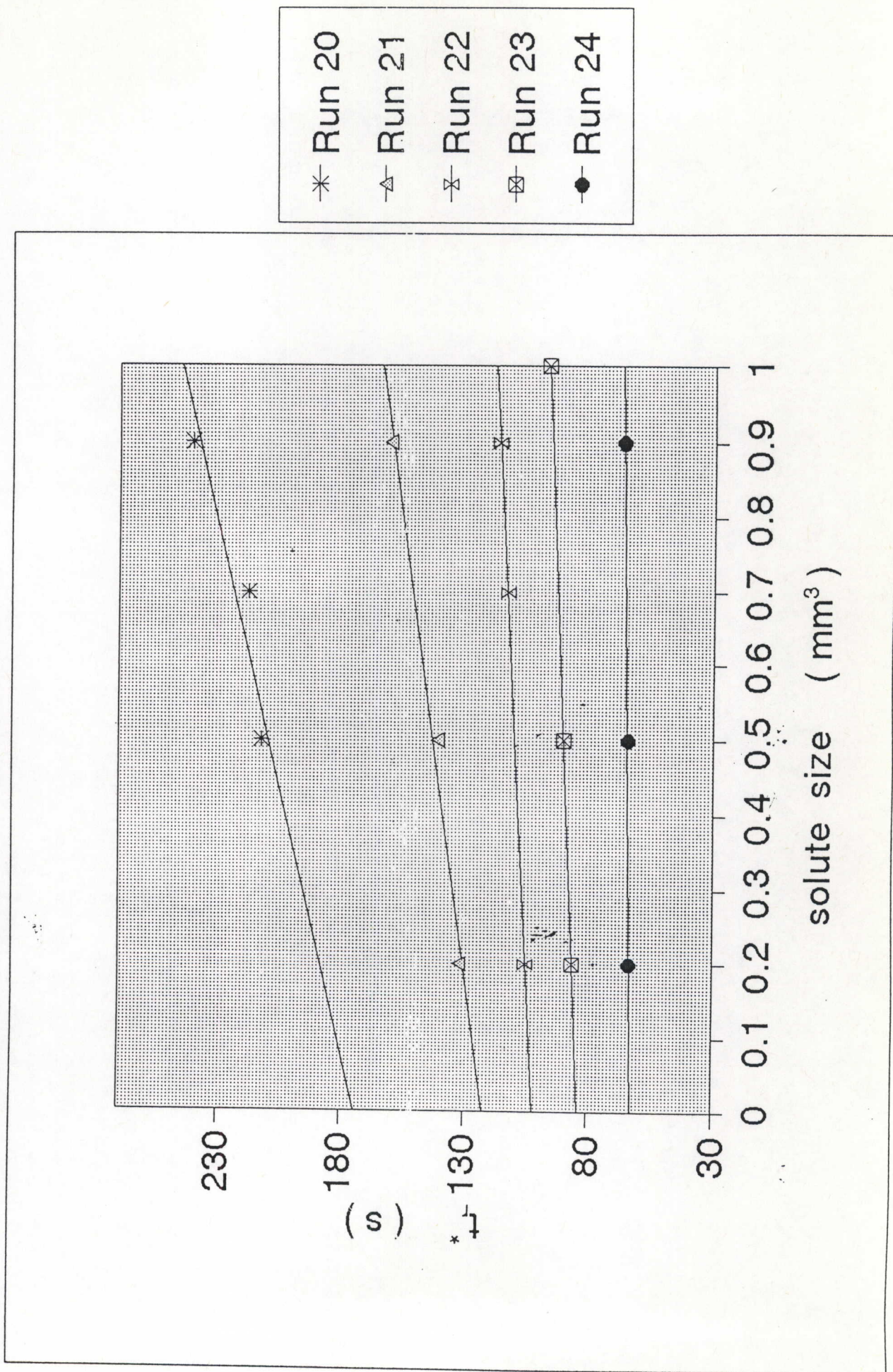


FIG.7. Methanol on column 3 at 293.15 K

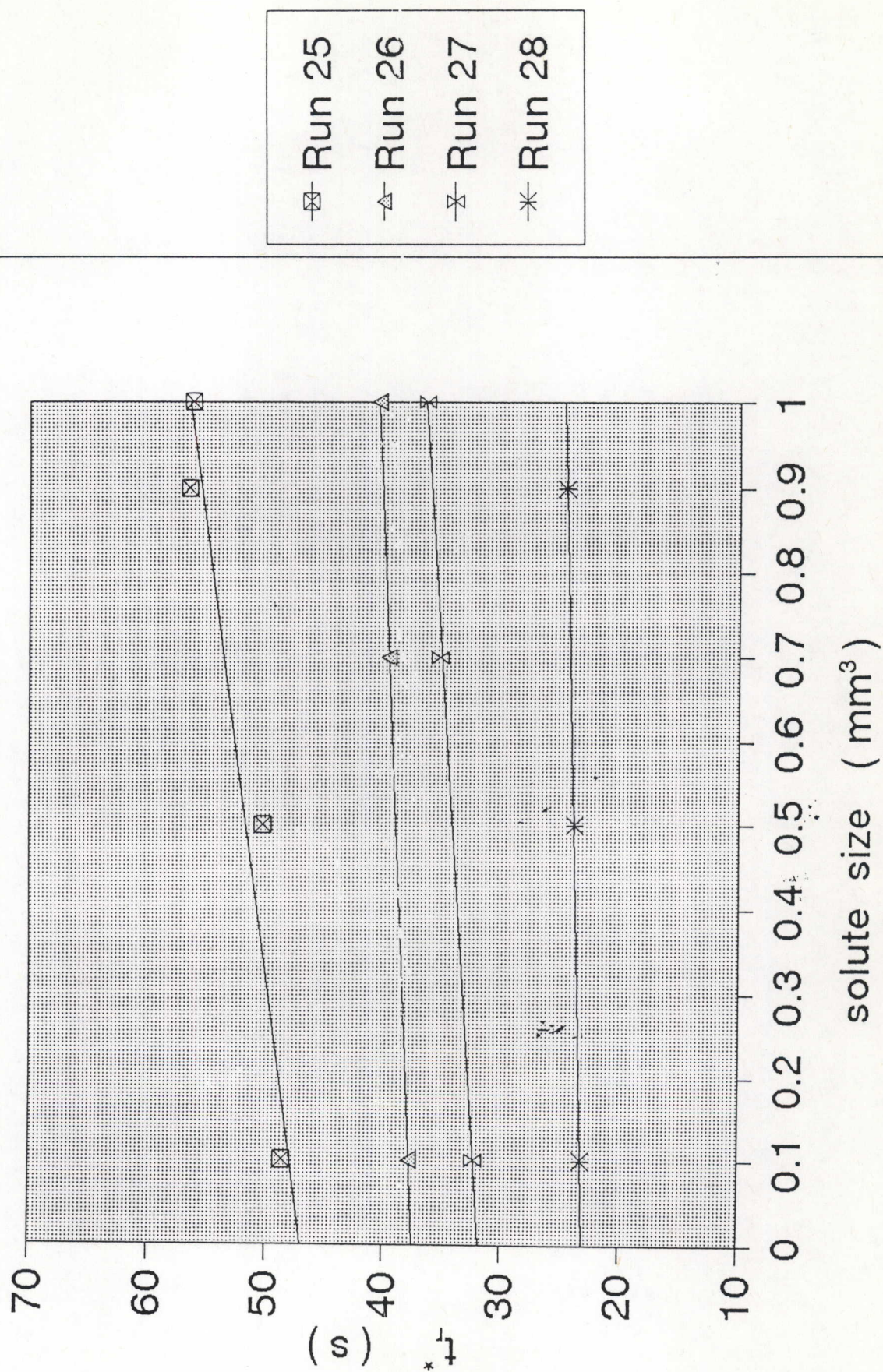


FIG.8. Ethanol on column 3 at 293.15 K

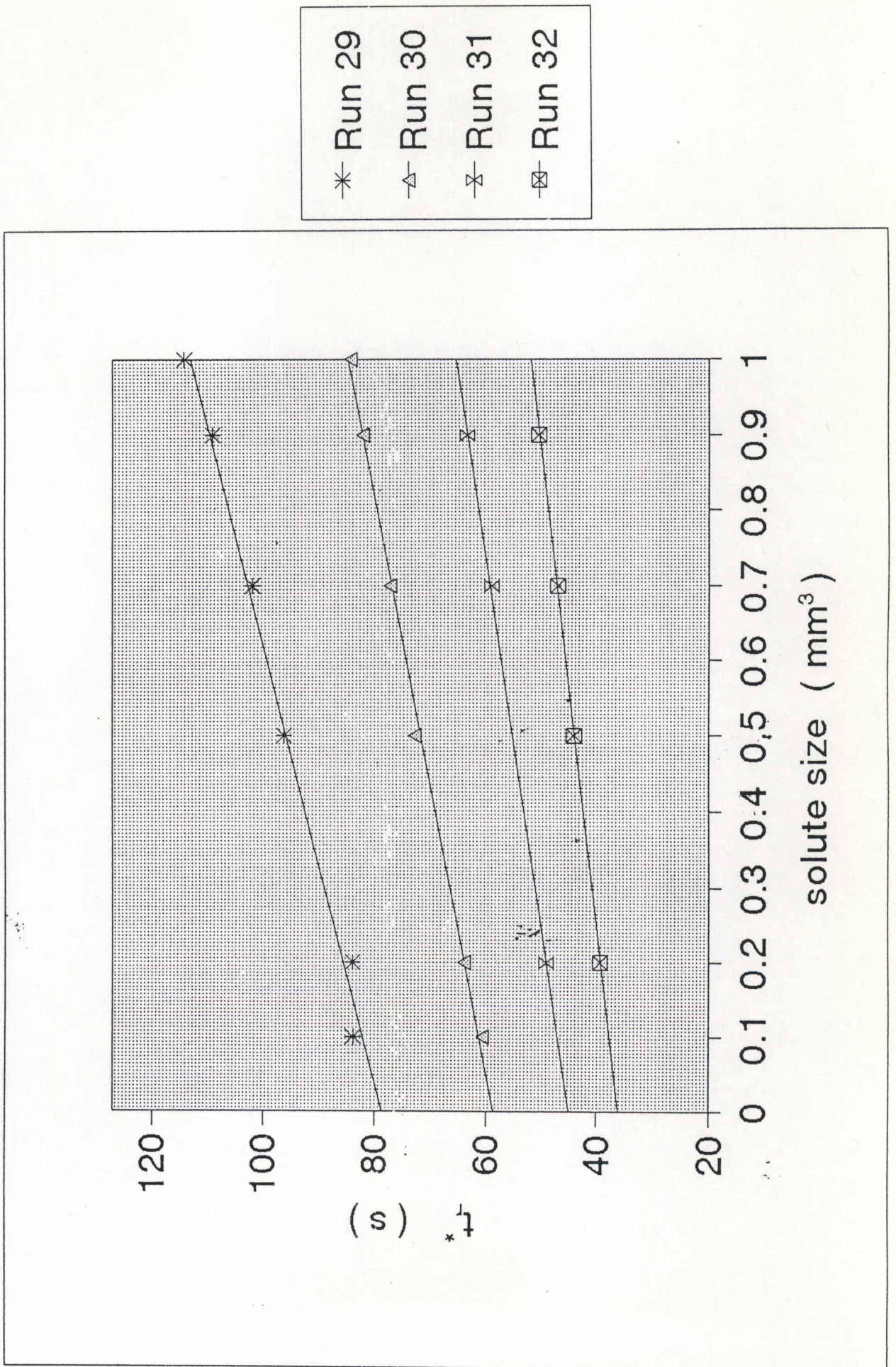


FIG.9. Propan-2-ol on column 3 at 293.15 K

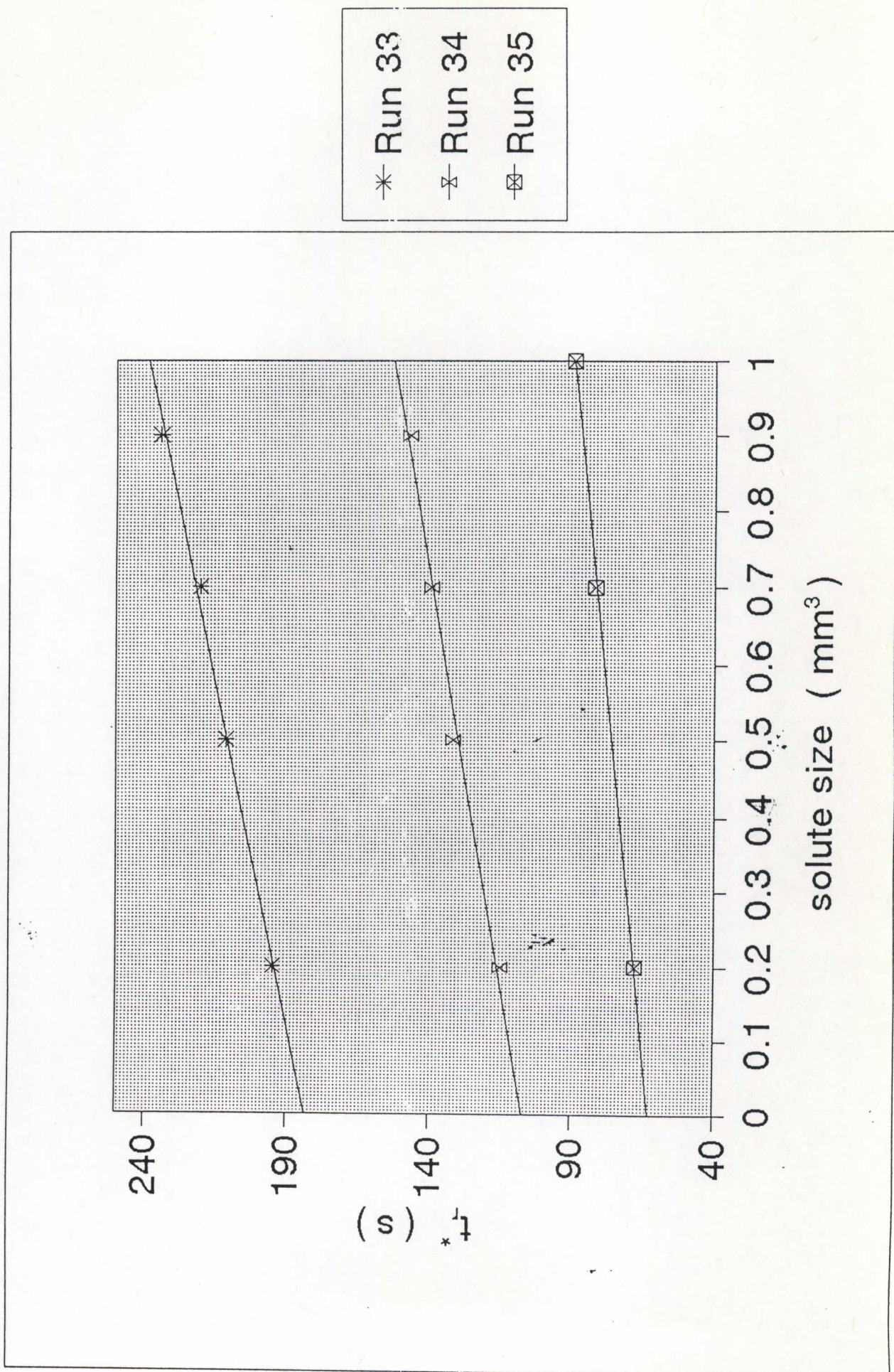


FIG.10. Methanol on column 4 at 303.15 K

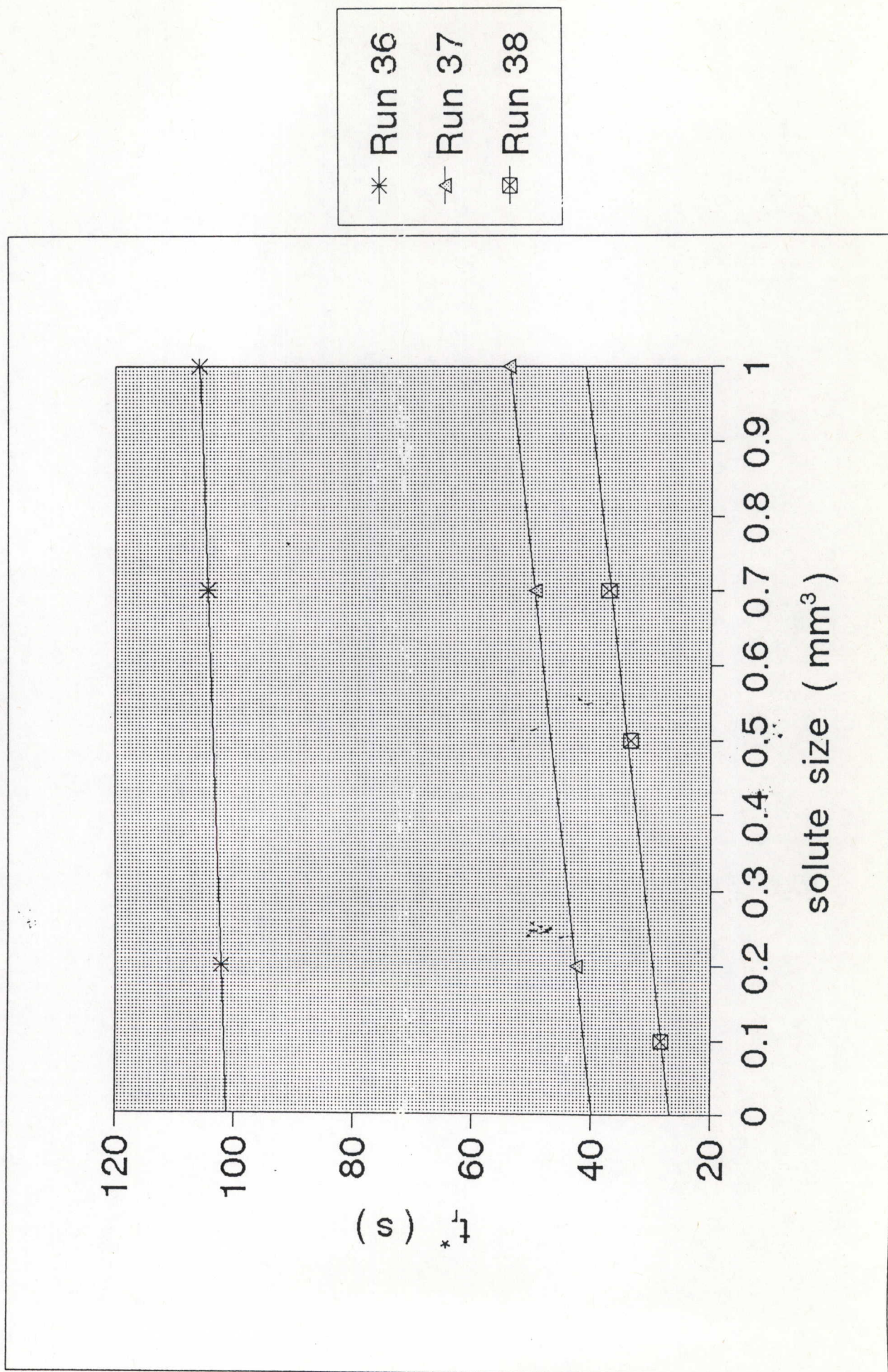


FIG.11. Ethanol on column 4 at 303.15 K

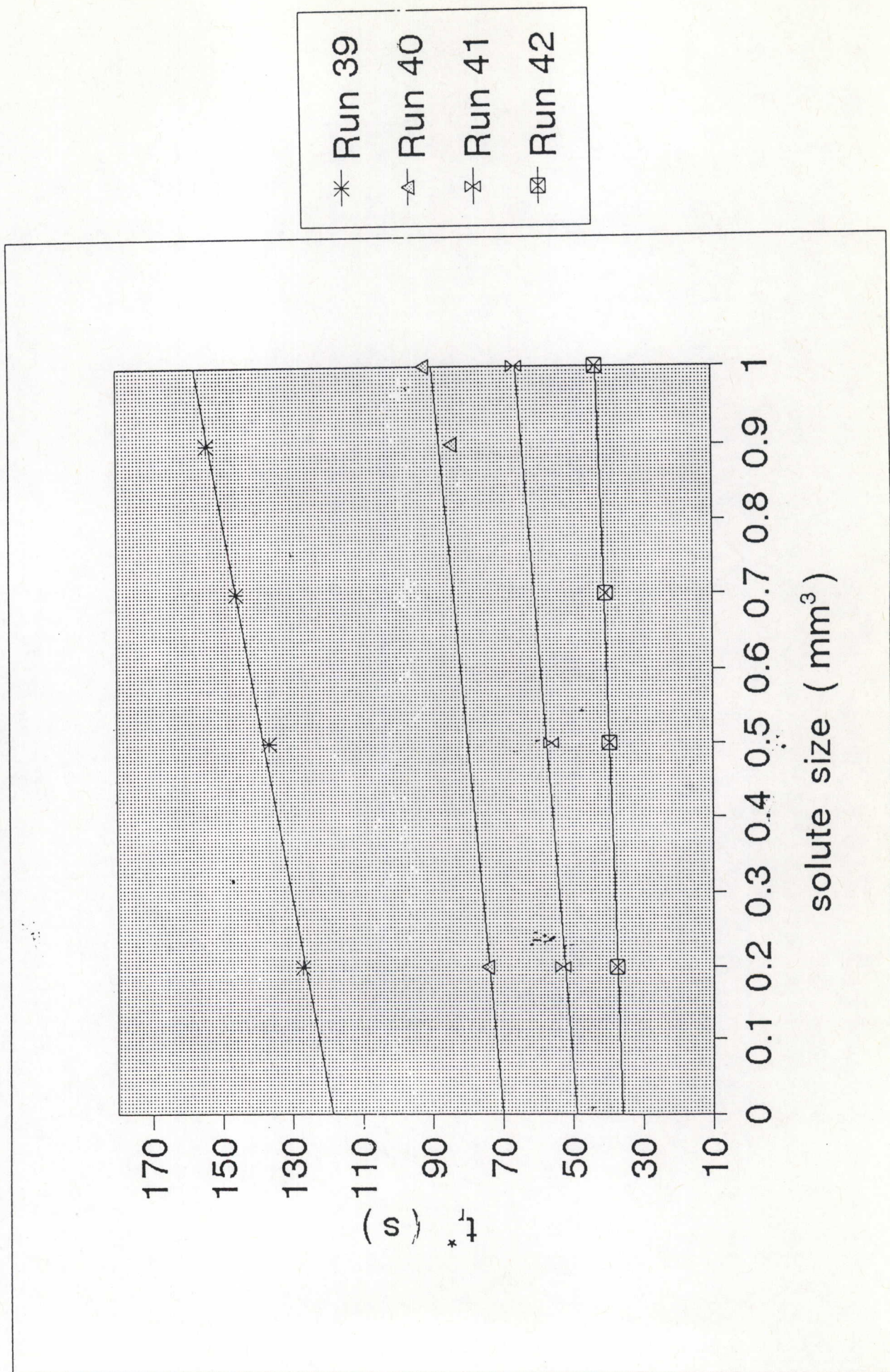


FIG.12. Propan-1-ol on column 4 at 303.15 K

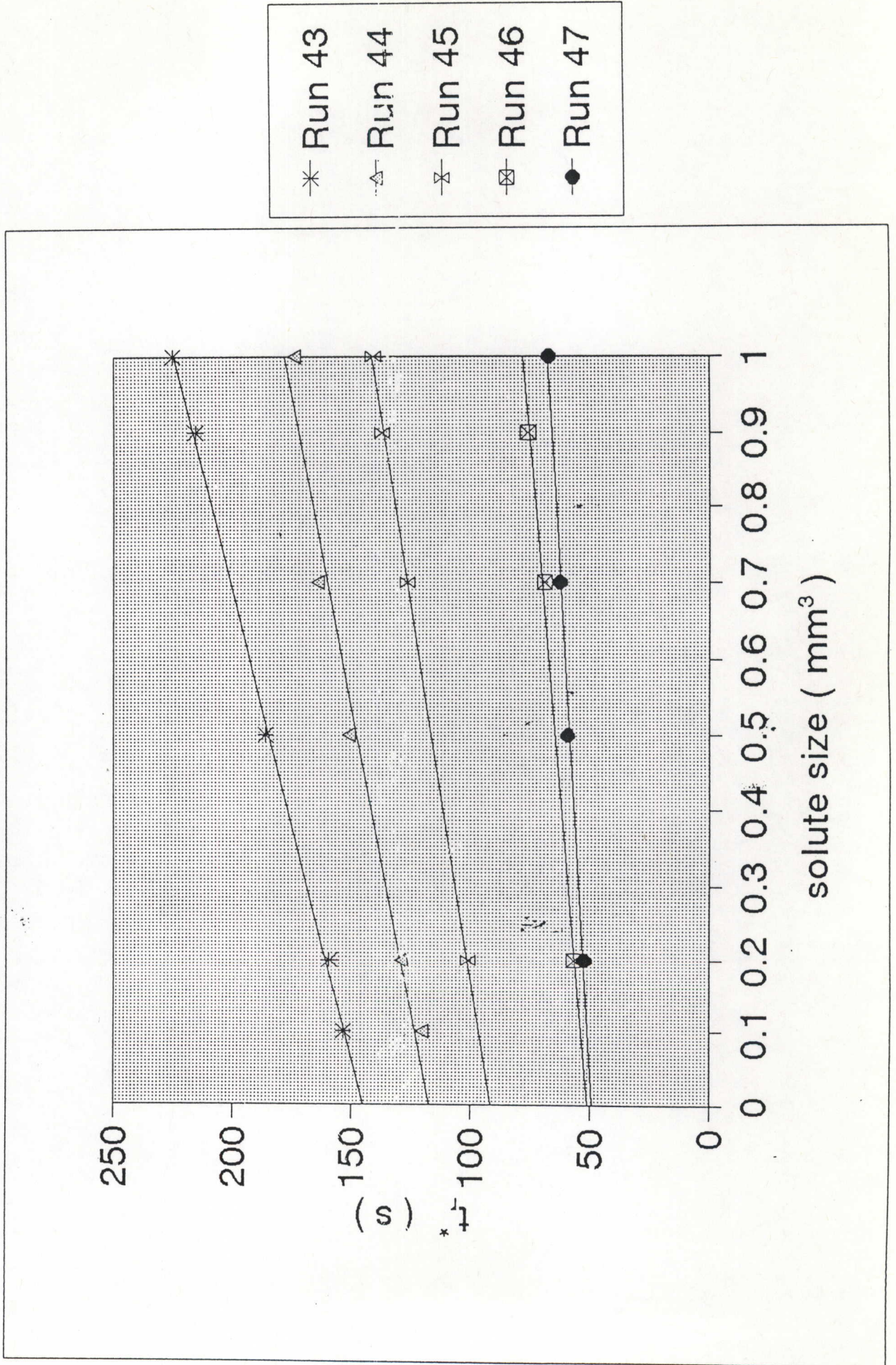


FIG. 13. Propan-2-ol on column 4 at 303.15 K

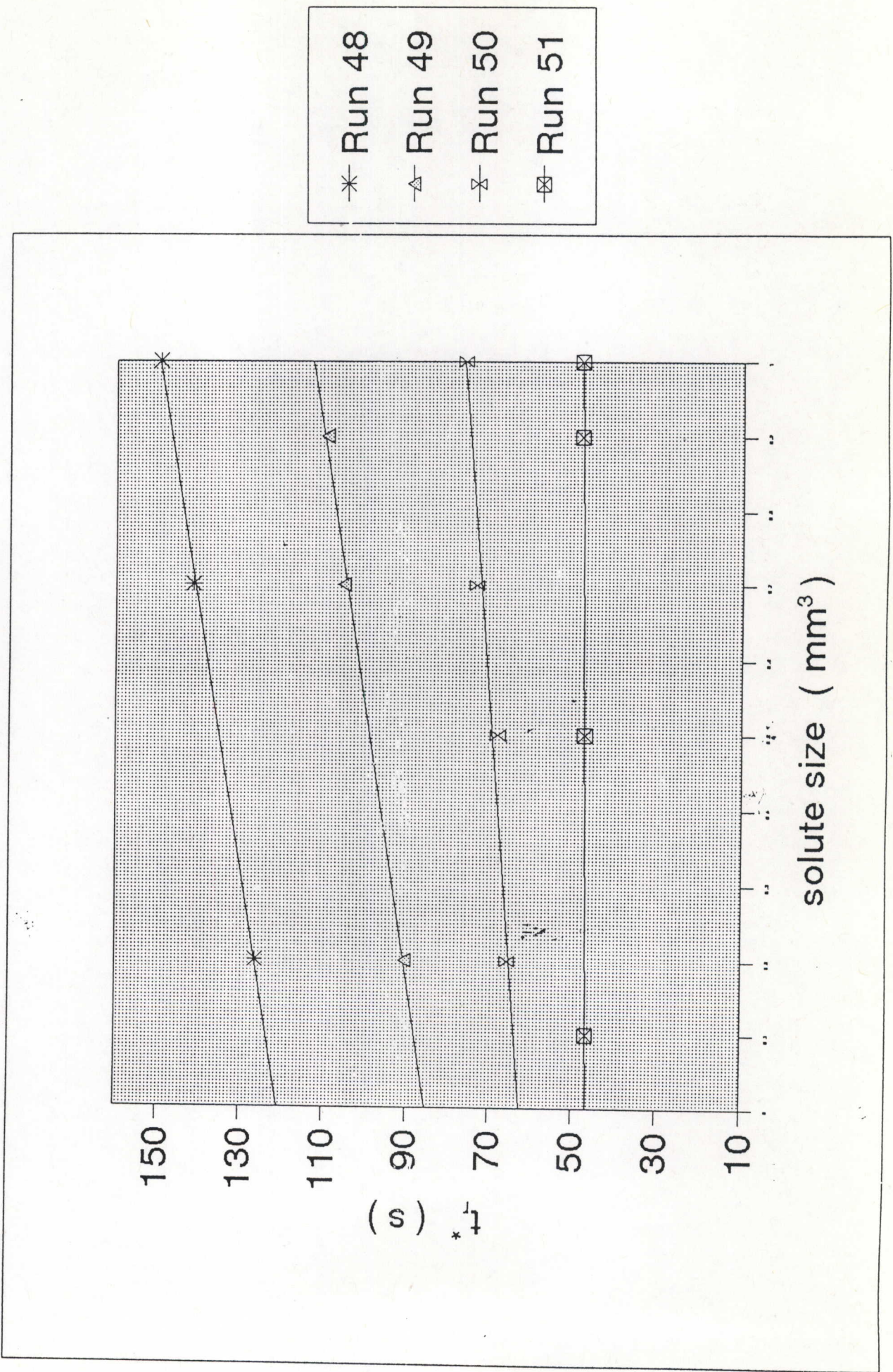


FIG.14. Propan-1-ol on column 5 at 303.15 K

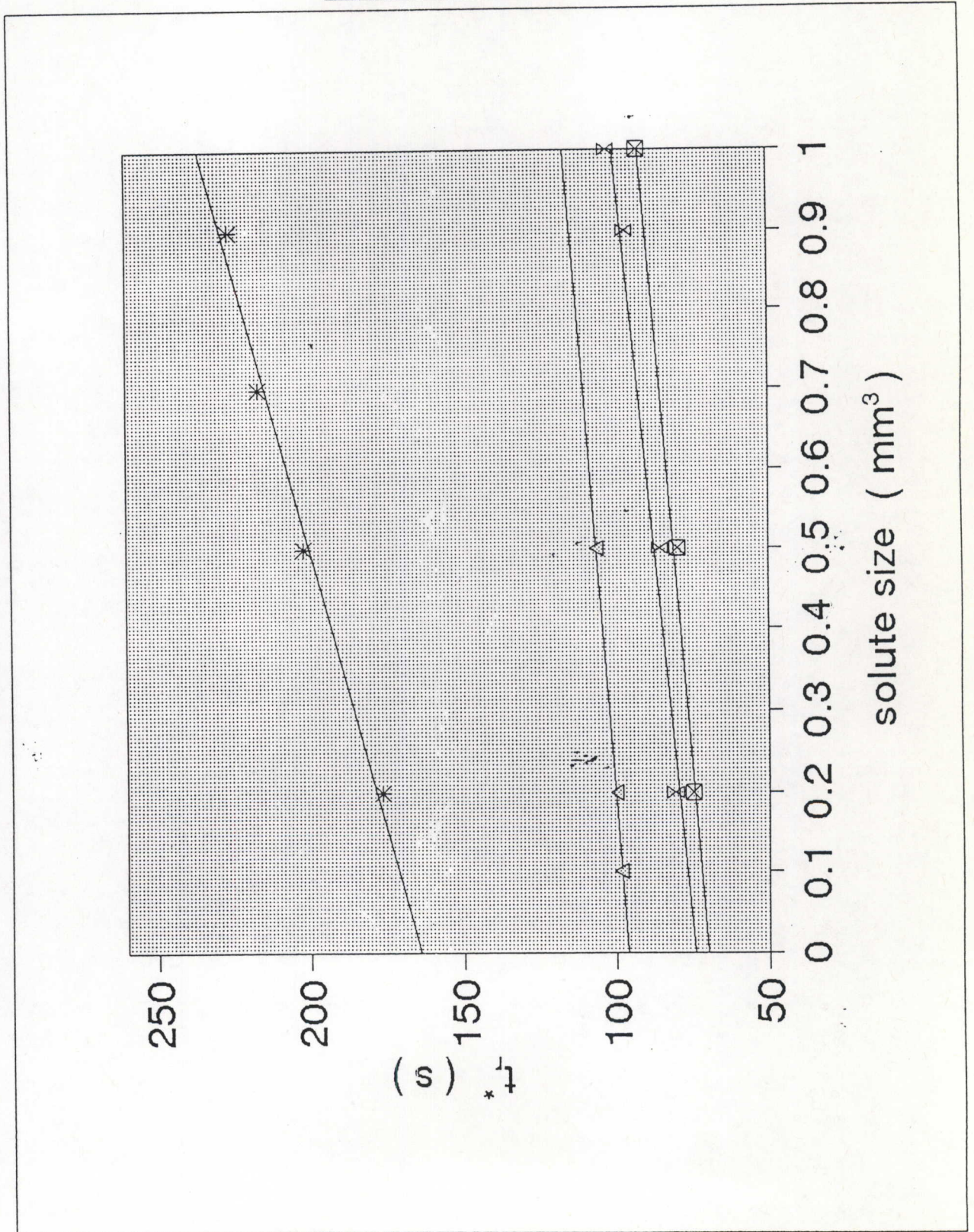


FIG.15. Methanol on column 6 at 303.15 K

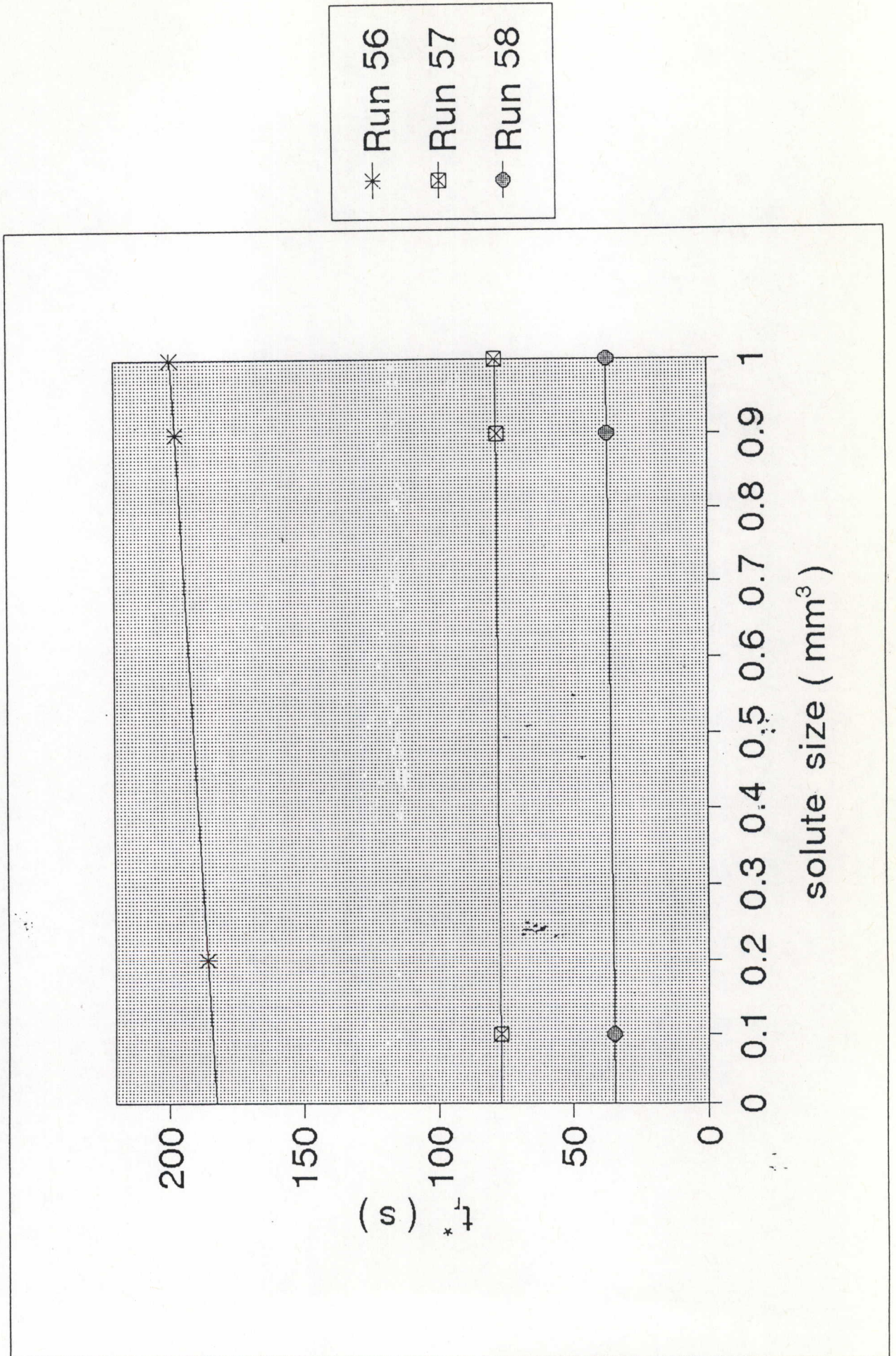


FIG. 16. Ethanol on column 4 at 303.15 K

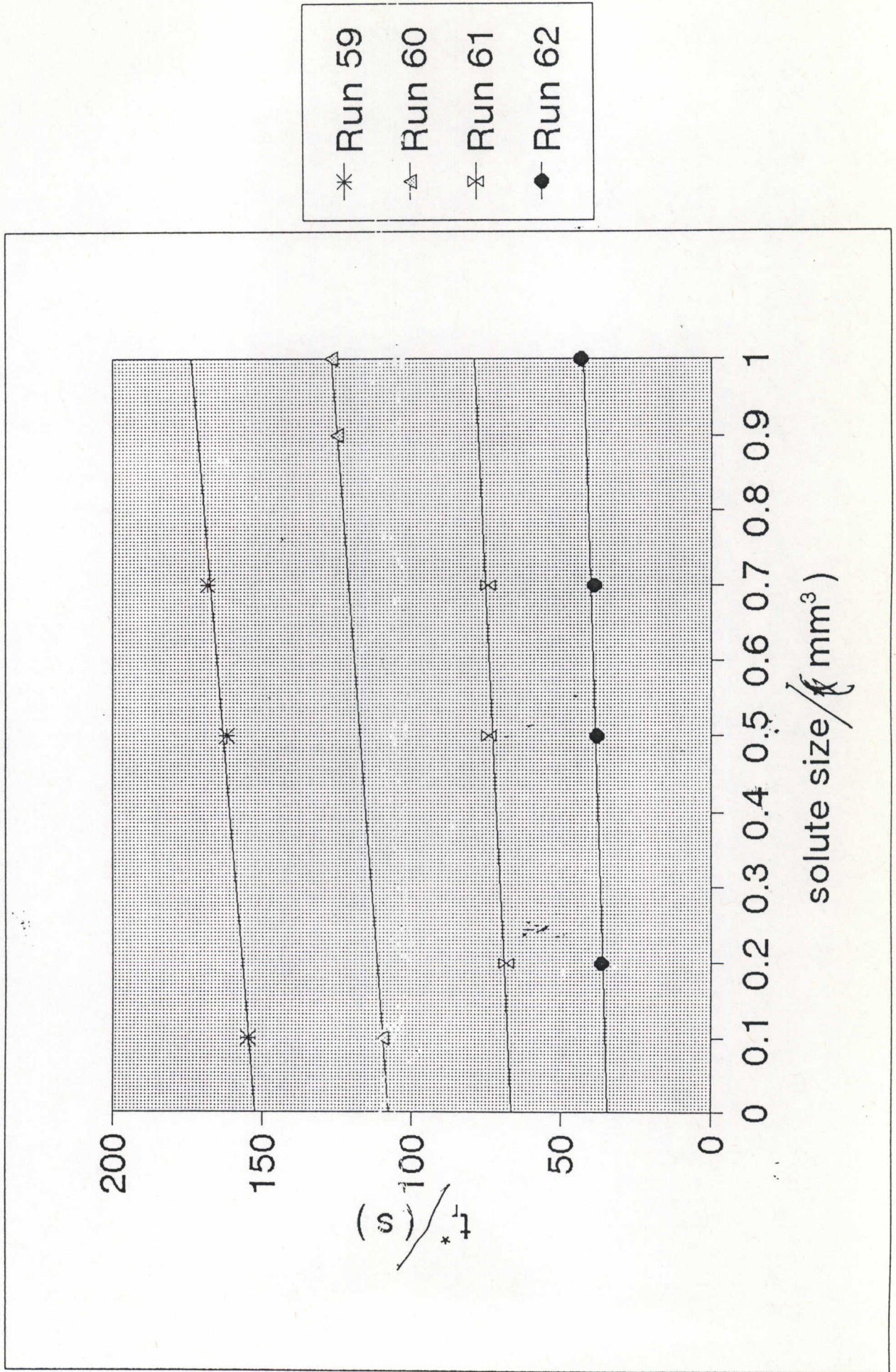


FIG.17. Propan-1-ol on column 6 at 303.15 K

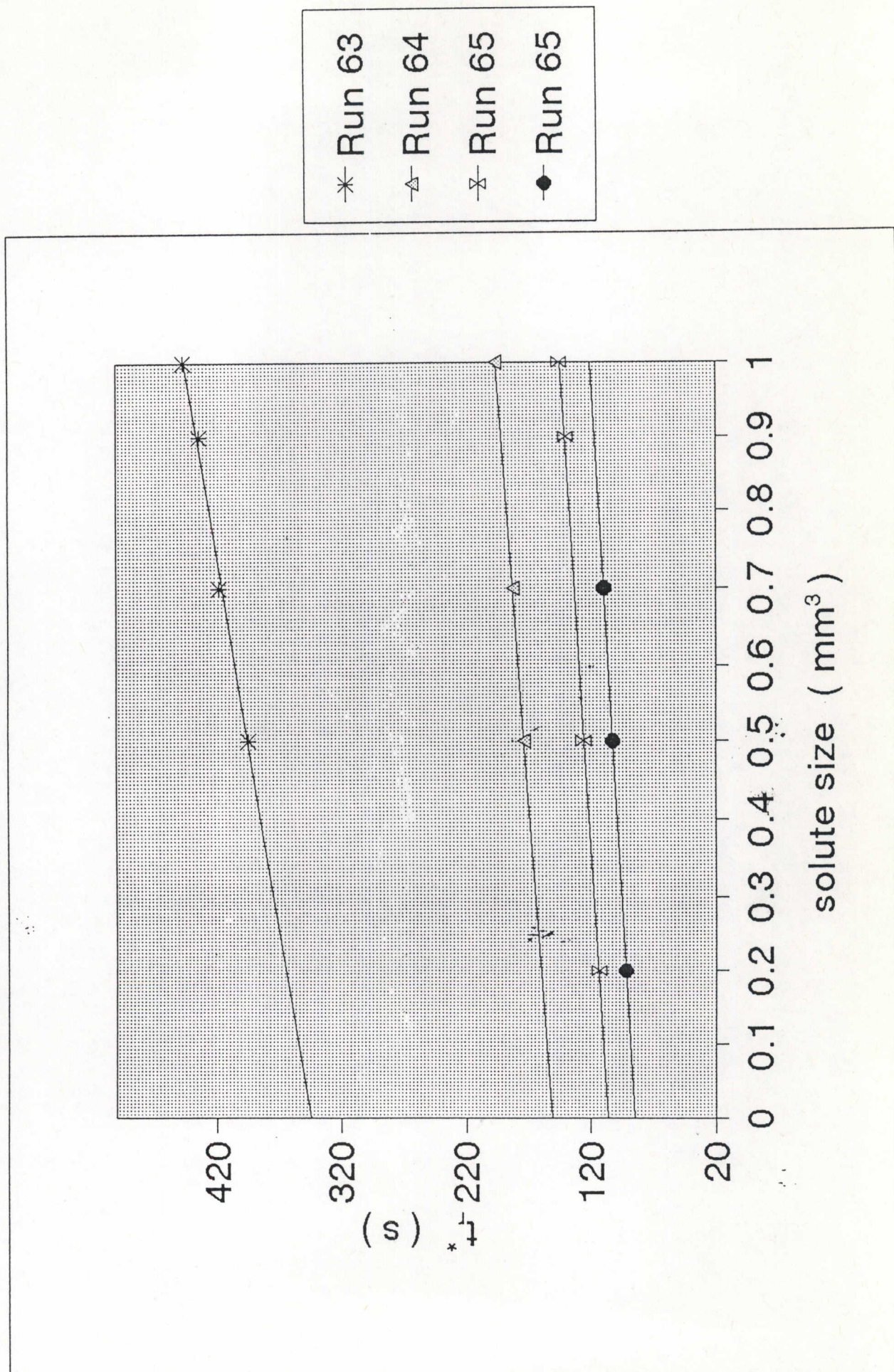


FIG.18. Propan-2-ol on column 6 at 303.15 K

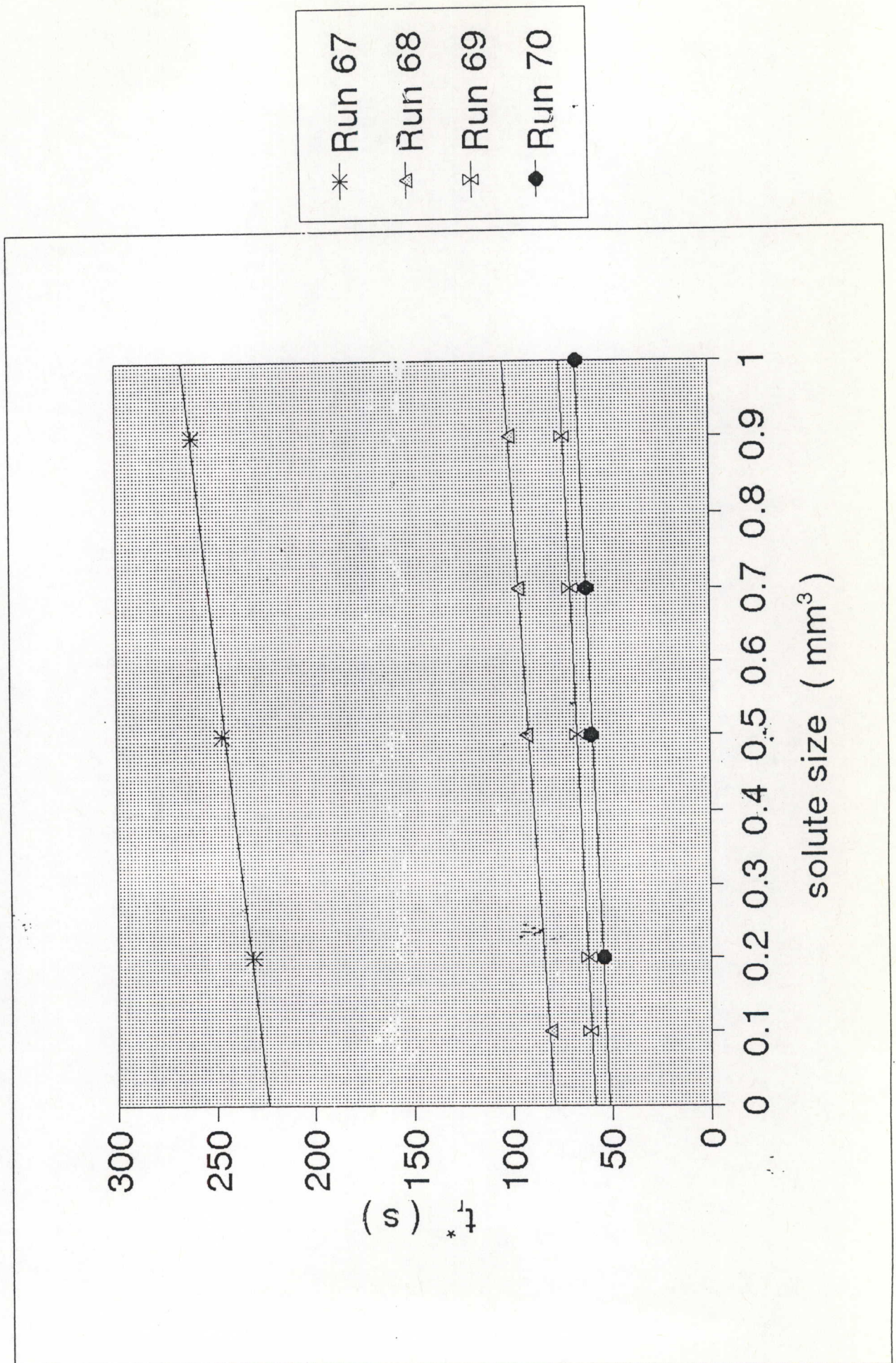


FIG.19. Methanol on column 7 at 303.15 K

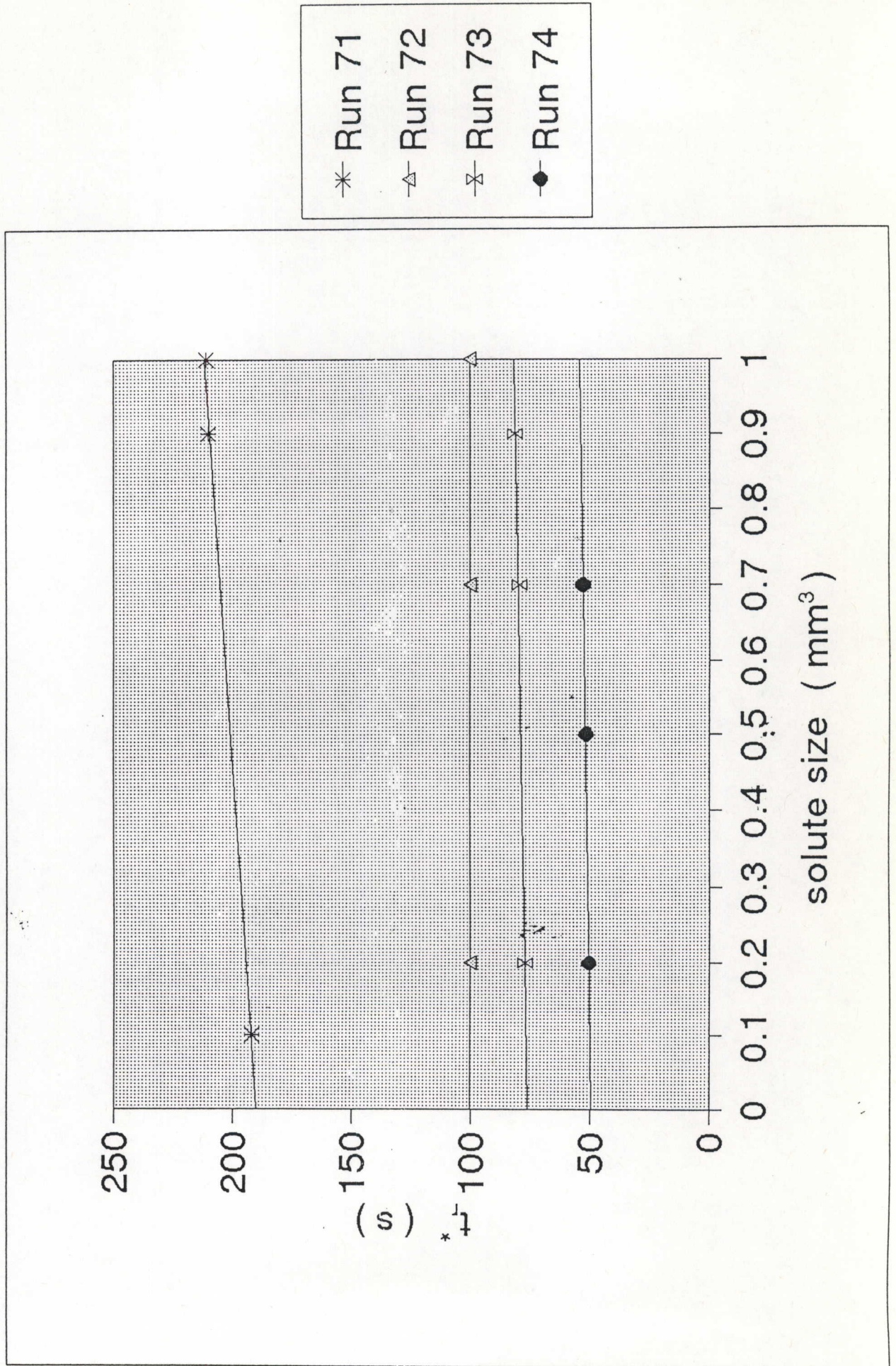


FIG.20. Ethanol on column 7 at 303.15 K

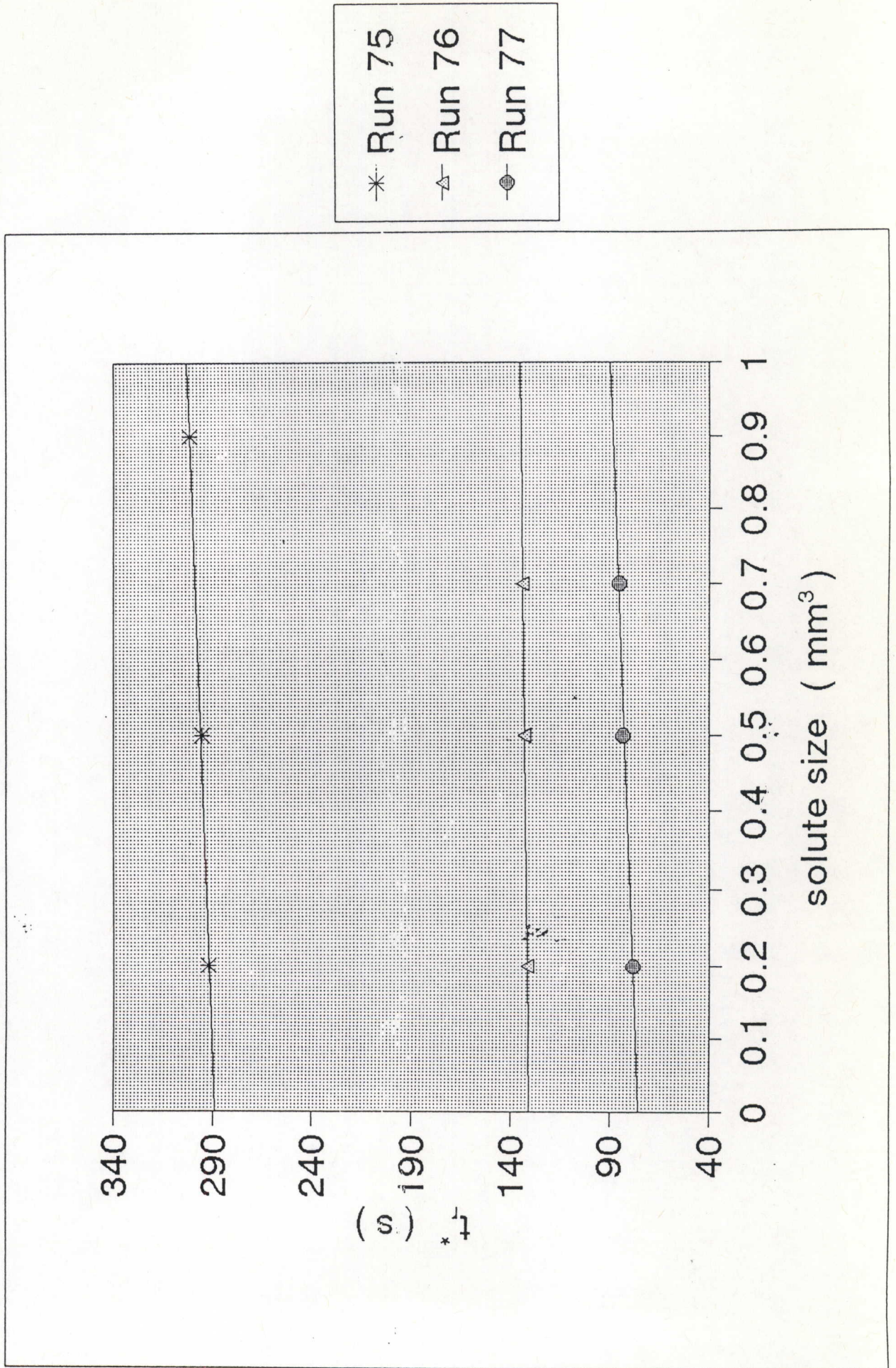
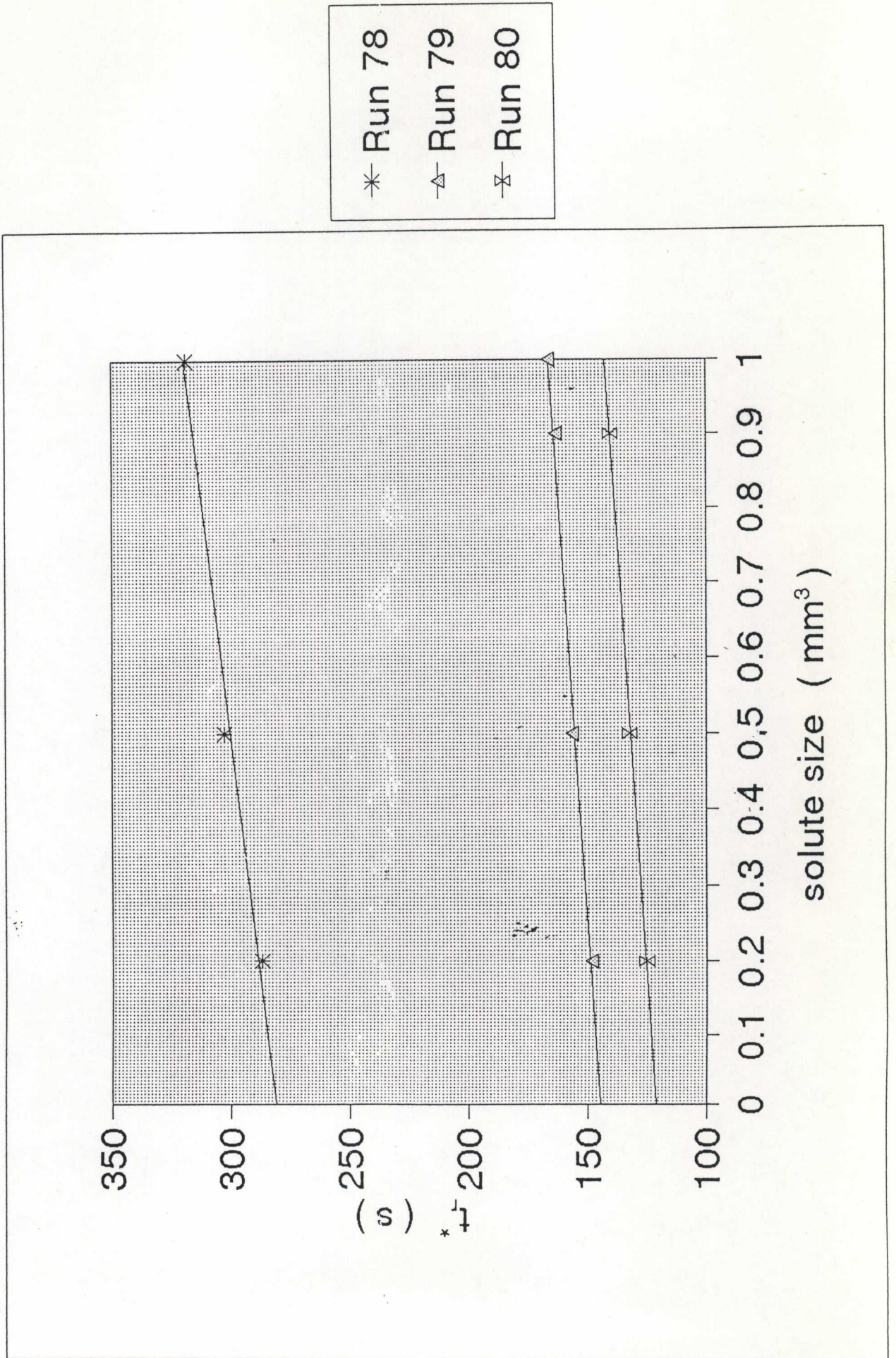


FIG.21. Propan-2-ol on column 7 at 303.15 K



REFERENCES

1. A.J.P.Martin, R.L.M.Synge, *Biochem.J.*, 1941, 35, 1358.
2. D.H.Everett, *Trans.Faraday Soc.*, 1965, 61, 1637.
3. A.J.B.Cruickshank, B.W.Gainey, G.P.Hicks, T.M.Letcher, R.W.Moody, and C.L.Young, *Trans. Faraday Soc.*, 1969, 64, 1014.
4. Bayles J.C.;T.M.Letcher and W.C.Moollan, *J. Chem. Thermodynamics*, 1993, 27,781- 788.
5. S.L. Sandler, "Thermodynamics Conference on Liquid-Liquid Mixtures", Colorado, 1995.
6. T.M.Letcher, and G. Netherton, *J.Chem.Thermodyn.*, 1975, 7, 353-357.
7. E.A.Guggenheim, *Mixtures*. Oxford University Press; London, 1952.
8. M.L.Huggins, *J.Chem. Phys.*, 1941, 9, 446.
9. P.J.Flory. *J.Chem.Phy.*, 1942, 10, 51.
10. D.H.Everett, and R.J Munn, *Trans. Faraday Soc.*, 1964, 60, 1951.
11. C.A. Eckert, and S.R. Sherman, "Thermodynamics Conference on Liquid-Liquid Mixtures", Colorado, (1995).
12. J.A. Zarkarian, F.E.Anderson, J.A.Boyd, and J.M.Prausnitz, *Ind.Eng.Chem.Proc.Des.Devel.*, 1979, 18:657.
13. D.M. Trampe and C.A. Eckert, *J. Chem. Eng. Data*, 1990, 35, 156.
14. D.M. Trampe and C.A. Eckert, *AIChEJ.*, 1993, 39, 1045.
15. A.Hussam and P.W. Carr, *Anal. Chem.*, 1985, 57, 793.
16. P.Alessi and M. Fermeglia, S.L. Sandler, *J.Chem. Eng. Data*, 1992, 37, 484.
17. R.B. Poe, S.C.Rutan, M.J.Hait, C.A.Eckert and P.W.Carr, *Anal.Chim.Acta.*, 1993, 277, 223.
18. J.C.Leroi, J.C. Mason, H.Renon, J.F.Fabries and Sannie, *Ind. Eng. Chem. Process Des.Dev.*, 1977, 16, 1, 139-144.
19. A.J.P.Martin, and A.T.James, *Biochem.J.*, 1952, 50, 679.
20. P.E.Porter, C.H.Deal, and F.H.Stross, *J.Amer.Chem.Soc.*, 1956, 78, 2999

21. D.H.Desty, A.Goldup, G.R.Luckhurst, and W.T.Swandon, "Gas Chromatography 1962", (Butterwoths, 1962).
22. R.J.Laub, and R.L.Pecsock, "Physiochemical Application of Gas Chromatography, John Wiley and Sons Ltd. U.S.A., 1978, 8.
23. H.Purnell, Gas Chromatography, John Wiley and Sons Ltd. U.S.A., 1962, 89
24. H.K.Onnes and W.H.Keesom, Commun.Phys.Lab. Univ.Leiden, 1912, 11, Suppl.23 .
25. E.A.Guggenheim, Thermodynamics, North-Holland, Amsterdam, 1967, Chapters 4-5.
26. A.Goldup, G.R. Luckhurst and W.T.Swanton, 1962, Nature, 193, 333.
27. D.H.Everett, B.W.Gainey and C.L.Young, Trans. Faraday Soc., 1968, 64, 2667.
28. A.J.B.Cruickshank, M.L.Windsor, and C.L.Young, Proc. Roy. Soc. Ser.A, 1966, 295, 259, 271.
29. A.J.B.Cruickshank, B.W.Gainey, and C.L.Young, Trans.Faraday Soc. 1968, 64, 337, in Gas Chromatography 1968, C.L.A.
30. S.Chapman and I.G.Cowling, Mathematical Theory of Non-Uniform Gases, Cambridge Press, Cambridge, England, 1939.
31. A.D.Buckingham. The Laws and Applications of Thermodynamics, Peramon, Oxford, England, 1964.
32. P.W. Atkins, Physical Chemistry, Third Edition, Oxford University Press, 1986.
- 33 J.R.Conder and C.L. Young, Physiochemical Measurements by Gas Chromatography, John Wiley and Sons.; 1979, 165.
34. W.C.Moollan, M.Sc. thesis, 1993.
35. R.L.Pecsok, A.de Yllana, and A.Abdul-Karim, Anal.Chem., 1964, 36, 452.
36. J.H.Dymond, and E.B.Smith, "The Virial Coefficient of Gases", Charendon Press, Oxford, 1969.
37. J.A.Riddick, W.B.Bunger, and T.K.Sakano "Organic Sovents", Wiley-

Interscience, New York, N.Y., 1970.

38. M.L.McGlashan, and D.J.B.Potter, Proc.Roy.Soc.Ser.A. 1962, 267, 478.
39. G.H. Hudson, and J.C. McCoubrey, Trans. Faraday Soc., 1960, 56, 761.27.
40. T.M. Letcher, R.C. Baxter, A. Bean, and J.D.Sewry, J.Chem. Thermodynamics, 988, 20, 581.
41. N.D.Gritchina, Die Stationare Phase in der GLC, Moskau, 1970, 42.
42. A.Kwantes and G.W.A.Rijnders, GC-Symposium Amsterdam, 1958, 125, Editor: D.Desty, Butterworth, London, 1958.
43. A.IGnat and L.I.Mel'der, Eesti NSV Tead., Akad.Toim.,Keem.Geol., 1985, 34, 210.
44. P.Alessi, J.Kikic, A.Alessandrini, and M.Fermeglia, J.Chem.Eng.Data, 1982, 27, 4, 445-448.
45. J.H.Park, A.Hussam, P.Couasnom, D.Fritty, and P.W.Carr, Anal.Chem., 1987, 59, 1970.
46. D.E.Martire, and P.Riedl, J.Phys. Chem., 1968, 72, 10, 3479.
47. J.A.Beattie, and O.C.Bridgeman, J.Am.Chem.Soc.; 1927, 49, 1665.
48. T.M.Letcher, and R.C.Baxter, J.Solution Chem.; 1989, 18, 65.
49. T.M.Letcher, and R.C.Baxter, J.Solution Chem.; 1989, 18, 81.
50. J.Gmehling, J. Menke, and M.Schiller, Activity Coefficients at Infinite Dilution, Chemistry Data Series, Vol IX, Part 4, 1410 -1411.
51. J.F. Carruth, R.Kobayashi, J.Chem. Eng. Data; 1973, 18, 2.
52. TRC Thermodynamic Tables of Hydrocarbons, A.P.I. Project 44, 23-2, 1.
53. T.M.Letcher, and P.J.Jerman, Journal of South African Chemical Institute, 1976, 16, 1, 55-62.